Comment R1.1: *I appreciate the Editor to give me a chance to review an interesting and valuable paper. I found some merits in the both methodology and results. In my opinion, this paper has a good potential to be published in the journal. However, I have also some concerns on the different parts of the manuscript. If only the author(s) address carefully to all of my comments, I'll recommend publication of the manuscript in the journal.*
Response: We would like to thank the reviewer for the constructive comments. We followed his suggestions for improving the manuscript. Our responses to specific comments are given below. We also suggest the reviewer to check carefully the responses to the comments of Reviewer 2, since his suggestions led to substantial changes in the manuscript.

Comment R1.2: *What was the criterion to select the stations? Why the USA and Australia? Are they covering all climates?*
Response: The reasons for choosing the CIMIS-database of California (USA) and AGBM database of Australia are:
- The first database includes stations from California-USA and it was selected because: a) it has been used as a basis for the development of Hargreaves-Samani method (Hargreaves and Samani, 1985; Hargreaves and Allen, 2002) and CIMIS method (Snyder and Pruitt, 1985, Snyder and Pruitt, 1992) and b) provides a dense and descriptive network of stations for a specific region that combines coastal, plain, mountain and desert environments (Table 1, Fig.1a in the manuscript). The second database includes stations from Australia and it was selected because the stations network covers a large territory with large variety of climate classes (Table 1, Fig.1b in the manuscript), but also because the Priestley-Taylor method has been calibrated for locations of eastern Australia (Priestley and Taylor, 1972). For the stations of AGBM database, the selection of stations was performed in such way in order to cover all the possible existing Köppen climatic types and elevation ranges of Australian continent (Table 1 in the manuscript). (see text in Page 9, lines 25-35, Page 10, lines 0-5)

- Additional reason for choosing these two databases was that they provide a large number of stations with complete data for estimating ASCE-ET_o covering large observation periods before and after the year 2000 (Table 1 in the manuscript). This was a prerequisite in this study because the rasters of the new coefficients were developed based on mean monthly climatic parameters of 1950-2000. Thus, using stations with many available data after 2000, we could prove that the derived coefficients also work for current conditions. (see text in Page 10, lines 8-10)

- We have to mention that the combination of the databases provided a wide range of the mean monthly values of the parameters used for the ET_o estimations (this is an additional reason for their selection). The general statistics of the aforementioned parameters are also given in Table R1 below, which was included in the supplementary material as Table S1 (reference for Table S1 exist in the text in Page 10, line 24). In order to show the high variability in the parameters of the validation dataset, we provide frequency diagrams of mean monthly T_{max}, T_{min}, R_s, RH%, u_2 and P are given below in Fig.R1a,b,c,d,e,f, respectively.

- Taking into account the last column of Table 1 (Köppen-Geiger classification), we provided the climatic classification of each station. According to Table 1, from the 140 stations, 9 belong to A Köppen-Geiger group (tropical/megathermal), 69 to B group (Arid/semi-arid), 59 to C group (temperate/mesothermal) and 3 to D group (continental/microthermal). We believe, that apart from the D group, the number of stations for the rest climatic groups are enough for validating the results. As concern the D group, we couldn't find more stations with adequate data inside the aforementioned databases. Other databases, which may provide data for stations from other parts of the world, were not used in order to fully exploit the two aforementioned databases but also to give the opportunity to other scientists to test our revised coefficients for their territories using other complete databases and not selected stations from various databases. Many existing databases of observed data may show differences in the methods used for measuring and presenting data. Such differences were also observed in the CIMIS and AGBM databases and they were used to justify many uncertainties observed during the implementation of this work (see response to comment R2.3 of reviewer 2 and the new section in the discussion with title "*Uncertainties in the data used for calibrating and validating the revised coefficients of P-T and H-S methods*". It would be difficult to identify such uncertainties using stations from multiple databases.

Table R1. General statistics* of the mean monthly observed values of climatic parameters from the 140 stations of California-USA and Australia that participate in the estimation of reference evapotranspiration with the ASCE method.

Parameter	T_{max}	T_{min}	R_s	RH	u_2	P	ET_o ASCE-short	ET_o ASCE-tall
Unit	°C	°C	MJ m^{-2} d^{-1}	%	m s^{-1}	mm $month^{-1}$	mm $month^{-1}$	mm $month^{-1}$
Average	25.3	11.4	18.8	56.4	2.6	41.5	138.4	190.5
Minimum	5.3	-7.2	4.9	19.0	0.9	0.0	17.9	26.2
Lower quartile	19.7	6.5	13.5	45.5	1.8	11.7	82.2	112.7
Upper quartile	31.1	15.8	24.4	68.2	3.2	50.6	186.9	254.2
Maximum	41.2	26.3	30.1	90.3	6.8	470.4	377.5	563.8
Range	**35.9**	**33.5**	**25.2**	**71.3**	**5.9**	**470.4**	**359.6**	**537.6**
Standard deviation	7.1	6.4	6.5	15.4	1.0	51.5	69.5	98.9
Coeff. of variation %	28.11%	56.13%	34.32%	27.36%	37.05%	123.90%	50.17%	51.93%

*The statistics are based on 1680 values (140 stations × 12 months)

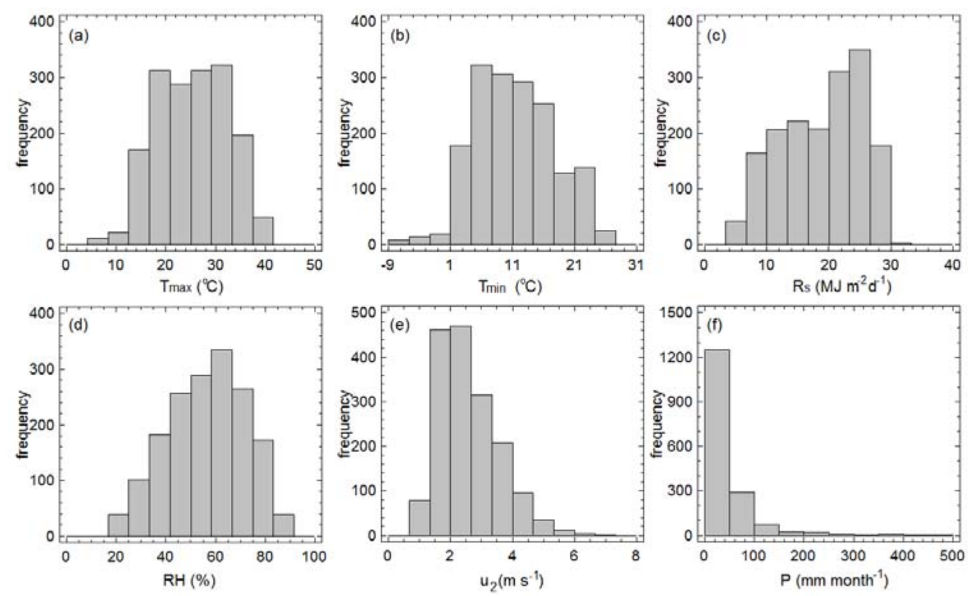

Fig.R1 Frequency diagrams (number of monthly values) based on the mean monthly data of the 140 stations of CA-USA and Australia for a) maximum temperature T_{max}, b) minimum temperature T_{min}, c) solar radiation R_s, d) relative humidity RH, e) wind speed u_2 at 2 m height and f) precipitation P. The frequencies are based on a total number of observations equal to 1680 (140 stations × 12 months).

Comment R1.3: *Lns 7-8, cite also these three useful papers to enhance the literature:*
- Selecting the best model to estimate potential evapotranspiration with respect to climate change and magnitudes of extreme events.
- Temporal analysis of reference evapotranspiration to detect variation factors.
- Analysis of potential evapotranspiration using limited weather data.
Response: The proposed citations were added at the proposed locations in the text and in the references list.

Comment R1.4: *Lns 15-16, cite also these two useful papers to enhance the literature:*
- Application of new mass transfer formulae for computation of evapotranspiration
- Ability of Box-Jenkins Models to Estimate of Reference Potential Evapotranspiration (A Case Study: Mehrabad Synoptic Station, Tehran, Iran)
Response: The proposed citations were added at the proposed locations in the text and in the references list.

Comment R1.5: *In the last paragraph of the Introduction, the authors should clearly mention the weakness point of former works (identification of the gaps) and describe the novelties of the current investigation to justify us the paper deserves to be published in this journal.*
Response: The most significant novelty of the study is that provides, for the first time, global maps of revised coefficients for the P-T and H-S evapotranspiration methods and revised coefficients for the H-S radiation formula. Such attempt has never been made in the past at the global scale, despite the fact that many studies for recalibrating the respective coefficients have been presented for many parts of the world. The final maps allow the comparison of the revised coefficients among regions under a common base since they were built using common datasets and using the same technique (Eqs.7), while they provide a global overview of the variation in these coefficients.
Other novelties of the study are:

- the development of global maps for the revised coefficients for P-T and H-S evapotranspiration methods for tall reference crop.
- the development of global maps for the possible mean annual error, when the P-T and H-S are applied using the standard coefficients of the original methods (maps of *MAD*% parameter, Fig.4b,c,d in the manuscript). These maps provide information about the uncertainty when the standard H-S and P-T methods are used. These maps were also combined to derive a new map (map of *DMAD* parameter, Fig.5a in the manuscript), which indentifies the optimum locations for the application of the standard H-S and P-T formulas based on their proximity to the results of ASCE for short reference crop. The *DMAD* map is an important tool, which can give a solution when someone has to choose between the two methods.
- the proposal of a method for deriving annual coefficients for the P-T and H-S methods. The procedure described by the set of Eqs.7, which estimates the partial weighted averages of the coefficients based on their monthly values, is a newly proposed method that can be easily applied in GIS environment, while it provides a solution when annual coefficients have to be derived under a common base for many stations or for global applications using raster data. This technique is proposed as an alternative of optimization methods, which are difficult to be incorporated in GIS environment (see more details about this comment in Page 18, lines 13-24 and the respective subsection of the

discussion). The method calibrates the basic coefficients without modifying or adding parameters in the original P-T and H-S equations.

Finally, we have to stress that the aim of the study is to provide tools for facilitating the estimation of ET_o and solar radiation for regions (especially those of developing countries), which face serious shortage of climatic data and not to propose the revised coefficients as an alternative method for regions, which have complete meteorological stations that provide detailed sets of all climatic variables. Of course, the use of such stations to validate the coefficients is the only solution. All the aforementioned aspects related to the novelties and the aims of the study are included in brief in the revised paragraph at the end of the introduction.

Comment R1.6: *Compare the results with modified/calibrated H-S and P-T models presented by other researchers in all of the world (particularly in the USA and Australia).*

Response: The requested task is quite difficult and there are many problems of comparability since either the majority of authors have modified the initial form of H-S and P-T models and not only the main coefficients, but also because the majority of the works provide H-S and P-T models, which are calibrated for regions outside California and Australia. For example, the popular recalibrated Priestley-Taylor model of Abtew (1996) for Florida-USA uses a recalibrated coefficient equal to 1.18, which is almost equal to our revised coefficient (1.17 from 0.5 degree resolution), but the model gives bad results in the validation procedure because Florida has a completely different environment from California and cannot cover the climatic variation of Australia stations. Other examples are the modified Makking model and other models given by Castañeda and Rao (2005), which were calibrated only for one station of southern California using 4 years of observations and the modified Hargreaves-Samani models and other models of Azhar and Perera (2011), which were recalibrated for three stations of southeastern Australia with very few years of observations. Similar problems were observed for too many other cases that we examined using a large list of models provided by Valipour (2015a,b; 2017) and Valipour et al. (2017) and by models obtained from the works cited in the introduction. Thus, it is unfair to examine the accuracy of such models using the complete validation dataset (both California and Australian stations), while it is not feasible in the context of this article to examine one by one all the modified models published in the international literature. Of course, the analysis of modified H-S and P-T models calibrated for other parts of the world was rejected from the beginning because the validation dataset does not include stations from these regions. The only models, which are absolutely comparable are the modified H-S models by Droogers and Allen (2002) because they have been calibrated using global datasets. In order to partly satisfy the request of the reviewer, we selected some models of reduced parameters, which have similar or additional requirements from the standard H-S and P-T models. The final selected models were also those who showed a) the best performance after examining an extremely large list of models using both California-USA and Australia stations data and b) a good performance to other studies using other datasets. The comparison with such models will also contribute to verify the value of our coefficients as alternative options for ET_o estimations with fewer variables.

Based on the aforementioned observations, the following 8 models were selected for comparisons with the standard and re-adjusted H-S and P-T models:

1. Two modified models of H-S by Droogers and Allen (2002) where the second one uses precipitation as additional parameter. The models were based on calibrations using global data.

2. Three models of reduced parameters given by Valiantzas (2013a,b; 2014) that were calibrated using 535 stations from Europe, Asia, Africa. The first model uses temperature and radiation data, while the other two use temperature, radiation, and humidity data. The models have been tested for California (Valiantzas, 2013c) and Australia conditions (Ahooghalandari et al., 2017).
3. Two models of reduced parameters by Ahooghalandari et al. (2016) calibrated using 18 stations from various locations of Australia. The models use temperature and relative humidity data. Ahooghalandari et al. (2017) also made recalibration of Valiantzas equations and other models but for a restricted region of Western Australia considering 8 stations, and for this reason these modified versions were not used.
4. The Copais model of Alexandris et al. (2006) that uses temperature, radiation and humidity data. The model was calibrated/validated using data from Greece, California and Oregon-USA, while it has shown a very good response to many other regions of the world including Australia (Ahooghalandari et al., 2017).

The aforementioned observations and the description of the additional models used for comparisons were added as a new paragraph in the page 10 (lines 32-35) and 11 (lines 0-25) together with the new Table 2, which gives the equations of the additional models. The results of the models were added in Page 14 (lines 25-35), and 15 (lines 0-15). The comparisons of the models were included in new Fig.8 and their statistics in the new Table 5.

Comment R1.7: *The Discussion section should be broken to sub-sections for better understanding of readers.*
Response: we followed the suggestion of the reviewer and the discussion section was broken to sub-sections.

Comment R1.8: *Explain the variations of the spatial extent of the major climatic groups CGs from Köppen-Geiger climate map.*
Response: The variations of the spatial extent of the major climatic groups CGs from Köppen-Geiger climate map, which are given in the first column of Table 4 in the revised manuscript, are results obtained from the respective raster Köppen-Geiger climate map of Peel et al. (2007) and they are described in detailed in their article. We believe that is beyond the scope of the paper to discuss the observed % of CGs in the map of Peel et al. (2007) (keep in mind that % values are re-adjusted after excluding Antarctica and they are slightly different from those given by Peel). If the reviewer means to explain the results of the other columns of new Table 4 (i.e. why for example the typical H-S method is better from the typical P-T method in more arid environments or why P-T is better in more humid environments) the explanation is based on the fact that the standard H-S method was calibrated for the conditions of California, which include arid and semi-arid environments, while the standard coefficient 1.26 of Priestley-Taylor method was obtained based on experiments of more humid environments. This justification was added in the text (see Page 13, lines 8-11).

Comment R1.9: *Discuss the comparison of the average and standard deviation of RMSEs of the validation dataset between different pixel Resolutions more thoroughly.*
Response: The comparison between different pixel resolutions was removed based on the objections of Reviewer 2. Reviewer 2 suggested not to use the resolutions below 0.5 degree due to interpolation limitations in the initial raster data for solar radiation, humidity and wind speed, which were at 0.5 degree. See comments of Reviewer 2. All the manuscript was revised from the beginning using only the results of 0.5 degree resolution.

Comment R1.10: *What are the strategies/recommendations to reduce uncertainties in this study?*
Response: a new subsection was added in the Discussion. See the new subsection with title "*Recommendations for reducing the uncertainties when the re-adjusted coefficients of P-T and H-S models are used"*.

Comment R1.11: *At the end of the manuscript, explain the implications and future works considering the outputs of current study.*
Response: we added new text about it (see the last paragraph in the Conclusions section)

Comment R1.12: *The quality of the language needs to improve by a native English speaker for grammatically style and word use.*
Response: We examined carefully the language, and English corrections were made with the help of native English speaker.

Other major corrections made in the text:

1. Some affiliations changed because some authors were transferred to other institutions or because one of the Institutions changed name.
2. The abstract reformed in order to be more descriptive.
3. Any analysis related to finer resolutions below 0.5 degrees was removed from the text following the comments of reviewer 2. For this reason, the 30 arc-sec resolution maps given in Figs.2,3,4,5,6,7 were substituted with the ones of 0.5 degree resolution with respective changes in the range of values in their legends. Any discussion about the comparison of different resolutions was also removed from the discussion section. Additionally, all the results and tables changed based on 0.5 degree resolution. Similar changes were also made in the supplementary material. The only reference about the finer resolutions is given in section 5. Data availability, where we added the following text: *"Apart from the 0.5 degree resolution raster datasets, the database contains the same datasets at finer resolution (30 arc-sec, 2.5 arc-min, 5 arc-min and 10 arc-min). These finer datasets are provided in order to cover the observed resolution range in the initial climatic data (e.g. the temperature data of Hijmans et al. (2005) are provided at 30 arc-sec resolution). The finer resolutions were produced using bilinear interpolation on solar radiation, humidity and wind speed data of Sheffield et al. (2006). This interpolation method is not the most appropriate for such purposes. The data of finer resolutions can only be used as a tool to assess uncertainties associated to temperature variation effects within a 0.5 degree pixel or to estimate average values of the coefficients for larger territories in order to capture a better representation of the coastlines or islands that do not exist in 0.5 degree resolution (use of values from individual pixels is not recommended). A complete list of the datasets is provided in the Table S5."*
4. Reviewer 2 also commented that the manuscript is quite long. For this reason we removed the accuracy analysis by splitting the stations based on their elevation, and we also removed the Taylor diagrams analysis since the criteria that we give in Table 5 are more than enough.
5. The Discussion section was completely reformed based on the comments of Reviewer 1.
6. We added another 8 models of short reference crop evapotranspiration for comparative purposes after the request of Reviewer 1.

7. An error was found in the coordinates of Australian station Paynes Find station (A-69) of the validation dataset and the associated coefficients extracted from the specific coordinates. The position of the station was corrected in Fig.1 and any information related to the station was corrected. An additional arithmetic error was found and corrected in the ET_o ASCE estimations of Australian stations. We performed a detailed check for all stations data, all the calculations/equations used for rasters development, all the calculations/equations used for analyzing stations data.

References

Abtew, W.: Evapotranspiration measurements and methoding for three wetland systems in South Florida. J. Am. Water Resour. Assoc. 32, 465-473, 1996.

Ahooghalandari, M., Khiadani, M., Jahromi, M. E.: Developing Equations for Estimating Reference Evapotranspiration in Australia. Water Resour. Manage., 30, 3815-3828, 2016.

Ahooghalandari, M., Khiadani, M., Jahromi, M. E.: Calibration of Valiantzas' reference evapotranspiration equations for the Pilbara region, Western Australia. Theor. Appl. Climat. 128, 845-856, 2017.

Alexandris, S., Kerkides, P., Liakatas, A.: Daily reference evapotranspiration estimates by the ''Copais'' approach. Agr. Water Manage. 82:371-386, 2006.

Azhar, A. H., Perera, B. J. C.: Evaluation of reference evapotranspiration estimation methods under Southeast Australian conditions. J. Irrig. Drain Eng., 137, 268-279, 2011.

Castañeda, L., Rao, P.: Comparison of methods for estimating reference evapotranspiration in Southern California. J. Environ. Hydrol. 13, 1-10, 2005.

Droogers, P., and Allen, R. G.: Estimating reference evapotranspiration under inaccurate data conditions. Irrig. Drain. Syst., 16, 33-45, 2002.

Hargreaves, G. H., and Samani, Z. A.: Reference crop evapotranspiration from ambient air temperature. *American Society of Agricultural Engineers*, 12 pp, 1985. http://libcatalog.cimmyt.org/download/reprints/97977.pdf

Hargreaves, G. H., and Allen, R. G.: History and evaluation of Hargreaves evapotranspiration equation. J. Irrig. Drain Eng. ASCE, 129 (1), 53-63, 2002.

Peel, M. C., Finlayson, B. L., and McMahon, T. A.: Updated world map of the Köppen-Geiger climate classification. Hydrol. Earth Syst. Sci., 11, 1633-1644, 2007.

Priestley, C. H. B., and Taylor, R. J.: On the assessment of surface heat flux and evaporation using large-scale parameters. Mon. Weather Rev., 100, 81-92, 1972.

Snyder, R. L., and Pruitt. W. O.: Estimating reference evapotranspiration with hourly data. VII-1-VII-3. R. Snyder, D. W. Henderson, W. O., Pruitt, and A. Dong (eds), *Calif. Irrig. Mgmt. Systems*, Final Rep., Univ. Calif., Davis, 1985.

Snyder, R. L., and Pruitt. W. O.: Evapotranspiration data management in California. Presented at the Amer. Soc. of Civil Engr. Water Forum '92', Aug. 2-6, 1992, Baltimore, MD, 1992.

Valiantzas, J. D.: Simple ETo forms of Penman's equation without wind and/or humidity data. I: Theoretical development. J. Irrig. Drain Eng., 139, 1-8, 2013a.

Valiantzas, J. D.: Simplified reference evapotranspiration formula using an empirical impact factor for penman's aerodynamic term. J. Hydrol. Eng., 18, 108-114, 2013b.

Valiantzas, J. D.: Closure to "Simple ETo forms of Penman's equation without wind and/or humidity data. I: Theoretical development" by John D. Valiantzas. J. Irrig. Drain Eng., 140, art. no. 07014017, 2014.

Valipour, M.: Investigation of Valiantzas' evapotranspiration equation in Iran. Theor. Appl. Clim., 121, 267-278, 2015a.

Valipour, M.: Evaluation of radiation methods to study potential evapotranspiration of 31 provinces. Meteorol. Atmos. Phys., 127, 289-303, 2015b.
Valipour, M.: Analysis of potential evapotranspiration using limited weather data. Appl. Water Sci., 7, 187-197, 2017.
Valipour, M., Gholami Sefidkouhi, M. A., and Raeini−Sarjaz, M.: Selecting the best model to estimate potential evapotranspiration with respect to climate change and magnitudes of extreme events. Agr. Water Manage., 180, 50-60, 2017.

High resolution global grids of revised Priestley-Taylor and Hargreaves-Samani coefficients for assessing ASCE-standardized reference crop evapotranspiration and solar radiation

Vassilis G. Aschonitis[1], Dimitris Papamichail[2], Kleoniki Demertzi[2], Nicolo Colombani[1], Micol Mastrocicco[3], Andrea Ghirardini[1], Giuseppe Castaldelli[1], Elisa-Anna Fano[1]

[1]Department of Life Sciences and Biotechnology, University of Ferrara, Ferrara, Italy
[2]Department of Hydraulics, Soil Science and Agricultural Engineering, Aristotle University of Thessaloniki, Thessaloniki, Greece
[3]Department of Environmental, Biological and Pharmaceutical Sciences and Technologies, University of Campania "Luigi Vanvitelli", Caserta, Italy

Correspondence to: Vassilis G. Aschonitis (schvls@unife.it)

Abstract. The objective of the study is to provide global grids (0.5 degree) of revised annual coefficients for the Priestley-Taylor (P-T) and Hargreaves-Samani (H-S) evapotranspiration methods after calibration based on ASCE-standardized Penman-Monteith method (ASCE method includes two reference crops: short clipped grass and tall alfalfa). The analysis also includes the development of a global grid of revised annual coefficients for solar radiation (R_s) estimations using the respective R_s formula of H-S. The analysis was based on global gridded climatic data of the period 1950-2000. The method for deriving annual coefficients of P-T and H-S methods was based on partial weighted averages (p.w.a.) of their mean monthly values. This method estimates the annual values considering the amplitude of the parameter under investigation (ET_o and R_s) giving more weight to the monthly coefficients of the months with higher ET_o values (or R_s values for the case of H-S radiation formula). The method also eliminates the effect of unreasonably high or low monthly coefficients that may occur during periods where ET_o and R_s fall below a specific threshold. The new coefficients were validated based on data from 140 stations located in various climatic zones of USA and Australia with expanded observations up to 2016. The validation procedure for ET_o estimations of short reference crop showed that the P-T and H-S methods with the new revised coefficients outperformed the standard methods reducing the estimated *RMSE* in ET_o values by 40% and 25%, respectively. The estimations of R_s using the H-S formula with revised coefficients reduced the *RMSE* by 28% in comparison to the standard H-S formula. Finally, a raster database was built consisting of: (a) global maps for the mean monthly ET_o values estimated by ASCE-standardized method for both reference crops, (b) global maps for the revised annual coefficients of the P-T and H-S evapotranspiration methods for both reference crops and a global map for the revised annual coefficient of the H-S radiation formula, (c) global maps that indicate the optimum locations for using the standard P-T and H-S methods and their possible annual errors based on reference values. The database can support estimations of ET_o and solar radiation for locations where climatic data are limited while it can support studies, which require such estimations at larger scales (e.g. country, continent, world). The datasets produced in this study are archived in PANGAEA database

(https://doi.pangaea.de/10.1594/PANGAEA.868808) and in ESRN-database (http://www.esrn-database.org or http://esrn-database.weebly.com).

1 Introduction

The reference crop evapotranspiration ET_o is defined as the maximum value of water losses by evaporation and transpiration above a reference crop (e.g. grass), which can be achieved under no water restrictions. It is also one of the most important parameters for water balance estimations and irrigation planning of crops (Allen et al., 1998). Several methods have been proposed for ET_o estimations (Itenfisu et al., 2003; Allen et al., 2005; Wang and Dickinson, 2012; McMahon et al., 2013; Valipour, 2017; Valipour and Gholami Sefidkouhi, 2017; Valipour et al., 2017) with the most popular the FAO-56 Penman-Monteith (Allen et al., 1998), the Priestley-Taylor (Priestley and Taylor, 1972) and the Hargreaves-Samani (Hargreaves and Samani, 1982; 1985) methods. The FAO-56 has been updated to the ASCE-standardized method (Allen et al., 2005), which reflects the current state-of-the-art, providing ET_o estimations for two reference crops (a short and a tall reference crop, which correspond to clipped grass and alfalfa, respectively). The ASCE-standardized method has been proposed by the ASCE-EWRI Task Committee as the most precise method and requires a wide range of climatic parameters, which in many cases are not available. The problem of data availability can be confronted by other methods, such as the Priestley-Taylor and Hargreaves-Samani, which require less information for their determination. In fact, they are considered as the most precise among the simplified methods with reduced parameters (Xu and Singh, 2002; Sumner and Jacobs, 2005; Valipour, 2012; 2014).

The Priestley-Taylor (P-T) method requires net solar radiation and temperature data. The P-T formula includes an empirical factor known as advection coefficient a_{pt}, which is usually set equal to 1.26 (Priestley and Taylor, 1972) and generally ranges between 1.08 and 1.34 (Tateishi and Ahn, 1996; Xu et al., 2013). Other studies for various climatic conditions have shown that a_{pt} presents significant spatial and seasonal variability (Castellvi et al., 2001; Moges et al., 2003; Pereira, 2004; Tabari and Talaee, 2011; Aschonitis et al., 2015). Weiß and Menzel (2008) used the value 1.26 for wet and the value 1.75 for dry climatic conditions, as suggested by Maidment (1992). The value a_{pt}=1.26 has been verified experimentally for bare irrigated soil (Eichinger et al., 1996). Theoretical simulations for the case of the reference crop in saturated soil have also verified the a_{pt}=1.26 for the case of non or restricted advection effects (Lhomme, 1997; McMahon et al., 2013). Lower values of the advection coefficient have been reported by Singh and Irmak (2011) (a_{pt}=1.14) for Nebraska (USA), by Abtew (1996) (a_{pt}=1.18) for Florida (USA), by Kellner (2001) (a_{pt}=0.8) for central Sweden, and by Xu and Singh (2002) (a_{pt}=0.9) for Switzerland. Values of a_{pt}<1 have been reported for forested steep areas (Shuttleworth and Calder, 1979; Giles et al. 1984; Flint and Childs, 1991). On the other hand, high values ranging between 1.82-2.14 have been reported for cold-dry lands of Iran (Tabari and Talaee, 2011). Aschonitis et al. (2015) analysed the monthly variation of a_{pt} for the Italian territories and observed through regression analysis that more than 90% of the spatial variability of the seasonal a_{pt} was explained by the spatial variability of vapour pressure deficit DE (positive correlation). The rate of a_{pt} variation per unit DE

was found significantly different between seasons and it was negatively correlated to net solar radiation and/or temperature. The general trends of a_{pt} led to the conclusion that colder-drier conditions due to low net radiation and high vapour pressure deficit tend to increase its values.

The Hargreaves-Samani (H-S) method requires only temperature data, including four empirical factors (or three depending on the formula). A part of the equation empirically describes the incident solar radiation R_s. A basic problem of the Hargreaves-Samani method is that it tends to underestimate ET_o under high wind conditions (u_2>3 m s^{-1}) and to overestimate ET_o under conditions of high relative humidity (Allen et al., 1998). The last years, many scientists have performed analysis and re-calibration of the Hargreaves-Samani method for various climates (Trajkovic, 2007; Tabari, 2010; Tabari and Talaee, 2011; Azhar and Perera, 2011; Aschonitis et al., 2012; Mohawesh and Talozi, 2012; Rahimikhoob et al., 2012; Ravazzani et al., 2012; Bachour et al., 2013; Long et al., 2013; Mendicino and Senatore, 2013; Ngongondo et al., 2013; Berti et al., 2014; Heydari and Heydari, 2014), which indicates a global interest for simplified methods, mainly driven by the lack of data.

The analysis of ET_o at global scale is of special interest since it provides a general view about the spatiotemporal variation of this parameter, while (together with rainfall) provides significant information about the aridity of terrestrial systems. A basic limitation of global analysis is the lack of homogeneously distributed meteorological stations around the globe and especially in mountainous regions. The last years, climatic models, advanced interpolation and other methods have succeeded to generate datasets of various climatic parameters (Hijmans et al., 2005; Sheffield et al., 2006; Osborn and Jones, 2014; Brinckmann et al., 2016), facilitating the attempts to develop ET_o maps. Significant works of global ET_o estimations have been performed from various scientists. Mintz and Walker (1993) used the Thorthwaite (1948) method and provided isoline maps of ET_o. Tateishi and Ahn (1996) used the Priestley-Taylor method and provided ET_o maps at 0.5 degree resolution. Droogers and Allen (2002) used FAO-56 Penman-Monteith method, providing ET_o maps at 10 arc-min resolution and a modified Hargreaves-Samani method, which considers rainfall. Weiß and Menzel (2008) compared four different methods (Priestley-Taylor, Kimberly Penman, FAO-56 Penman-Monteith and Hargreaves-Samani) and provided ET_o maps at 0.5 degree resolution. Zomer et al. (2008) used Hargreaves-Samani method and provided the highest resolution (30 arc-sec) available for ET_o maps.

The objectives of the study are: a) to develop mean monthly maps of ET_o for the period 1950-2000 at global scale using the most precise ASCE-standardized method for both reference crops (short clipped grass and tall alfalfa); b) to develop global maps that provide the possible annual error in ET_o estimations using the standard P-T and H-S evapotranspiration methods in comparison to ASCE method for short reference crop and the possible annual error in solar radiation estimations using the temperature-based H-S radiation formula (this attempt will allow to identify the optimum locations for the application of the standard H-S and P-T evapotranspiration formulas based on their proximity to the results of ASCE for short reference crop); c) to develop global maps of re-adjusted annual coefficients for the H-S and P-T evapotranspiration methods for both short and tall reference crop based on a new method that estimates partial weighted averages of the monthly coefficients (the same procedure was also followed for the coefficients of the H-S radiation formula); d) to validate the results of the re-adjusted P-T and H-S coefficients using data from meteorological stations from different locations with different climatic conditions; and e) to compare the predictive ability of the re-adjusted P-T and H-S coefficients for short reference crop evapotranspiration with the respective predictions obtained from other models that have low data requirements. The analysis and the produced datasets of this study were based on mean monthly climatic data of 0.5 degree resolution for the period 1950-2000. The final datasets of revised H-S and P-T coefficients will provide a global overview of the variation in their values and a common base for comparing the values of different regions since they are calibrated using common datasets and using the same technique. The produced global datasets of this study can support estimations of ET_o and solar radiation for locations where climatic data are limited while it can support studies, which require such estimations at larger scales (e.g. country, continent, world).

2 Data and methods

2.1 Global climatic data

The analysis presented in this study was based on global climatic data obtained from the following databases:

- The database of Hijmans et al. (2005) provides mean monthly values for the parameters of precipitation, maximum, minimum and mean temperature at 30 arc-sec spatial resolution. The data are provided as grids of mean monthly values of the period 1950-2000 (http://www.worldclim.org/). The database also includes a revised version of the GTOPO30 DEM based on SRTM DEM at 30 arc-sec spatial resolution, which was used for the estimation of atmospheric pressure. The DEM was also used as a base to calculate the distance from the coastlines in raster format at 30 arc-sec spatial resolution based on the Euclidean distance.
- The database of Sheffield et al. (2006) provides monthly values of parameters such as wind speed at the height of 10 m above the ground surface, solar radiation, specific humidity, precipitation and temperature for the period 1948-2006 at 0.5 degree spatial resolution. The data are available in the form of netcdf files of monthly values of each year for the period 1948-2006 (http://hydrology.princeton.edu/data.pgf.php).
- The database of Peel et al. (2007) provides the revised global Köppen-Geiger climate map. The data are provided in raster form with 0.1 degree spatial resolution. The climate map was developed using the GHCN version 2.0 dataset (Peterson and Vose, 1997), which includes precipitation data from 12396 stations and temperature data from 4844 stations data for the periods 1909-1991 and 1923-1993, respectively. The Köppen-Geiger map was used to obtain the climatic type of the meteorological stations used in the validation dataset.

In this study, the ET_o is estimated combining the databases of Hijmans et al. (2005) and Sheffield et al. (2006), as follows: a) mean monthly values of maximum, minimum, mean temperature and precipitation were obtained from Hijmans et al. (2005); while b) wind speed, specific humidity and incident solar radiation were obtained from Sheffield et al. (2006) database. The specific humidity was converted to actual vapour pressure using the equation given by Peixoto and Oort (1996). The final results and analysis presented in this study is based on the coarser 0.5 degree resolution.

All the calculations presented in the next sections were performed in ArcGIS 9.3 ESRI environment at WGS84 ellipsoid coordinate system. For area coverage calculations or for estimations of mean global values of various parameters, coordinate system conversions were performed from WGS84 to projected Cylindrical Equal Area system (Antarctica is not included in the maps, thus any % globe coverage calculations and derivation of mean global values of various parameters are referred to the rest terrestrial surface).

2.2 Methods

2.2.1 The ASCE standardized reference evapotranspiration method

The estimation of ET_o using the ASCE method is performed by the following equation (Allen et al. 2005):

$$ET_o = \frac{0.408\Delta\left(R_n - G\right) + \dfrac{\gamma u_2 (e_s - e_a) C_n}{\left(T_{\text{mean}} + 273.16\right)}}{\Delta + \gamma(1 + C_d u_2)} \tag{1}$$

where ET_o is the reference crop evapotranspiration (mm d^{-1}), R_n is the net solar radiation at the crop surface (MJ m^{-2} d^{-1}), u_2 is the wind speed at 2 m height above the soil surface (m s^{-1}), T_{mean} is the mean daily air temperature (^oC), G is the soil heat flux density at the soil surface (MJ m^{-2} d^{-1}), e_s is the saturation vapor pressure (kPa), e_a is the actual vapor pressure (kPa), Δ is the slope of the saturation vapor pressure-temperature curve (kPa $^oC^{-1}$), γ is the psychrometric constant (kPa $^oC^{-1}$), C_n and C_d are constants, which vary according to the time step and the reference crop type and describe the bulk surface resistance and aerodynamic roughness. The short reference crop (ASCE-short) corresponds to clipped grass of 12 cm height and surface resistance of 70 s m^{-1} where the constants C_n and C_d have the values 900 and 0.34, respectively. The tall reference crop (ASCE-tall) corresponds to full cover alfalfa of 50 cm height and surface resistance of 45 s m^{-1}, where the constants C_n and C_d have the values 1600 and 0.38, respectively (Allen et al., 2005). The use of Eq.1 at daily or monthly step for short reference crop is equivalent to FAO-56 method (Allen et al., 1998).

2.2.2 The Priestley-Taylor method

The calculation of Priestley-Taylor (P-T) method is performed by the following equation (Priestley and Taylor, 1972):

$$ET_o = a_{pt} \frac{\Delta}{\lambda\left(\Delta + \gamma\right)}\left(R_n - G\right) \tag{2}$$

where ET_o is the potential evapotranspiration (mm d^{-1}), R_n is the net solar radiation (MJ m^{-2} d^{-1}), G is the soil heat flux density at the soil surface (MJ m^{-2} d^{-1}), Δ is the slope of the saturation vapor pressure-temperature curve (kPa $^oC^{-1}$), γ is the psychrometric constant (kPa $^oC^{-1}$), λ is the latent heat of vaporization (MJ kg^{-1}) and a_{pt} is the P-T advection coefficient. The value of λ was considered equal to 2.45 MJ kg^{-1} (Allen et al., 1998) (this value is also constant in Eq.1 and appears as $1/\lambda$=0.408). Eq.1 strictly refers to the reference crop evapotranspiration (i.e. short or tall crop), whereas Eq.2 has been used for the calculation of evapotranspiration under non-limiting water conditions of short reference crop, bare soil or open water surface and for this reason is also called potential evapotranspiration, which is a more general term. Eq.2 is applied in this study as a reference crop evapotranspiration method and for this reason is compared with Eq.1 for short reference crop using the standard mean global value 1.26 for the factor a_{pt}.

2.2.3 The Hargreaves-Samani method

The Hargreaves-Samani (H-S) method (Hargreaves and Samani, 1982;1985) for ET_o includes an internal function, which estimates the incoming shortwave solar radiation R_s (MJ m^{-2} day^{-1}), as follows:

$$R_s = K_{RS} \cdot R_a \cdot (TD)^{0.5} \tag{3}$$

where K_{RS} is the adjustment coefficient for the H-S radiation formula (°C$^{-0.5}$), R_a is the extraterrestrial radiation (MJ m^{-2} day^{-1}) and TD is the temperature difference between maximum and minimum daily temperature (°C). According to Allen et al. (1998), the empirical K_{RS} coefficient differs for 'interior' or 'coastal' regions: a) K_{RS}=0.16 for "interior" locations, where land mass dominates and air masses are not strongly influenced by a large water body and b) K_{RS} =0.19 for "coastal" locations, situated on or adjacent to the coast of a large land mass and where air masses are influenced by a nearby water body. For general use of Eq.3, a mean global value of K_{RS}=0.17 has been adopted in this study. R_a and R_s divided by λ change units from MJ m^{-2} day^{-1} to mm day^{-1} as it is required in the next equation of ET_o. The formula for estimating the ET_o by H-S method is given by the following equation (Hargreaves and Samani, 1982; 1985):

$$ET_o = 0.0135\left(\mathrm{T}_{mean} + 17.8\right)\frac{R_s}{\lambda} = 0.0135\left(\mathrm{T}_{mean} + 17.8\right)K_{RS} \cdot \frac{R_a}{\lambda} \cdot (TD)^{0.5} \tag{4a}$$

Considering Eq.4a, the K_{RS} and the exponent 0.5 are adjustment factors of radiation formula (Eq.3), while the 0.0135 and 17.8 are adjustment factors of the ET_o formula leading to a total amount of four empirical coefficients. Using the mean global value of K_{RS}=0.17, Eq.4a is simplified according to the following (Allen et al., 1998):

$$ET_o = c_{hs2} \cdot \left(\mathrm{T}_{mean} + 17.8\right) \cdot \frac{R_a}{\lambda} \cdot (TD)^{0.5} = 0.0023\left(\mathrm{T}_{mean} + 17.8\right) \cdot \frac{R_a}{\lambda} \cdot (TD)^{0.5} \tag{4b}$$

where in both Eqs.4a and 4b, the ET_o is the potential evapotranspiration (mm d^{-1}), R_a is the extraterrestrial radiation (MJ m^{-2} d^{-1}), λ is the latent heat of vaporization (MJ kg^{-1}) and T_{mean} is the mean daily temperature (°C). The Eq.4b is applied in this study as a reference crop evapotranspiration method and for this reason is compared with Eq.1 for short reference crop. For the case of T_{mean}<-17.8 °C, the term of (T_{mean}+17.8) was set to zero, which is necessary for a global application (Weiß and Menzel, 2008). In further steps of analysis, the coefficient 0.0135 (Eq.4a) is symbolized as c_{hs1} while the coefficient 0.0023 is symbolized as c_{hs2}, which is equal to $c_{hs2} = c_{hs1} \cdot K_{RS}$.

In order to reduce the errors of the aforementioned methods in the high latitudes and altitudes (polar and alpine environments) where negative temperatures exist, a filter was used in all methods to set mean monthly ET_o=0 when mean monthly T_{max} is ≤0 (conditions of extreme frost).

2.2.4 Steps of analysis

Step 1: Comparative analysis between the standard ET_o formulas of ASCE, P-T and H-S, and error analysis of H-S radiation formula

The first step of the analysis includes the estimation of mean monthly and mean annual ET_o using the ASCE method (Eq.1) for the two reference crops (short and tall), the standard P-T method (Eq.2) with a_{pt}=1.26 and the standard H-S method according to Eq.4b with c_{hs2}=0.0023. The difference between the ET_o methods will be captured using as a base the mean annual and the mean monthly ET_o values of ASCE-short.

In the case of mean annual ET_o, the analysis is based on the % of mean annual difference (*MAD*%) of each method M versus the mean annual ET_o of ASCE-short, which is given by:

$$MAD\%_{(M)} = 100\left[YET_{o(M)} - YET_{os} \right] / \left(YET_{os} \right) \quad (5)$$

where YET_{os} is the mean annual ET_o of ASCE-short method, $YET_{o(M)}$ is the mean annual ET_o of M method (as M is used ASCE-tall either the standard P-T or the standard H-S). The *MAD*% for ASCE-tall was estimated in order to assess the effects of reference crop type at different climatic environments on the annual estimations of ET_o. The *MAD*% of P-T and H-S methods was used to investigate the strength of the two standard methods to approximate the annual ET_o of ASCE-short. Positive values of *MAD*% indicate overestimation of the mean annual ET_o values using the M method in comparison to ASCE-short method while negative values indicate underestimation, respectively. Furthermore, the difference between the absolute *MAD*% values (*DMAD*) of the standard P-T (with a_{pt}=1.26) and H-S (with c_{hs2}=0.0023) methods was estimated in order to assess which of the two methods is more appropriate to be used locally, based on its proximity to ASCE-short method. The *DMAD* is estimated as follows:

$$DMAD = |MAD\%_{(\text{H-S})}| - |MAD\%_{(\text{P-T})}| \quad (6)$$

where positive *DMAD* values indicate better performance of standard P-T while negative values indicate better performance of standard H-S method in a region. Regions that showed *DMAD* values between -1 and +1 were considered transitional zones where both methods showed approximately the same proximity to the annual ASCE-short estimations.

In the case of mean monthly ET_o, the coefficient of determination R^2 and the root mean square difference *RMSD* (equivalent to *RMSE*) (Droogers and Allen, 2002) were used to compare the mean monthly values of ASCE-tall, standard P-T (a_{pt}=1.26) and standard H-S (c_{hs2}=0.0023) methods with the respective values of the ASCE-short method.

The procedures of *MAD*%, R^2 and *RMSD* were also used to analyse the mean annual and mean monthly estimations of R_s by the standard solar radiation formula of H-S (Eq.3 with K_{RS}=0.17) versus the given R_s values of Sheffield et al. (2006).

Step 2: Readjustment of annual P-T and H-S coefficients for both reference crops

For the case of P-T, the readjustment of the mean monthly a_{pt} coefficient was performed directly for each location by solving for a_{pt} after equating Eq.1 with Eq.2 of each month. A filter was used in order to set a_{pt} equal to 0 when Eq.1 or/and

Eq.2 without a_{pt} were equal to 0. In this case, the a_{pt} changes its physical meaning in order to indicate that mean monthly ET_o approximates to 0. Doing the above procedures for both short and tall reference crop, twelve images of mean monthly readjusted a_{pt} coefficients were produced for each reference crop.

For the case of H-S method, the readjustment of the coefficients was performed in two stages. In the first stage, the readjustment was performed in the radiation formula (Eq.3) only for the K_{RS} coefficient while the exponent 0.5 (square root) of the DT remained the same. The mean monthly K_{RS} was estimated using the values of solar radiation R_s given by Sheffield et al. (2006). In the second stage, the readjustment was performed in the evapotranspiration formula (Eq.4b) for the coefficient of c_{hs2} using as a base the ASCE method for both reference crops, while the coefficients of 17.8 and 0.5 remained the same. In this way the readjusted values of c_{hs2} and K_{RS} would also provide readjusted values of the c_{hs1} since $c_{hs1} = c_{hs2}/K_{RS}$. A similar filter to set c_{hs2}=0 as in the case of a_{pt} was used, when Eq.1 or/and Eq.4b without c_{hs2} were equal to 0. Following the above procedures, twelve images of mean monthly readjusted c_{hs2} coefficients for each reference crop (short and tall) and twelve K_{RS} images were produced.

The new mean monthly a_{pt}, c_{hs2} and K_{RS} coefficients were used to build respective mean annual coefficients. The robustness of mean annual coefficients are strongly related to their ability to capture better the values of the dependent variable (i.e. ET_o and R_s), especially in the months that present larger values. For this reason, weighted annual averages of mean monthly a_{pt}, c_{hs2} and K_{RS} coefficients were estimated. Under cold conditions, the monthly coefficients may present unrealistic values that significantly affect the weighted averages. In order to solve this problem, threshold values for the mean monthly dependent variables (i.e. ET_o and R_s) were set before their inclusion in the weighted average estimations. Preliminary analysis for the readjustment of a_{pt} and c_{hs2} coefficients (based on the values of ASCE-short) showed that when the mean monthly ET_o values of ASCE-short, H-S and P-T were below 45 mm month^{-1} (~1.5 mm d^{-1}), then unrealistic mean monthly values of a_{pt} and c_{hs2} coefficients appeared. As unrealistic values were considered those that were at least one order of magnitude larger or smaller from the standard values of a_{pt}=1.26 and c_{hs2}=0.0023. Taking into account the above, the following procedure was performed in order to obtain partial weighted annual averages (after excluding months with $ET_o \leq 45$ mm month^{-1}) of mean monthly a_{pt} and c_{hs2} coefficients for short reference crop based on ASCE-short method:

$$\text{when } ET_{os\ i} > 45 \text{ mm month}^{-1} \quad \text{then} \quad Fr_i\text{=1 else =0} \tag{7a}$$

and

$$\text{when } ET_{oi\ (M)} > 45 \text{ mm month}^{-1} \quad \text{then} \quad Fm_i\text{=1 else =0} \tag{7b}$$

$$ET_{os\ adj.i} = ET_{os\ i} \cdot Fr_i \cdot Fm_i \tag{7c}$$

$$YET_{os\ adj.} = \sum_{i=1}^{12} \left(ET_{os\ adj.i} \right) \tag{7d}$$

$$C = \sum_{i=1}^{12} \left(\frac{ET_{os\,adj.i}}{YET_{os\,adj.}} \cdot C_i \right) \tag{7e}$$

where $ET_{os\,i}$ is the mean monthly value of ET_o (mm month^{-1}) obtained from the ASCE-short method, $ET_{oi\,(M)}$ is the mean monthly value of ET_o (mm month^{-1}) obtained from the M method (M is either P-T or H-S), Fr_i is the filter function of reference method with values 0 or 1, Fm_i is the filter function of M method with values 0 or 1, $ET_{os\,adj.\,i}$ is the adjusted mean monthly value of ET_o from ASCE-short method, which becomes 0 when Fr_i or Fm_i is 0, $YET_{os\,adj.}$ is the sum of the monthly adjusted $ET_{os\,adj.\,i}$ values, C_i is the mean monthly coefficient of M method (i.e. a_{pt} or c_{hs2}) calibrated based on ASCE-short method (results from the previous step of analysis), C is the partial weighted average (p.w.a.) of the mean monthly coefficients of M method (i.e. a_{pt} or c_{hs2}) for short reference crop and i is month.

For estimating the p.w.a. of mean monthly a_{pt} and c_{hs2} for tall reference crop, the same procedure of Eqs.7 was followed using the mean monthly values of ET_o from ASCE-tall to estimate the Fr_i values in Eq.7a, while the adjusted values of ET_o ASCE-tall were also used in Eqs.7c,d,e. For C_i values in Eq.7e, the estimated mean monthly values of a_{pt} or c_{hs2} based on ASCE-tall method were used. Even though the mean monthly values of ASCE-tall are generally higher from ASCE-short, the threshold of 45 mm month^{-1} in Eqs.7a,b remained the same since it was observed that the difference between ASCE-short and ASCE-tall is very small when $ET_{os\,i}$ falls below ~50 mm month^{-1}.

A similar procedure (using the set of Eqs.7) was also followed to obtain the p.w.a. of mean monthly K_{RS} of H-S method for R_s estimations. The Fr_i values in Eq.7a were estimated using as reference the mean monthly R_s values of Sheffield et al. (2006), which were also used after adjustment in Eqs.7c,d,e. The Fm_i values in Eq.7b were estimated using the respective R_s values of the standard H-S with K_{RS}=0.17. For C_i values in Eq.7e, the mean monthly values of K_{RS} calibrated based on R_s values of Sheffield et al. (2006) were used. The threshold used for adjusting R_s values in Eqs.7a,b was set equal to 3.61 MJ m^{-2} d^{-1} (~110 MJ m^{2} month^{-1}), which is equivalent to 45 mm month^{-1} (conversion of mm month^{-1} to MJ m^{-2} month^{-1} was performed after multiplying with λ=2.45 MJ kg^{-1}). The threshold for R_s adjustment was tested before its use and it was found that works satisfactorily excluding unrealistic monthly values of K_{RS}. As unrealistic values were considered those values that were at least one order of magnitude larger or smaller from the standard value of K_{RS}=0.17.

Step 3: Use of stations for the validation of the p.w.a. coefficients of P-T and H-S methods and comparisons with other models of reduced parameters

Stations from two databases (California Irrigation Management System - CIMIS database, http://www.cimis.water.ca.gov, and Australian Government – Bureau of Meteorology AGBM database, http://www.bom.gov.au/), were used in this study in order to validate the p.w.a. coefficients of P-T and H-S methods. The first database includes stations from California-USA and it was selected for the following reasons: a) it has been used as a basis for the development of Hargreaves-Samani method (Hargreaves and Samani, 1985; Hargreaves and Allen, 2002) and CIMIS method (Snyder and Pruitt, 1985, Snyder and Pruitt, 1992) and b) provides a dense and descriptive network of stations for a specific region that combines coastal, plain, mountain and desert environments (Table 1, Fig.1a). The second database includes stations from Australia and it was selected because the stations network covers a large territory with large variety of climate classes (Table 1, Fig.1b) but also because the Priestley-Taylor method has been calibrated for locations of eastern Australia (Priestley and Taylor, 1972). The selection of stations from AGBM database was performed in such way in order to cover all the possible existing Köppen climatic types and elevation ranges of Australian continent (Table 1). In total, 140 stations were used, 60 stations were selected from CIMIS and 80 stations from the AGBM that have at least 15 years of observations (some stations, that do not follow this rule, were selected due to their special climate Köppen class or the high elevation of their location). Observations from years after 2000 up to 2016 were included (when they were available) in the stations data, in order to show that the new revised coefficients are applicable for recent periods.

[FIGURE 1]

[TABLE 1]

In the case of CIMIS stations, the monthly data for all climatic parameters were obtained, including ET_o estimations using the CIMIS method (Snyder and Pruitt, 1985, Snyder and Pruitt, 1992), but they required quality control before their use. Quality control signs are provided by the database for all climatic data, indicating extreme values, while possible errors are flagged but they are not automatically excluded. For this reason, the user should consider the signs in order to prepare a robust dataset. For this study, proper control was performed and very extreme or erroneous monthly values were excluded. Excluded values were less than 1‰ of the total values of all stations and all parameters. The final clean dataset was subjected to a secondary but indirect quality control through the comparison between the estimated mean monthly values of ET_o of ASCE-short method (Eq.1) using the clean climatic data of all USA-CA stations versus the respective mean monthly ET_o values given by CIMIS database (linear regression result between mean monthly values for n obs.=12×60=720: y=0.994x-1.07 with R^2=0.98) (see Fig.S1 in the supplementary material). Data cleaning was not followed in the case of Australia stations, since the AGBM database provides the mean monthly values of the climatic parameters for the total periods of observation and not for individual years. The general statistics of the mean monthly observed values of climatic parameters obtained from the 140 stations of California-USA and Australia are given in Table S1 of the supplementary material. A comparison of T_{max}, T_{min}, R_s, R_n, DE (vapour pressure deficit) and u_2 parameters between the rasters (0.5 degree) and the stations data are provided in Figs.S2a,b,c,d,e,f of the Supplementary material.

The validation procedure was performed using the data of the stations in Table 1 by comparing the mean monthly values of ET_o derived by the P-T (Eq.2) and H-S (Eq.4b,c) methods with the standard a_{pt} and c_{hs2} coefficients and with the re-adjusted ones versus the ASCE method for short reference crop (Eq.1). The same procedure was also performed for the new a_{pt} and c_{hs2} coefficients for the tall reference crop and for the re-adjusted coefficient K_{RS} in the radiation formula of H-S (Eq.3). For the case of ASCE method for short reference crop, additional models of reduced parameters were used from the literature in order to perform comparisons with the standard and re-adjusted P-T and H-S models. The selection of these models was made in such way in order to satisfy the following criteria/characteristics:

- The selected models have been calibrated either using global data or a representative amount of data from California or

Australia. Models that have been tested for California and Australia and showed good performance were also included.

- The selected models showed better performance when tested using the validation datasets of California and Australia stations in comparison to other tested models but also a good performance to other regions based on studies from the literature. It has to be mentioned that an extremely large amount of models were examined taking into account the modified H-S and P-T models obtained from works that have been already mentioned in the introduction and the large lists of models presented in the works of Valipour (2015a,b; 2017) and Valipour et al. (2017). Strict modifications of P-T and H-S models with fixed coefficients calibrated for local conditions were not used because they cannot adapt their coefficients to the large climatic variability of the validation dataset.
- The majority of the selected models require additional parameters in comparison to P-T and H-S models. This criterion was used in order to compare the strength of the re-adjusted P-T and H-S coefficients versus such models.

Based on the aforementioned criteria, the following eight models were selected for comparisons with the standard and re-adjusted H-S and P-T models (Table 2):

- Two modified models of H-S by Droogers and Allen (2002), where the second one uses precipitation as additional parameter. The models were calibrated using global data.
- Three models of reduced parameters given by Valiantzas (2013a,b; 2014), which were calibrated using 535 stations from Europe, Asia, Africa. The first model uses temperature and radiation data, while the other two use temperature, radiation, and humidity data. The models have been tested for California (Valiantzas, 2013c) and Australia conditions (Ahooghalandari et al., 2017).
- Two models of reduced parameters by Ahooghalandari et al. (2016) calibrated/validated using stations from various locations of Australia. The models use temperature and relative humidity data.
- The Copais model of Alexandris et al. (2006) that uses temperature, radiation and humidity data. The model was calibrated/validated using data from Greece, California and Oregon-USA while it has shown a very good response to many other regions of the world including Australia (Ahooghalandari et al., 2017).

[TABLE 2]

The following statistical criteria were used in the validation procedure: coefficient of determination R^2, modified coefficient of determination bR^2 based on y=*b*x (Krause et al., 2005), mean absolute error *MAE*, root mean square error *RMSE*, percent bias *PBIAS%*, Nash-Sutcliffe efficiency *NSE* (Nash and Sutcliffe, 1970), index of agreement *d* (Willmott, 1981) and Kling-Gupta efficiency (Gupta et al., 2009). The criteria were calculated using the package {HydroGOF} in R language (Zambrano-Bigiarini, 2015, see the package manual for formulas).

3. Results

3.1 Comparative analysis between the standard ET_o formulas of ASCE, P-T and H-S and error analysis of H-S radiation formula

The global maps of mean monthly ET_o at 0.5 degree resolution for the period 1950-2000 using a) the methods of ASCE (Eq.1) for both reference crops (ASCE-short and ASCE-tall), b) the standard P-T method (Eq.2) for a_{pt}=1.26 and c) the standard H-S method (Eq.4b) for c_{hs2}=0.0023, were developed. The respective mean annual ET_o maps are given in Fig.2a,b,c,d, respectively. Similarly, the mean annual R_s values provided by Sheffield et al. (2006) and the respective R_s values estimated by the standard H-S radiation formula (Eq.3 with K_{RS}=0.17) are given in Fig.3a,b, respectively.

[FIGURE 2]

[FIGURE 3]

The *MAD*% (Eq.5) maps of ASCE-tall, standard P-T and standard H-S methods versus ASCE-short are given in Fig.4a,b,c, respectively, while in Fig.4d is also given the *MAD*% of the standard solar radiation formula of H-S versus the R_s values given by Sheffield et al. (2006). The percentage globe coverage (excluding Antarctica) for different classes of *MAD*% and the R^2 and *RMSD* based on respective comparisons of the mean monthly values of ET_o and R_s methods are given in Table 3.

[FIGURE 4]

[TABLE 3]

The case of *MAD*% between the ET_o methods of ASCE-tall and ASCE-short (Fig.4a and Table 3) indicates that there is a 25.2% of map coverage in the *MAD*% class of ±10% where the effects of reference crop type are significantly minimized (Table 3). These territories include the regions of tropical rainforests in Latin America, central Africa and Indonesia, regions of large mountain formations-ranges of high elevation and regions of taigas and tundras of North America and Asia (Fig.4a). The low values of vapor pressure deficit is the main characteristic of these regions. On the contrary, the largest differences between the two reference crops appear in arid and semi-arid environments due to the high values of vapor pressure deficit. The high correlation R^2=0.98 (Table 3) between the mean monthly ET_o values of ASCE-tall and ASCE-short suggests that it is feasible to develop reliable regional monthly coefficients or regression models, which can convert the ET_o estimations from short to tall reference crop especially when the ET_o of short reference crop is estimated with a method of reduced parameters (e.g. P-T or H-S) (a paradigm has been presented by Aschonitis et al., 2012).

Even though *MAD%*, R^2 and *RMSD* for the standard P-T and H-S methods (Fig.4b and c, Table 3) indicate a better performance of the second one to approximate the ASCE-short in a global scale, both methods seem to be equally valuable because their proximity to ASCE-short is maximized at relatively different climatic regions. This is indicated by the difference between the absolute *MAD%* values (*DMAD*) (Eq.6) of the P-T and H-S methods (Fig.5a). The interpretation of Fig.5a was performed using as a base the major Climatic Groups (CGs) of the Köppen-Geiger climate map obtained by Peel et al. (2007) (Fig.5b). The spatial extent of the major CGs of the Köppen-Geiger climate classification (without Antarctica) and the percentage prevalence of P-T versus H-S in the CGs based on the *DMAD* values are given in Table 4. According to Table 4 and Figs.5a,b, the H-S method prevails in regions of B group (arid and semi-arid) and E group (polar/alpine/tundras), while the P-T method prevails in the regions of A group (tropical/megathermal), C group (temperate/mesothermal climates) and D group (continental/microthermal). Even though the P-T method seems to be more powerful in more climatic zones, in reality the H-S method prevails in the 49.3% of the regions while P-T in the 46.6% (the remaining proportion of 4.1% mainly corresponds to inner Greenland and very high mountain areas with annual ET_o=0 or to regions where both methods gave equal results). The prevalence of standard H-S method to drier environments and the respective prevalence of standard P-T method in more humid environments can be explained by the fact that the standard coefficient of H-S was calibrated for California conditions (semi-arid/arid environments) (Hargreaves and Samani, 1985) while the standard coefficient of P-T was calibrated taking into account more humid environments (Priestley and Taylor, 1972).

[FIGURE 5]

[TABLE 4]

The spatial variation of *MAD*% for the case of R_s estimations using the standard solar radiation formula of H-S for K_{RS}=0.17 (Eq.3) versus the mean annual R_s values of Sheffield et al. (2006) is given in Fig.4d. It is indicative that 55.3% of the territories are included in the *MAD*% range ±10%, while the 95.2% is included in the range between ±25% (Table 3). Significant deviations of R_s estimations using the standard H-S method appear mostly in the region of Greenland (Fig.4d). The values of R^2 και *RMSD* (Table 3) indicate a good performance of the method in the case of monthly estimations. The overall results indicate that the use of the standard value K_{RS}=0.17 can provide satisfactory indirect estimations of R_s for the most part of the world only by the use of temperature data.

3.2 Partial weighted averages of mean monthly a_{pt}, c_{hs2} and K_{RS}

The p.w.a. of mean monthly a_{pt} and c_{hs2} for short (p.w.a.s.) and tall (p.w.a.t.) reference crop were derived from the application of Eqs.7 and they are given in Figs.6, while the respective p.w.a. of mean monthly K_{RS} values are given in Fig.7. The global means of p.w.a. of a_{pt} and c_{hs2} for short reference crop (presented below each map of Fig.6a,c), and the global mean of p.w.a. of K_{RS} values for R_s (presented below Fig.7) approximate to the standard values of a_{pt}=1.26, c_{hs2}=0.0023 and K_{RS}=0.17, respectively.

[FIGURE 6]

[FIGURE 7]

As regards the spatial variation of a_{pt} for short reference crop (Fig.6a), the higher values were observed in extremely arid and desert environments exceeding the value of 1.8 (due to extremely high vapour pressure deficit), while the extremely cold and extremely humid environments presented values <1.0. Interesting cases are the alpine-tundra and extreme humid tropical environments, which presented similar values between ~0.8-1.0, due to the low values of vapour pressure deficit. Values of a_{pt} below 0.8 were observed in sub-polar areas. The spatial variation of a_{pt} for tall reference crop (Fig.6b) follows similar patterns with a_{pt} of short reference crop but with increased values, which can be described by the following relationship $a_{pt(\text{p.w.a.t.})}=1.73 \cdot a_{pt(\text{p.w.a.s.})} - 0.58$, $R^2=0.996$, $p<0.0001$. This relationship is valid for $a_{pt(\text{p.w.a.s.})}>0.8$ for preserving $a_{pt(\text{p.w.a.t.})} \geq a_{pt(\text{p.w.a.s.})}$.

As regards the spatial variation of c_{hs2} for short reference crop (Fig.6c), the higher values were observed in extremely arid and desert environments exceeding 0.0026 (due to extremely high vapour pressure deficit), while the extremely cold and extremely humid environments presented values <0.0018. Similarities appear again in the case of alpine-tundra and extreme humid tropical environments, which presented values between ~0.0014-0.0018, due to the low values of vapour pressure deficit. Values of c_{hs2} below 0.0014 were observed in sub-polar areas. The spatial variation of c_{hs2} for tall reference crop (Fig.6d) follows similar patterns with c_{hs2} of short reference crop but with increased values, which can be described by the following relationship $c_{hs2(\text{p.w.a.t.})}=1.793 \cdot c_{hs2(\text{p.w.a.s.})} - 0.00114$, $R^2=0.967$, $p<0.0001$. This relationship is valid for $c_{hs2(\text{p.w.a.s.})}>0.0014$ for preserving $c_{hs2(\text{p.w.a.t.})} \geq c_{hs2(\text{p.w.a.s.})}$.

In the case of K_{RS} (Fig.7), extreme deviations from the value of 0.17 were observed in Greenland with values above 0.21 and in south-east China with values below 0.13 (regions of Chongqing, Guizhou, Hunan, Jiangxi, Guangxi). The spatial variation of K_{RS} does not follow a specific pattern in relation to climate zones, while in many cases, it was observed an increasing trend of its values closer to the coastlines (Fig.7). Additional observations about the effect of distance from the coastline Dc on K_{RS} are given in the discussion section.

3.3 Validation of the re-adjusted a_{pt}, c_{hs2} and K_{RS} coefficients

The validation of the re-adjusted a_{pt}, c_{hs2} coefficients for ET_o estimations (for both reference crops) and the K_{RS} coefficient for R_s was performed taking into account the mean monthly values of the climatic parameters of all stations from Table 1. The re-adjusted coefficients for each station obtained from the 0.5 degree resolution maps are given in Table S2 of the Supplementary material while the comparison between ET_o estimations (for both reference crops) between rasters and stations is provided in Figs.S2g,h, respectively. The comparison of different methods is described in the next paragraphs, while the overall results of the statistical criteria for all the examined cases are given in Table 5.

[TABLE 5]

Table 5a and Fig.8 show the ET_o (mm month^{-1}) comparisons between the ASCE-short values versus the values of the P-T and H-S methods with the standard and the re-adjusted (p.w.a.s.) coefficients and versus the values of the additional models given in Table 2. From the results of Fig.8 together with the results of the statistical criteria (Table 5a), the following observations were derived:

- The P-T(p.w.a.s.) and H-S(p.w.a.s.) models (Fig.8b,d) outperformed to all the statistical criteria (Table 5a) in comparison to the respective standard P-T(1.26) and H-S(0.0023) models (Fig.8a,c) reducing the *RMSE* values at 40 and 25%, respectively.

- The comparison of statistical criteria between H-S(0.0023), H-S(p.w.a.s.), DRAL1 and DRAL2, which follow the general formula of H-S method and are based on calibrations with global data, showed the following order of accuracy H-S(p.w.a.s.)>DRAL1> DRAL2>H-S(0.0023).
- The standard P-T(1.26) showed the worst results to all criteria (Table 4a), while the use of P-T(p.w.a.s.) succeeded to improve the predictions giving better results from H-S(0.0023), DRLA2, VAL1 and AKJ2 models.
- The H-S(p.w.a.s.) provided better results from DRAL1, DRAL2, VAL1, AKJ1, AKJ2 where the latter four require data for more climatic parameters.
- The order of accuracy of the models was the following: VAL3>VAL2>Copais>H-S(p.w.a.s.)>AKJ1>P-T(p.w.a.s.)>DRAL1> DRAL2>H-S(0.0023)>AKJ2>VAL1>P-T(1.26) (the order was based on absolute comparisons of the accuracy rankings for each criterion, see Table S3 in Supplementary material). The *RMSE* difference between H-S(p.w.a.s.) and the best VAL3 model was 6.8 mm month^{-1} (or 0.23 mm d^{-1}), while the respective difference between P-T(p.w.a.s.) and VAL3 was 13.5 mm month^{-1} (or 0.45 mm d^{-1}). These differences are satisfactory, especially for the case of H-S(p.w.a.s.), which uses less climatic data from VAL3. Of course, these differences are even smaller when compared to VAL2 and Copais, which also use more climatic parameters. Justifications for the less satisfactory performance of P-T(p.w.a.s.) are given in the Discussion section.

[FIGURE 8]

Table 5b and Fig.9a,b show the ET_o (mm month^{-1}) comparisons between the ASCE-tall values versus the values of P-T and H-S method using the readjusted a_{pt} and c_{hs2} coefficients for tall reference crop (p.w.a.t.), respectively. Since there are not currently other methods of reduced parameters calibrated based on ASCE ET_o for tall reference crop, the comparison is restricted between the two methods. The results of Fig.9a,b together with the results of the statistical criteria (Table 5b) indicate a better performance of the H-S (with c_{hs2}=p.w.a.t.). The higher errors observed in H-S(p.w.a.t.) and P-T(p.w.a.t) in comparison to the respective errors of H-S(p.w.a.s.) and P-T(p.w.a.s) for short reference crop is justified by the fact that ASCE-tall is significantly higher from ASCE-short, especially in the drier environments (ASCE-tall was found ~28% higher from ASCE-short at global scale based on the mean values given in Fig.2a,b, and ~38% higher based on the comparison of the total mean values estimated by the California-USA and Australia stations data).

[FIGURE 9]

Table 5c and Fig.10a,b show the comparisons between the R_s (MJ m^{-2} d^{-1}) of stations data versus the respective values of standard radiation formula of H-S (Eq.3) with K_{RS}= 0.17 and with K_{RS}= p.w.a, respectively. The results of Fig.10a,b together with the results of the statistical criteria (Table 5c) indicate a better performance of the H-S R_s with K_{RS}= p.w.a. even though the performance of the standard H-S R_s is also satisfactory.

[FIGURE 10]

4. Discussion

Uncertainties in the data used for calibrating and validating the revised coefficients of P-T and H-S methods

The re-calibrated coefficients of the H-S and P-T methods were estimated using raster datasets that cover the period 1950-2000 assuming stationary climate conditions, while the validation datasets of California-USA and Australia stations are expanded up to 2016. Recent studies have shown changes/anomalies after 2000 in temperature (Hansen et al., 2010; Sun et al., 2017), solar radiation (Wild et al., 2013), wind speed (McVicar et al., 2012a,b) and atmospheric humidity (Willet et al., 2014) and such changes could affect the validity of the revised coefficients. The comparisons of T_{max}, T_{min}, R_s, R_n, DE (vapour pressure deficit), and u_2 values between the rasters data and the stations data, showed a very good correspondence for the case of T_{max}, T_{min}, R_s, R_n (Fig.S2a,b,c,d) and a relatively good correspondence for the case of DE (Fig.S2e). In the case of u_2, a discrepancy was observed between the rasters and stations data (Fig.S2f). The separate examination of u_2 for the CA-USA and Australia stations (Fig.S3), showed that the total average of mean monthly u_2 values of CA-USA stations was lower from the rasters data of Sheffield et al. (2006) (data extracted from the stations' positions) while the opposite trend was found for u_2 values of Australia stations. This discrepancy between the u_2 values of rasters and stations can be justified by:

- Possible changes in wind speeds after 2000, since the majority of wind speed data in the stations datasets correspond to periods after 2000.
- Uncertainties in the Sheffield et al. (2006) wind data due to the scarce existing wind data for calibrating their model at global scale during the period of 1950-2000 and especially during the years belonging to the first half of the simulation period.
- The effect of the equation $u_2=4.87u_z/\ln(67.8z-5.42)$ (Allen et al., 1998; 2005), which was used to adjust the wind rasters of Sheffield et al. (2006) and the wind data of Australia stations from z=10 to 2 m height. The degree of accuracy of the aforementioned equation to convert wind data at 2 m is unknown. This equation is usually not calibrated for meteorological stations with anemometers positioned above 2 m height, while the uncertainty is even larger when is applied at global scale and for a pixel of 0.5 degree resolution, which may contain high topographic variability.
- The bias that may have been introduced after cleaning extreme wind values in the data of CA-USA stations, which may be associated to hurricane events. The region of California is strongly affected by hurricanes and the higher wind speeds in the rasters of Sheffield et al. (2006) data may partly occurred because they have included such events in their climatic simulations.
- The bias that may have been introduced by the wind data of Australia stations. The AGBM database (Australian Government – Bureau of Meteorology) provides 12 values of mean monthly wind speeds of the total observation periods for 9am and another 12 values for 3pm local time. In order to get the mean monthly wind speeds of the stations, the average value of 9 am and 3 pm conditions was used for each month.

- Combinations of all the aforementioned cases.

Uncertainties may also exist in the case of $DE=e_s-e_a$ (Fig.S2e), since Sheffield et al. (2006) provides data of specific humidity that were directly converted to actual vapour pressure e_a using the equation of Peixoto and Oort (1996), which uses the additional parameter of atmospheric pressure as internal parameter. The atmospheric pressure in the case of rasters was estimated based on elevation data of 1 km resolution (30 arc-sec), which were further converted to 0.5 degree resolution. The use of e_a data from 0.5 degree resolution pixels may also added additional error, especially when there is large topographic variability within the 0.5 degree pixel. On the other hand, the e_a of stations was estimated by relative humidity and temperature data.

Thus, uncertainties exist in both rasters and stations data. In future studies, further improvements in the revised coefficients can be made by using global raster data, which incorporate the conditions after 2000, and by solving many of the aforementioned problems related to both stations data and raster data produced by climatic models.

Reasons for using annual p.w.a. coefficients instead of monthly or seasonal ones in the case of H-S and P-T methods

The analysis presented in this study passed through various stages before the selection of the annual p.w.a. form of the coefficients (Eqs.7). Some steps in the preliminary analysis were to analyse: (a) the different forms of averages (e.g. mean, mode, median, geometric mean, harmonic mean etc) for deriving annual coefficients, and (b) the strength of the derived mean monthly and seasonal coefficients versus the annual p.w.a. coefficients and versus the coefficients of the standard methods,.

As regards the use of weighted annual average (w.a.) of the mean monthly coefficients instead of other forms of averages (e.g. mean, mode, median, geometric mean - g.m., harmonic mean – h.m.), preliminary analysis was performed using data extracted by the climatic rasters from many positions of the world. During this analysis, trials to derive annual coefficients were made using an optimization algorithm separately for each position. The results showed that the optimized annual values were always closer to the monthly coefficients of the warmer months since the optimization algorithms try to reduce the total error, which is mainly dominated by the months that show larger ET_o values (or R_s for the case of K_{RS} calibration). The optimized values were also compared to the different types of annual averages (e.g. mean, mode, median, g.m., h.m., w.m.), which were estimated after excluding values of monthly coefficients associated to months with ET_o and R_s values <45 mm month^{-1} (for R_s the equivalent is 3.61 MJ m^{-2} d^{-1}) The w.a. outperformed in all cases because it is the only form that considers the amplitude of the parameter under investigation (ET_o and R_s) (Eq.7), giving more weight to the monthly coefficients that are related to the warmer months. This attribute of w.a. is extremely significant since it is the only type that considers the seasonal observed differences in monthly ET_o (for a_{pt} and c_{hs2}) and R_s (for K_{RS}) minimizing the possible errors during warmer months.

The case of mean monthly coefficients was also examined (results not shown). The results showed that the assessment of annual ET_o and seasonal ET_o during the warm season using the mean monthly coefficients outperforms in comparison to the standard methods, but their predictive strength was not as good as p.w.a. coefficients especially during cold season. Similar findings were observed when different time intervals for calculating seasonal averages of the coefficients were used (e.g. 3-months averages or 6-months averages). The basic observed problem with monthly/seasonal coefficients associated to the global scale application of this study was that many parts of the world presented unreasonably high or low monthly/seasonal values of the coefficients (at least one order of magnitude larger or smaller from the standard values) during cold seasons. This problem occurred because P-T and H-S evapotranspiration models do not include the effect of humidity and wind, which becomes greater when temperature is low (in very low temperatures even the ASCE results can be questioned). Such values may lead to significant errors in monthly/seasonal ET_o estimations during cold periods when there are deviations of climatic conditions (seasonal shifts/disturbances or climate changes in general) from those used for calibrating the coefficients. These were the reasons for using the threshold of 45 mm month^{-1} to exclude such values from p.w.a. of the coefficients. Thus, the pw.a. annual values were chosen as the best solution for a global application because they counterbalance the errors that could be introduced by intra-annual/intra-seasonal climatic variability or other errors such as those described in the previous section of the Discussion (errors associated to the data).

It is also important to note that the derivation of annual coefficients is a pure optimization problem when stations data are used. For example, Cristea et al. (2013) derived coefficients of the P-T method for 106 stations that represent a range of climates across the contiguous USA. The coefficients were estimated for each station by minimizing the sum of the squared residuals between the benchmark FAO-56 and P-T using data only for the period April-September. The obtained optimized values of the coefficients were interpolated in order to make a map of the a_{pt} coefficient. In this study, the maps of the coefficients were produced based on raster data and not stations data, which means that optimization should be performed pixel by pixel (~62000 pixels globally for the 0.5 degree resolution excluding Antarctica). This procedure would require special programming since readily available tool to perform this procedure does not exist in commercial or free GIS software packages. This is the main reason for using as an alternative method the Eqs.7 in GIS environment, since it can be calculated easily in raster calculators incorporated in the GIS packages. A solution could be the development of a tool for GIS purposes using rasters data that could be able to run using 24 rasters; 12 for the benchmark ET_o and another 12 for the P-T or H-S ET_o formula without the 1.26 and 0.0023 factors, respectively, in order to provide optimized annual values of their coefficients (for a global application filters to remove unreasonable values are also required).

Observations derived by the application of H-S radiation formula

Special attention was also given in the case of K_{RS} coefficient for estimating R_s. Although there were indications that the spatial variation of p.w.a. a_{pt} and c_{hs2} coefficients at global scale may be linked to general climatic characteristics (Fig.5), the respective variation of p.w.a. K_{RS} coefficient could not clearly be linked with a specific climatic or topographic characteristic. The only observed dependence, which showed some relevance to the spatial variation of K_{RS}, was a relatively negative correlation with the distance from the coastline *Dc*. This observed dependence can be only used as a general observation and not as a basis for applying in general the empirical rule of Allen et al. (1998) (K_{RS}=0.16 for “interior” and K_{RS} =0.19 for “coastal” locations). The large uncertaintiy in the aforementioned rule was also indicated by Samani (2000) and it is verified by the analysis presented in Fig.S4a of the supplementary material. Fig.S4a shows a relatively negative correlation between K_{RS} and Dc (for Dc<500 km) but also shows an extremely high variability of K_{RS} close to the coastlines where K_{RS} values are not necessarily higher in comparison to the values observed in the interior regions. The observed lower variability of K_{RS} at interior regions is probably related to the fact that coastlines are more affected by oceanic-climatic phenomena, which anyway present high spatial variability at global scale. The raster data of K_{RS} (Fig.7) can be used as indicator to control the validity of the rule but also to control the validity of the given values 0.16-0.19 for a specific region. Samani (2000) also observed that the monthly K_{RS} values may be influenced by the difference between monthly maximum and minimum temperature TD. This effect was also investigated through correlation between the mean monthly K_{RS} coefficients and the mean monthly TD values of the stations data (Fig.S4b, in supplementary material). The results showed that the hypothesis related to the effect of TD on K_{RS} may be stronger locally in comparison to the effect of Dc, but again the variation of K_{RS} is extremely large in the TD range between 8-15 $^{\circ}$C (Fig.S4b), not allowing secure conclusions for a global scale application. The result of Fig.S4b is based only on the stations of Table 1, and for this reason the variation in a global scale is expected much larger.

Recommendations for reducing the uncertainties when the re-adjusted coefficients of P-T and H-S models are used

The uncertainties, which may be introduced by climate disturbances/changes or other uncertainties related to the data used for calibrating the coefficients, can be reduced taking into account some of the following observations and recommendations.

A separate analysis using only the stations of California showed that a regional mean value of the coefficients derived by p.w.a. values may present even better performance because it probably counterbalances other uncertainties associated to the spatial climatic variability within a specific region. A factor for such uncertainties may be rainfall, which may not show significant seasonal deviations or deviations from the expected annual values for a large region but may show different spatial patterns every year within the region affecting the accuracy of the coefficients. The aforementioned observation was verified by the application of H-S method for ET_o of short reference crop for the stations of California when the average value of c_{hs2}=0.0024 obtained from the respective p.w.a.s values of the stations (Table S.2) was used (this value also approximates the standard value of 0.0023). The average value of sixty p.w.a.s. coefficients of the CA-USA stations gave better results from the individual coefficients (Fig.S5 and Table S4, in supplementary material). The aforementioned observations suggest that a robust territorial segmentation based on general topographic characteristics (e.g. elevation, slope, latitude and longitude, distance from the coastline etc) and general climatic characteristics (e.g. Köppen class, general precipitation and temperature patterns) can provide a proper zonation of large territories for deriving very robust mean values of a_{pt}, c_{hs2} and K_{RS} coefficients using the respective p.w.a. values of each zone. Robust zonations based on grids of mean monthly precipitation and temperature using the data of Hijmans et al. (2005), or the mean monthly ET_o rasters provided by this study can easily be performed using cluster analysis in GIS environment (Demertzi et al., 2014; Aschonitis et al., 2016a,b).

The comparison between P-T and H-S evapotranspiration methods with re-adjusted coefficients but also their comparison with the other models of Table 2 also provided significant information. From the comparison between P-T and H-S with re-adjusted coefficients, it was observed that H-S provided better results in both short and tall reference crop. The prevalence of H-S can be attributed to the fact that more than ~80% of stations from Table 1 are located in territories with negative *DMAD* values (Fig.5a) giving a general advantage to H-S method for more robust estimations. This observation can justify the better performance of the standard H-S (with c_{hs2}=0.0023) in comparison to the standard P-T (with a_{pt}=1.26) for short reference crop (Table 5a) and indirectly validates the *DMAD* map. Considering these observations, it is recommended to take into account both the *MAD* (Fig.4,b,c) and *DMAD* (Fig.5a) maps before selecting one of the two methods either using the standard or the p.w.a. coefficients. From the comparisons with the other models of Table 2, it was observed that three models, which use temperature, radiation and humidity data (i.e. VAL3, VAL2, Copais, and especially VAL3), provided better estimations. These models have shown very good performance using data from other case studies (Pan et al., 2011; Shiri et al., 2014; Kisi, 2014; Gao et al., 2015; Valipour, 2015a,2015c; Djaman et al., 2015, 2016, 2017; Ahooghalandari et al., 2017), and their use is recommended instead of the P-T and H-S with re-adjusted coefficients, when the only missing climatic parameter is wind speed.

A very interesting observation was also made about the tall reference crop based on the results of *MAD%* map (Fig.4a). In the *MAD*% class of ±10% of Fig.4a were observed some small negative values, which correspond to the ~2% of map coverage. These values indicate slightly larger annual values of ASCE-short in comparison to ASCE-tall. This result was observed in regions of extremely small vapour pressure deficit (areas of very high elevation, either of very cold, or extremely humid conditions scattered around the world) and it is a peculiarity of Eq.1 and probably an artefact. This result occurred because the second term of the nominator in Eq.1 (which includes the vapour pressure deficit term and the C_n coefficient) approximates to 0 when e_s-e_a becomes extremely small, while the denominator of Eq.1 is always larger in ASCE-tall in comparison to ASCE-short due to the difference in C_d value (0.34 for short and 0.38 for tall reference crop). A recommendation for partly solving this problem for tall reference crop applications is to use the revised coefficients of P-T and H-S methods derived for short reference crop in the places were the annual value of ASCE-tall is lower from ASCE-short. This recommendation is based on the fact that annual ASCE-tall is expected to be always larger from the respective value of ASCE-short. This peculiarity was not corrected in the ASCE-tall maps and the respective a_{pt} and c_{hs2} coefficients for tall reference crop in order to show the absolute estimations of the ASCE-tall and the respective coefficients. Taking into account the *MAD* map (Fig.4a), the users can found the location of these pixels.

5. Data availability

The produced datasets of this study have been archived in PANGAEA database (https://doi.pangaea.de/10.1594/PANGAEA.868808) and in ESRN-database, which is currently supported by the University of Ferrara (Italy), Aristotle university of Thessaloniki (Greece) and University of Campania "Luigi Vanvitelli" (Italy) (http://www.esrn-database.org/gis-data.html or http://esrn-database.weebly.com/gis-data.html). Apart from the 0.5 degree resolution raster datasets, the database contains the same datasets at finer resolution (30 arc-sec, 2.5 arc-min, 5 arc-min and 10 arc-min). These finer datasets are provided in order to cover the observed resolution range in the initial climatic data (e.g. the temperature data of Hijmans et al. (2005) are provided at 30 arc-sec resolution). The finer resolutions were produced using bilinear interpolation on solar radiation, humidity and wind speed data of Sheffield et al. (2006). This interpolation method is not the most appropriate for such purposes. The data of finer resolutions can only be used as a tool to assess uncertainties associated to temperature variation effects within a 0.5 degree pixel or to estimate average values of the coefficients for larger territories in order to capture a better representation of the coastlines or islands that do not exist in 0.5 degree resolution (use of values from individual pixels is not recommended). A complete list of the datasets is provided in the Table S5.

6. Conclusions

The study provided global grids of revised annual coefficients for the Priestley-Taylor (P-T) and Hargreaves-Samani (H-S) methods for estimating ET_o for both short and tall reference crop. The coefficients were calibrated using respective grids of ET_o estimated with the ASCE-standardized method. Respective grids of annual coefficients were also derived for the radiation formula of H-S. The calibration procedures were based on global gridded climatic data of the period 1950-2000. The method for deriving annual coefficients of P-T and H-S methods was based on partial weighted averages (p.w.a.) of the respective mean monthly coefficients. This method estimates the annual values considering the amplitude of the parameter under investigation (ET_o and R_s) giving more weight to the monthly coefficients of the months with higher ET_o values (or R_s values for the case of H-S radiation formula). The method also eliminates the effect of unreasonable monthly coefficients that may occur during periods when ET_o and R_s fall below a specific threshold. The new coefficients were validated based on data from 140 stations located at various climatic zones of USA and Australia with expanded observations up to 2016. Additional tests were also performed for the case of short reference crop evapotranspiration using additional models with low requirements for climatic data. The validation procedure for ET_o estimations of short reference crop showed that the P-T and H-S methods with revised coefficients outperformed the standard methods reducing the estimated *RMSE* in ET_o values by 40% and 25%, respectively. The estimations of R_s using the H-S formula with revised coefficients reduced the *RMSE* by 28% in comparison to the standard formula. The comparisons with other models of short reference crop, showed that the P-T and H-S methods with revised coefficients can compete models of additional climatic parameters. In the case where only wind speed is missing from available data, the use of VAL2, VAL3 and Copais methods (temperature, radiation and humidity data requirements) is recommended. Finally, a raster database of 0.5 degree resolution was built consisting of: (a) global maps for the mean monthly ET_o values estimated by ASCE-standardized method for both reference crops, (b) global maps for the revised annual coefficients of the P-T and H-S evapotranspiration methods for both reference crops and a global map for the revised annual coefficients of the H-S radiation formula, (c) global maps that indicate the optimum locations for using the standard P-T and H-S methods and their possible annual errors based on reference values (*MAD%* and *DMAD* maps). The online free availability of the database can support estimations of ET_o and solar radiation for locations where climatic data are limited while it can support studies, which require such estimations at larger scales (e.g. country, continent, world).

The methods used in this study, their respective results and the observed uncertainties can be used as a base for future works focusing on: (a) the validation of the coefficients for other parts of the world, especially using climatic data obtained after 2000, and the comparison with other models of low data requirements (b) the recalibration of the coefficients using data from climatic models that include observations from more recent years and analysis of climate change effects on the coefficients, (c) the use of the available climatic datasets obtained from climatic models in order to calibrate models of the coefficients for various locations and not fixed values such as the ones given in this study, (d) analysis of alternative methods for deriving annual coefficients that approximate optimized values or incorporation of optimization algorithms in GIS environment for capturing the optimum solution per pixel, (e) the confrontation of uncertainties related to the data used for calibration and validation (e.g. low representativity of interpolated climatic parameters due to the lack of data in many parts of the world, errors associated to commonly used equations; such as the one used for adjusting wind data at 2 m height; uncertainties associated to the observed data etc).

Supplementary material. Supplementary information related to the article is given in the following supplementary file (to be added by the journal).

Acknowledgements. This study was performed in the context of two Post-Doctoral research studies by Dr.Vassilis Aschonitis financed by Ferrara University (Italy) and Aristotle University of Thessaloniki (Greece).

References

Abtew, W.: Evapotranspiration measurements and methoding for three wetland systems in South Florida. J. Am. Water Resour. Assoc. 32, 465-473, 1996.

Ahooghalandari, M., Khiadani, M., and Jahromi, M. E.: Developing Equations for Estimating Reference Evapotranspiration in Australia. Water Resour. Manage., 30, 3815-3828, 2016.

Ahooghalandari, M., Khiadani, M., and Jahromi, M. E.: Calibration of Valiantzas' reference evapotranspiration equations for the Pilbara region, Western Australia. Theor.Appl. Climatol., 128, 845-856, 2017.

Allen, R. G., Pereira, L. S., Raes, D., and Smith, M.: Crop Evapotranspiration: Guidelines for computing crop water requirements. Irrigation and Drainage Paper 56, Food and Agriculture Organization of the United Nations, Rome, 1998.

Allen, R. G., Walter, I. A., Elliott, R., Howell, T., Itenfisu, D., and Jensen M.: The ASCE standardized reference evapotranspiration equation. Final Report (ASCE-EWRI). Pr. In: Allen RG, Walter IA, Elliott R, Howell T, Itenfisu D, Jensen M (Eds.) Environmental and Water Resources Institute, 2005. Task Committee on Standardization of Reference

Evapotranspiration of the Environmental and Water Resources Institute, 2005.

Alexandris, S., Kerkides, P., and Liakatas, A.: Daily reference evapotranspiration estimates by the ‘‘Copais’’ approach. Agr. Water Manage., 82, 371-386, 2006.

Aschonitis, V. G., Antonopoulos, V. Z., and Papamichail, D. M.: Evaluation of pan coefficient equations in a semi-arid Mediterranean environment using the ASCE standardized Penman-Monteith method. Agr. Sci., 3, 58-65, 2012.

Aschonitis, V., Demertzi, K., Papamichail, D., Colombani, N., and Mastrocicco, M.: Revisiting the Priestley-Taylor method for the assessment of reference crop evapotranspiration in Italy. Ital. J. Agrometeorol., 20, 5-18, 2015.

Aschonitis, V., Miliaresis, G., Demertzi, K., and Papamichail, D.: Terrain segmentation of Greece using the spatial and seasonal variation of reference crop evapotranspiration. Adv. Meteorol., art. no. 3092671, 2016a.

Aschonitis, V. G., Awe, G.O., Abegunrin, T. P., Demertzi, K. A., Papamichail, D. M., and Castaldelli, G.: Geographic segmentation, spatial dependencies, and evaluation of the relative position of rain-gauges based on gridded data of mean monthly precipitation: application in Nigeria. Hydrol. Res., nh2016095, 2016b, (in press) DOI: 10.2166/nh.2016.095

Azhar, A. H., and Perera, B. J. C.: Evaluation of reference evapotranspiration estimation methods under Southeast Australian conditions. J. Irrig. Drain Eng., 137, 268-279, 2011.

Bachour, R., Walker, W. R., Torres-Rua, A. F., and McKee, M.: Assessment of reference evapotranspiration by the hargreaves method in the Bekaa Valley, Lebanon. J. Irrig. Drain. Eng. ASCE, 139 (11), 933-938, 2013.

Berti, A., Tardivo, G., Chiaudani, A., Rech, F., and Borin, M.: Assessing reference evapotranspiration by the Hargreaves method in north-eastern Italy. Agr. Water Manage., 140, 20-25, 2014.

Brinckmann, S., Krähenmann, S., and Bissolli, P.: High-resolution daily gridded data sets of air temperature and wind speed for Europe, Earth Syst. Sci. Data, 8, 491-516, 2016.

Castellvi, F., Stockle, C. O., Perez, P. J., and Ibanez, M.: Comparison of methods for applying the Priestley-Taylor equation at a regional scale. Hydrol. Process., 15, 1609-1620, 2001.

Cristea, N. C., Kampf, S. K., and Burges, S. J.: Revised coefficients for Priestley-Taylor and Makkink-Hansen equations for estimating daily reference evapotranspiration. J. Hydrol. Eng., 18, 1289-1300, 2013.

Demertzi, K., Papamichail, D., Aschonitis, V., and Miliaresis, G.: Spatial and seasonal patterns of precipitation in Greece: The terrain segmentation approach. Global Nest J., 16, 988-997, 2014.

Djaman, K., Balde, A. B., Sow, A., Muller, B., Irmak, S., N'Diaye, M. K., Manneh, B., Moukoumbi, Y. D., Futakuchi, K., Saito, K.: Evaluation of sixteen reference evapotranspiration methods under sahelian conditions in the Senegal River Valley. J. Hydrol. Reg. Stud., 3, 139-159, 2015.

Djaman, K., Irmak, S., Kabenge, I., and Futakuchi, K.: Evaluation of FAO-56 penman-monteith model with limited data and the valiantzas models for estimating grass-reference evapotranspiration in Sahelian conditions. Journal of Irrigation and Drainage Engineering, 142 (11), art. no. 04016044, 2016.

Djaman, K., Irmak, S., and Futakuchi, K.: Daily reference evapotranspiration estimation under limited data in eastern Africa. J. Irrig. Drain Eng., 143 (4), art. no. 06016015, 2017.

Droogers, P., and Allen, R. G.: Estimating reference evapotranspiration under inaccurate data conditions. Irrig. Drain. Syst., 16, 33-45, 2002.

Eichinger, W. E., Parlange, M. B., and Strickler, H.: On the concept of equilibrium evaporation and the value of the Priestley-Taylor coefficient. Water Resour. Res., 32, 161-164, 1996.

Flint, A. L, and Childs, S. W.: Use of the Priestley-Taylor evaporation equation for soil water limited conditions in a small forest clearcut. Agric. Forest Meteorol., 56, 247-260, 1991.

Gao, X., Peng, S., Xu, J., Yang, S., and Wang, W.: Proper methods and its calibration for estimating reference evapotranspiration using limited climatic data in Southwestern China. Arch. Agron. Soil Sci., 61, 415-426, 2015.

Giles, D. G., Black, T. A., and Spittlehouse, D. L.: Determination of growing season soil water deficits on a forested slope using water balance analysis. Can. J. For. Res. 15, 107-114, 1984.

Gupta, H. V., Kling, H., Yilmaz, K. K., and Martinez, G. F.: Decomposition of the mean squared error and NSE performance criteria: Implications for improving hydrological modelling. J. Hydrol., 377, 80-91, 2009.

Hansen, J., Ruedy, R., Sato, M., and Lo K.: Global surface temperature change, Rev. Geophys., 48, RG4004, 2010.

Hargreaves, G. H., and Samani, Z. A.: Estimating potential evapotranspiration. J. Irrig. Drain Eng. ASCE, 108, 223-230, 1982.

Hargreaves, G. H., and Samani, Z. A.: Reference crop evapotranspiration from ambient air temperature. *American Society of Agricultural Engineers*, 12 pp, 1985. http://libcatalog.cimmyt.org/download/reprints/97977.pdf

Hargreaves, G. H., and Allen, R. G.: History and evaluation of hargreaves evapotranspiration equation. J. Irrig. Drain Eng. ASCE, 129, 53-63, 2002.

Heydari, M. M., and Heydari, M.: Calibration of Hargreaves-Samani equation for estimating reference evapotranspiration in semiarid and arid regions. Arch. Agron. Soil Sci., 60, 695-713, 2014.

Hijmans, R. J., Cameron, S. E., Parra, J. L., Jones, P. G., and Jarvis, A.: Very high resolution interpolated climate surfaces for global land areas. Int. J. Climatol., 25, 1965-1978, 2005.

Itenfisu, D., Elliott, R.L., Allen, R. G., and Walter, I. A.: Comparison of reference evapotranspiration calculations as part of the ASCE standardization effort. J. Irrig. Drain Eng. ASCE, 129, 440-448, 2003.

Kellner, E.: Surface energy fluxes and control of evapotranspiration from a Swedish Sphagnum mire. Agr. Forest Meteorol., 110, 101-123, 2001.

Kisi, O.: Comparison of different empirical methods for estimating daily reference evapotranspiration in mediterranean climate. J. Irrig. Drain Eng., 140, art. no. 04013002, 2014.

Krause, P., Boyle, D. P., and Bäse, F.: Comparison of different efficiency criteria for hydrological model assessment. Adv. Geosci., 5, 89-97, 2005.

Lhomme, J. -P.: A theoretical basis for the Priestley-Taylor coefficient. Bound.-Lay. Meteorol., 82, 179-191, 1997.

Long, H., Shuai, X., Lei, Q., and Zhang, R.: Spatiotemporal distribution of calibration coefficients of hargreaves equation for estimating potential evapotranspiration in Mainland China. J. Irrig. Drain Eng. ASCE, 139, 293-299, 2013.

Maidment, D. R.: Handbook of hydrology. McGraw-Hill, New York, 1992.

McMahon, T. A., Peel, M. C., Lowe, L., Srikanthan, R., and McVicar, T. R.: Estimating actual, potential, reference crop and pan evaporation using standard meteorological data: a pragmatic synthesis. Hydrol. Earth Syst. Sci., 17, 1331-1363, 2013.

McVicar, T. R., Roderick, M. L., Donohue, R. J., and Van Niel, T. G.: Less bluster ahead? ecohydrological implications of global trends of terrestrial near-surface wind speeds. Ecohydrology, 5, 381-388, 2012a.

McVicar, T. R., Roderick, M. L., Donohue, R. J., Li, L. T., Van Niel, T. G., Thomas, A., Grieser, J., Jhajharia, D., Himri, Y., Mahowald, N. M., Mescherskaya, A. V., Kruger, A. C., Rehman, S., and Dinpashoh, Y.: Global review and synthesis of trends in observed terrestrial near-surface wind speeds: implications for evaporation. J. Hydrol., 416-417, 182-205, 2012b.

Mendicino, G., and Senatore, A.: Regionalization of the hargreaves coefficient for the assessment of distributed reference evapotranspiration in Southern Italy. J. Irrig. Drain. Eng. ASCE, 139, 349-362, 2013.

Mintz, Y., and Walker, G. K.: Global fields of soil moisture and land surface evapotranspiration derived from observed precipitation and surface air temperature. J. Appl. Meteor., 32, 1305-1334, 1993.

Moges, S. A., Katambara. Z., and Bashar, K.: Decision support system for estimation of potential evapotranspiration in Pangani Basin. Phys. Chem. Earth 28, 927-934, 2003.

Mohawesh, O. E., and Talozi, S. A.: Comparison of Hargreaves and FAO56 equations for estimating monthly evapotranspiration for semi-arid and arid environments. Arch. Agron. Soil Sci., 58, 321-334, 2012.

Nash, J. E., and Sutcliffe, J. V.: River flow forecasting through conceptual models, Part I - A discussion of principles. J Hydrol., 10, 282-290, 1970.

Ngongondo, C., Xu, C. -Y., Tallaksen, L. M., and Alemaw, B.: Evaluation of the FAO Penman-montheith, Priestley-Taylor and Hargreaves models for estimating reference evapotranspiration in southern Malawi. Hydrol. Res., 44, 706-722, 2013.

Osborn, T. J. and Jones, P. D.: The CRUTEM4 land-surface air temperature data set: construction, previous versions and dissemination via Google Earth, Earth Syst. Sci. Data, 6, 61-68, 2014.

Pan, Y., Gong, H.-L., Li, X.-J., Zhu, L., and Zhang, J.: Application of Valiantzas approach to estimating reference evapotranspiration in China. Shuikexue Jinzhan/Adv.Water Sci., 22 (1), 30-37, 2011.

Peel, M. C., Finlayson, B. L., and McMahon, T. A.: Updated world map of the Köppen-Geiger climate classification. Hydrol. Earth Syst. Sci., 11, 1633-1644, 2007.

Peixoto, J. P., and Oort, A. H.: The climatology of relative humidity in the atmosphere. J. Climate, 9, 3443-3463, 1996.

Pereira, A. R.: The Priestley–Taylor parameter and the decoupling factor for estimating reference evapotranspiration. Agr. Forest Meteorol., 125, 305-313, 2004.

Peterson, T. C., and Vose, R. S.: An overview of the global historical climatology network temperature database. B. Am. Meteorol. Soc., 78, 2837-2849, 1997.

Priestley, C. H. B., and Taylor, R. J.: On the assessment of surface heat flux and evaporation using large-scale parameters.

Mon. Weather Rev., 100, 81-92, 1972.

Rahimikhoob, A., Behbahani, M. R., and Fakheri, J.: An evaluation of four reference evapotranspiration models in a subtropical climate. Water Resour. Manage., 26, 2867-2881, 2012.

Ravazzani, G., Corbari, C., Morella, S., Gianol, P., and Mancini, M.: Modified Hargreaves-Samani equation for the assessment of reference evapotranspiration in alpine river basins. J. Irrig. Drain. Eng. ASCE, 138, 592-599, 2012.

Samani, Z.: Estimating solar radiation and evapotranspiration using minimum climatological data. J. Irrig. Drain. Eng. ASCE, 126, 265-267, 2000.

Sheffield, J., Goteti, G., and Wood, E. F.: Development of a 50-yr high-resolution global dataset of meteorological forcings for land surface modeling. J. Climate, 19, 3088-3111, 2006.

Shiri, J., Nazemi, A.H., Sadraddini, A.A., Landeras, G., Kisi, O., Fakheri Fard, A., and Marti, P.: Comparison of heuristic and empirical approaches for estimating reference evapotranspiration from limited inputs in Iran. Comput. Electron. Agr., 108, 230-241, 2014.

Shuttleworth, W. J., and Calder, I. R.: Has the Priestley-Taylor equation any relevance to forest evaporation? J. Appl. Meteorol., 18, 639-646., 1979.

Singh, R. K., and Irmak, A.: Treatment of anchor pixels in the METRIC model for improved estimation of sensible and latent heat fluxes. Hydrol. Sci. J. 56, 895-906, 2011.

Snyder, R. L., and Pruitt. W. O.: Estimating reference evapotranspiration with hourly data. VII-1-VII-3. R. Snyder, D. W. Henderson, W. O., Pruitt, and A. Dong (eds), *Calif. Irrig. Mgmt. Systems*, Final Rep., Univ. Calif., Davis, 1985.

Snyder, R. L., and Pruitt. W. O.: Evapotranspiration data management in California. Presented at the Amer. Soc. of Civil Engr. Water Forum '92', Aug. 2-6, 1992, Baltimore, MD, 1992.

Sumner, D. M., and Jacobs, J. M.: Utility of Penman–Monteith, Priestley–Taylor, reference evapotranspiration, and pan evaporation methods to estimate pasture evapotranspiration. J. Hydrol., 308, 81-104, 2005.

Sun, X., Ren, G., Xu, W., Li, Q., and Ren, Y.: Global land-surface air temperature change based on the new CMA GLSAT data set. Sci. Bull., 62, 236-238, 2017.

Tabari, H.: Evaluation of reference crop evapotranspiration equations in various climates. Water Resour. Manage., 24, 2311-2337, 2010.

Tabari, H., and Talaee, P. H.: Local calibration of the Hargreaves and Priestley–Taylor equations for estimating reference evapotranspiration in arid and cold climates of Iran based on the Penman–Monteith model. J. Hydrol. Eng., 16, 837-845, 2011.

Tateishi, R., and Ahn, C. H.: Mapping evapotranspiration and water balance for global land surfaces. ISPRS J. Photogramm., 51, 209-215, 1996.

Thornthwaite, C. W.: An approach toward a rational classification of climate.. Geogr. Rev., 38, 55-94, 1948.

Trajkovic, S.: Hargreaves versus Penman–Monteith under humid condition. J. Irrig. Drain. Eng., 133, 38-42, 2007.

Valiantzas, J. D.: Simple ETo forms of Penman's equation without wind and/or humidity data. I: Theoretical development. J. Irrig. Drain Eng., 139, 1-8, 2013a.

Valiantzas, J. D.: Simplified reference evapotranspiration formula using an empirical impact factor for penman's aerodynamic term. J.Hydrol.Eng., 18, 108-114, 2013b.

Valiantzas, J. D.: Simple ETo forms of Penman's equation without wind and/or humidity data. II: Comparisons with reduced set-FAO and other methodologies. J. Irrig. Drain. Eng., 139, 9-19, 2013c.

Valiantzas, J. D.: Closure to "Simple ETo forms of Penman's equation without wind and/or humidity data. I: Theoretical development" by John D. Valiantzas. J. Irrig. Drain Eng., 140, art. no. 07014017, 2014.

Valipour, M.: Ability of Box-Jenkins models to estimate of reference potential evapotranspiration (A Case Study: Mehrabad synoptic station, Tehran, Iran). IOSR J. Agr. Vet. Sci., 1, 1-11, 2012.

Valipour, M.: Application of new mass transfer formulae for computation of evapotranspiration. J. Appl. Water Eng. Res., 2, 33-46, 2014.

Valipour, M.: Investigation of Valiantzas' evapotranspiration equation in Iran.Theor. Appl. Clim., 121, 267-278, 2015a.

Valipour, M.: Evaluation of radiation methods to study potential evapotranspiration of 31 provinces. Meteorol. Atmos. Phys., 127, 289-303, 2015b.

Valipour, M.: Importance of solar radiation, temperature, relative humidity, and wind speed for calculation of reference evapotranspiration. Arch. Agron. Soil Sci., 61, 239-255, 2015c.

Valipour, M.: Analysis of potential evapotranspiration using limited weather data. Appl. Water Sci., 7, 187-197, 2017.

Valipour, M., Gholami Sefidkouhi, M. A.: Temporal analysis of reference evapotranspiration to detect variation factors. Int. J. Global Warm., (in press), 2017 doi: 10.1504/IJGW.2018.10002058

Valipour, M., Gholami Sefidkouhi, M. A., and Raeini−Sarjaz, M.: Selecting the best model to estimate potential evapotranspiration with respect to climate change and magnitudes of extreme events. Agr. Water Manage., 180, 50-60, 2017.

Wang, K., and Dickinson, R. E.: A review of global terrestrial evapotranspiration: Observation, modeling, climatology, and climatic variability. Rev. Geophys., 50, RG2005, 2012.

Weiß, M., and Menzel, L.: A global comparison of four potential evapotranspiration equations and their relevance to stream flow modelling in semi-arid environments. Adv. Geosci., 18, 15-23, 2008.

Wild, M., Folini, D., Schär, C., Loeb, N., Dutton, E.G., and König-Langlo, G.: The global energy balance from a surface perspective, Clim. Dyn., 40, 3107-3134, 2013.

Willett, K. M., Dunn, R. J. H., Thorne, P. W., Bell, S., De Podesta, M., Parker, D. E., Jones, P. D., and Williams, C. N.: HadISDH land surface multi-variable humidity and temperature record for climate monitoring. Clima. Past, 10, 1983-2006, 2014.

Willmot, C. J.: On the validation of models. Phys.Geogr., 2, 184-194, 1981.

Xu, C. -Y., and Singh V. P.: Cross comparison of empirical equations for calculating potential evapotranspiration with data from Switzerland. Water Resour. Manage., 16, 197-219, 2002.

Xu, J., Peng, S., Ding, J., Wei, Q., and Yu, Y.: Evaluation and calibration of simple methods for daily reference evapotranspiration estimation in humid East China. Arch. Agron. Soil Sci., 59, 845-858, 2013.

Zambrano-Bigiarini, M.: Hydrogof: Goodness-of-fit functions for comparison of simulated and observed hydrological time series. R package, version 0.3-8, 2015. https://cran.r-project.org/web/packages/hydroGOF/hydroGOF.pdf

Zomer, R. J., Trabucco, A., Bossio, D. A., van Straaten, O., and Verchot, L. V.: Climate change mitigation: A spatial analysis of global land suitability for clean development mechanism afforestation and reforestation. Agr. Ecosyst. Environ, 126, 67-80, 2008.

TABLES

Table 1. Meteorological stations from USA-California (CIMIS database) and Australia (AGBM database).

No.	Code	Station	Country	Elevation (m)	Lat (Dec.deg.)	Long (Dec.Deg.)	Period	Köppen Class*
CA-1	006	Davis	USA-CA	18	38.54	-121.78	Sep 1982 - Aug 2016	Csa
CA-2	002	FivePoints	USA-CA	87	36.34	-120.11	Jun 1982 - Aug 2016	BWk
CA-3	005	Shafter	USA-CA	110	35.53	-119.28	Jun 1982 - Aug 2016	BSk
CA-4	007	Firebaugh/Telles	USA-CA	56	36.85	-120.59	Sep 1982 - Aug 2016	BWk
CA-5	012	Durham	USA-CA	40	39.61	-121.82	Oct 1982 - Aug 2016	Csa
CA-6	008	Gerber	USA-CA	76	40.04	-122.17	Sep 1982 - Aug 2014	Csa
CA-7	015	Stratford	USA-CA	59	36.16	-119.85	Nov 1982 - Aug 2016	BSk
CA-8	019	Castroville	USA-CA	3	36.77	-121.77	Nov 1982 - Aug 2016	Csb
CA-9	021	Kettleman	USA-CA	104	35.87	-119.89	Nov 1982 - Aug 2016	BWk
CA-10	027	Zamora	USA-CA	15	38.81	-121.91	Dec 1982 - May 2006	Csa
CA-11	030	Nicolaus	USA-CA	10	38.87	-121.55	Jan 1983 - Dec 2011	Csa
CA-12	032	Colusa	USA-CA	17	39.23	-122.02	Jan 1983 - Aug 2016	Csa
CA-13	033	Visalia	USA-CA	107	36.30	-119.22	Jan 1983 - Feb 2007	BSk
CA-14	035	Bishop	USA-CA	1271	37.36	-118.41	Feb 1983 - Aug 2016	BSk
CA-15	039	Parlier	USA-CA	103	36.60	-119.50	May 1983 - Aug 2016	BSk
CA-16	041	Calipatria/Mulberry	USA-CA	-34	33.04	-115.42	Jul 1983 - Aug 2016	BWh
CA-17	043	McArthur	USA-CA	1009	41.06	-121.46	Dec 1983 - Aug 2016	Csb
CA-18	044	U.C.Riverside	USA-CA	311	33.96	-117.34	Jun 1985 - Aug 2016	BSk
CA-19	047	Brentwood	USA-CA	14	37.93	-121.66	Nov 1985 - Aug 2016	Csb
CA-20	049	Oceanside	USA-CA	15	33.26	-117.32	Mar 1986 - Oct 2003	BSk
CA-21	054	Blackwells Corner	USA-CA	215	35.65	-119.96	Oct 1986 - Aug 2016	BWk
CA-22	056	Los Banos	USA-CA	29	37.10	-120.75	Jun 1988 - Aug 2016	BSk
CA-23	061	Orland	USA-CA	60	39.69	-122.15	May 1987 - May 2010	Csa
CA-24	062	Temecula	USA-CA	433	33.49	-117.23	Nov 1986 - Aug 2016	BSk
CA-25	064	Santa Ynez	USA-CA	149	34.58	-120.08	Nov 1986 - Aug 2016	Csb
CA-26	068	Seeley	USA-CA	12	32.76	-115.73	May 1987 - Aug 2016	BWh
CA-27	070	Manteca	USA-CA	10	37.83	-121.22	Nov 1987 - Aug 2016	BSk
CA-28	071	Modesto	USA-CA	11	37.65	-121.19	Jul 1987 - Aug 2016	BSk
CA-29	077	Oakville	USA-CA	58	38.43	-122.41	Jan 1989 - Aug 2016	Csb
CA-30	075	Irvine	USA-CA	125	33.69	-117.72	Oct 1987 - Aug 2016	BSk
CA-31	078	Pomona	USA-CA	223	34.06	-117.81	Mar 1989 - Aug 2016	Csa
CA-32	080	Fresno State	USA-CA	103	36.82	-119.74	Oct 1988 - Aug 2016	BSk
CA-33	083	Santa Rosa	USA-CA	24	38.40	-122.80	Jan 1990 - Aug 2016	Csb
CA-34	084	Browns Valley	USA-CA	287	39.25	-121.32	Apr 1989 - Aug 2016	Csa
CA-35	085	Hopland F.S.	USA-CA	354	39.01	-123.08	Sep 1989 - Apr 2016	Csa
CA-36	086	Lindcove	USA-CA	146	36.36	-119.06	May 1989 - Aug 2016	Csa
CA-37	087	Meloland	USA-CA	-15	32.81	-115.45	Dec 1989 - Aug 2016	BWh
CA-38	088	Cuyama	USA-CA	698	34.94	-119.67	May 1989 - Aug 2016	BSk
CA-39	091	Tulelake F.S.	USA-CA	1230	41.96	-121.47	Mar 1989 - Aug 2016	Dsb

CA-40	092	Kesterson	USA-CA	23	37.23	-120.88	Oct 1989 - Aug 2016	BSk
CA-41	094	Goletta foothills	USA-CA	195	34.47	-119.87	Jul 1989 - Jul 2016	Csb
CA-42	099	Santa Monica	USA-CA	104	34.04	-118.48	Dec 1992 - Aug 2016	Csb
CA-43	103	Windsor	USA-CA	26	38.53	-122.83	Dec 1990 - Aug 2016	Csb
CA-44	104	De Laveaga	USA-CA	91	37.00	-122.00	Sep 1990 - Aug 2016	Csb
CA-45	105	Westlands	USA-CA	58	36.63	-120.38	Apr 1992 - Aug 2016	BWk
CA-46	106	Sanel Valley	USA-CA	160	38.98	-123.09	Feb 1991 - Aug 2016	Csa
CA-47	57	Buntingville	USA-CA	1221	40.29	-120.43	June 1986 - Sep 2016	Dsb
CA-48	90	Alturas	USA-CA	1343	41.44	-120.48	Apr 1989 - Sep 2016	Dsb
CA-49	151	Ripley	USA-CA	77	33.53	-114.63	Dec 1998 - Sep 2016	BWh
CA-50	183	Owens Lake North	USA-CA	1123	36.49	-117.92	Dec 2002 - Sep 2016	BWk
CA-51	147	Otay Lake	USA-CA	177	32.63	-116.94	Apr 1999 - Sep 2016	Csb
CA-52	175	Palo Verde II	USA-CA	70	33.38	-114.72	Jan 2001 - Sep 2016	BWh
CA-53	135	Blynthe NE	USA-CA	84	33.66	-114.56	Jan 1997 - Sep 2016	BWh
CA-54	155	Bryte	USA-CA	12	38.60	-121.54	Dec 1998 - Sep 2016	Csa
CA-55	159	Monrovia	USA-CA	181	34.15	-117.99	Oct 1999 - Sep 2016	Csa
CA-56	161	Patterson	USA-CA	56	37.44	-121.14	Aug 1999 - Sep 2016	BSk
CA-57	174	Long Beach	USA-CA	5	33.80	-118.09	Sep 2000 - Sep 2016	Csb
CA-58	173	Torrey Pines	USA-CA	102	32.90	-117.25	Nov 2000 - Sep 2016	Csa
CA-59	150	Miramar	USA-CA	136	32.89	-117.14	Apr 1999 - Sep 2016	Csa
CA-60	153	Escondido SPV	USA-CA	119	33.08	-116.98	Feb 1999 - Sep 2016	Csb
A-1	32040	Townsville Aero	Australia	4	-19.25	146.77	(1940/1996-2016)#	Aw
A-2	33307	Woolshed	Australia	556	-19.42	146.54	(1990/2003-2016)	Aw
A-3	2056	Kununurra Aero	Australia	44	-15.78	128.71	(1971/1990-2016)	BSh
A-4	35264	Emerald	Australia	189	-23.57	148.18	(1990/1998-2016)	BSh
A-5	24024	Loxton R.C.	Australia	30	-34.44	140.6	(1984/1998-2016)	BSk
A-6	74037	Yanco AG.I.	Australia	164	-34.62	146.43	(1957/1999-2016)	BSk
A-7	74258	Deniliquin Airp.AWS	Australia	94	-35.56	144.95	(1990/2003-2016)	BSk
A-8	75041	Griffith Airp.AWS	Australia	134	-34.25	146.07	(1958/1990-2016)	BSk
A-9	76031	Mildura Airp.	Australia	50	-34.24	142.09	(1946/1993-2016)	BSk
A-10	24048	Renmark Apt.1	Australia	32	-34.2	140.68	(1990/2003-2016)	BWk
A-11	40082	University of QLD G.	Australia	89	-27.54	152.34	(1897/1990-2016)	Cfa
A-12	40922	Kingaroy Airp.	Australia	434	-26.57	151.84	(1990/2003-2016)	Cfa
A-13	41359	Oakey Aero	Australia	406	-27.4	151.74	(1970/1996-2016)	Cfa
A-14	41522	Dalby Airp.	Australia	344	-27.16	151.26	(1990/2006-2016)	Cfa
A-15	41525	Warwick	Australia	475	-28.21	152.1	(1990/2000-2016)	Cfa
A-16	41529	Toowoomba Airp.	Australia	641	-27.54	151.91	(1990/1997-2016)	Cfa
A-17	80091	Kyabram	Australia	105	-36.34	145.06	(1964/1990-2016)	Cfa
A-18	81049	Tatura I.S.A.	Australia	114	-36.44	145.27	(1942/1990-2016)	Cfa
A-19	81124	Yarrawonga	Australia	129	-36.03	146.03	(1990/2003-2016)	Cfa
A-20	81125	Shepparton Airp.	Australia	114	-36.43	145.39	(1990/1996-2016)	Cfa
A-21	41175	Applethorpe	Australia	872	-28.62	151.95	(1966/2006-2016)	Cfb
A-22	81123	Bendigo Airp.	Australia	208	-36.74	144.33	(1990/2004-2016)	Cfb
A-23	85072	East Sale Airp.	Australia	5	-38.12	147.13	(1943/1996-2016)	Cfb
A-24	85279	Bairnsdale Airp.	Australia	49	-37.88	147.57	(1942/2003-2016)	Cfb

A-25	85280	Morwell L.V.Airp.	Australia	56	-38.21	146.47	(1984/1999-2016)	Cfb
A-26	85296	Mount Moornapa	Australia	480	-37.75	147.14	(1990/2003-2016)	Cfb
A-27	90035	Colac	Australia	261	-38.23	143.79	(1990/2003-2016)	Cfb
A-28	9538	Dwellingup	Australia	267	-32.71	116.06	(1934/1990-2016)	Csb
A-29	9617	Bridgetown	Australia	179	-33.95	116.13	(1990/2003-2016)	Csb
A-30	23373	Nuriootpa Pirsa	Australia	275	-34.48	139.01	(1990/1996-2016)	Csb
A-31	26021	Mount Gambier Aero	Australia	63	-37.75	140.77	(1942/1994-2016)	Csb
A-32	26091	Coonawarra	Australia	57	-37.29	140.83	(1985/1990-2016)	Csb
A-33	66062	Sydney (Obs.Hill)	Australia	39	-33.86	151.21	(1858/1990-2016)	Cfb
A-34	33002	Ayr DPI Res.St.	Australia	17	-19.62	147.38	(1951/1994-2016)	Cwa
A-35	7176	Newman Aero	Australia	524	-23.42	119.8	(1971/2003-2016)	BWh
A-36	13017	Giles	Australia	598	-25.03	128.3	(1956/1990-2016)	BWh
A-37	11052	Forrest	Australia	159	-30.85	128.11	(1990/2003-2016)	BWh
A-38	11003	Eucla	Australia	93	-31.68	128.9	(1876/1995-2016)	BSk
A-39	12071	Salmon Gums	Australia	249	-32.99	121.62	(1932/2003-2016)	BSk
A-40	7045	Meekatharra Airp.	Australia	517	-26.61	118.54	(1944/1992-2016)	BWh
A-41	1025	Doongan	Australia	385	-15.38	126.31	(1988/1990-2016)	Aw
A-42	2012	Halls Creek Airp.	Australia	422	-18.23	127.66	(1944/1996-2016)	BSh
A-43	13015	Carnegie	Australia	448	-25.8	122.98	(1942/1990-2016)	BWh
A-44	3080	Curtin Aero	Australia	78	-17.58	123.83	(1990/2003-2016)	BSh
A-45	6022	Gascoyne Junction	Australia	144	-25.05	115.21	(1907/1990-2016)	BWh
A-46	9789	Esperance	Australia	25	-33.83	121.89	(1969/1990-2016)	Csb
A-47	91223	Marrawah	Australia	107	-40.91	144.71	(1971/1990-2016)	Cfb
A-48	18106	Nullarbor	Australia	64	-31.45	130.9	(1888/2006-2016)	BWk
A-49	16090	Coober Pedy Airp.	Australia	225	-29.03	134.72	(1990/2004-2016)	BWh
A-50	16085	Marla Police St.	Australia	323	-27.3	133.62	(1985/1990-2016)	BWh
A-51	13011	Warburton Airfield	Australia	459	-26.13	126.58	(1940/2003-2016)	BWh
A-52	15528	Yuendumu	Australia	667	-22.26	131.8	(1952/1990-2016)	BWh
A-53	15666	Rabbit Flat	Australia	340	-20.18	130.01	(1990/1996-2016)	BWh
A-54	14829	Lajamanu Airp.	Australia	316	-18.33	130.64	(1952/1990-2016)	BSh
A-55	15135	Tennant Creek Airp.	Australia	376	-19.64	134.18	(1969/1992-2016)	BSh
A-56	37010	Camooweal Township	Australia	231	-19.92	138.12	(1891/2003-2016)	BWh
A-57	14707	Wollogorang	Australia	60	-17.21	137.95	(1967/1990-2016)	Aw
A-58	14938	Mango Farm	Australia	15	-13.74	130.68	(1980/1990-2016)	Aw
A-59	69134	Batemans Bay	Australia	11	-35.72	150.19	(1985/1991-2016)	Cfb
A-60	14198	Jabiru Airp.	Australia	27	-12.66	132.89	(1971/1990-2016)	Aw
A-61	28008	Lockhart River Airp.	Australia	19	-12.79	143.3	(1956/2001-2016)	Am
A-62	34084	Charters Towers Airp.	Australia	290	-20.05	146.27	(1990/1992-2016)	BSh
A-63	29038	Kowanyama Airp.	Australia	10	-15.48	141.75	(1912/1999-2016)	Aw
A-64	32078	Ingham Composite	Australia	12	-18.65	146.18	(1968/1990-2016)	Am
A-65	40854	Logan City W.T.P.	Australia	14	-27.68	153.19	(1990/1992-2016)	Cfa
A-66	8095	Mullewa	Australia	268	-28.54	115.51	(1896/1990-2016)	BSh
A-67	8251	Kalbarri	Australia	6	-27.71	114.17	(1970/1990-2016)	BSh
A-68	8225	Eneabba	Australia	100	-29.82	115.27	(1964/1990-2016)	Csa
A-69	7139	Paynes Find	Australia	339	-29.27	117.68	(1919/1990-2016)	BWh

A-70	10007	Bencubbin	Australia	359	-30.81	117.86	(1912/1990-2016)	BSh
A-71	10092	Merredin	Australia	315	-31.48	118.28	(1903/1990-2016)	BSk
A-72	12038	Kalgoorlie-Boulder Airp.	Australia	365	-30.78	121.45	(1939/1994-2016)	BSh
A-73	16098	Tarcoola Aero	Australia	123	-30.71	134.58	(1990/1999-2016)	BWh
A-74	18195	Minnipa Pirsa	Australia	165	-32.84	135.15	(1990/2003-2016)	BSk
A-75	46126	Tibooburra Airp.	Australia	176	-29.44	142.06	(1990/2003-2016)	BWh
A-76	48245	Boorke Airp. AWS	Australia	107	-30.04	145.95	(1990/2002-2016)	BSh
A-77	55325	Tamworth Airp. AWS	Australia	395	-31.07	150.84	(1990/2006-2016)	Cfa
A-78	38026	Birdsville Airp.	Australia	47	-25.9	139.35	(1990/2001-2016)	BWh
A-79	30161	Richmond Airp.	Australia	206	-20.7	143.12	(1990/2003-2016)	BSh
A-80	33013	Collinsville Airp.	Australia	196	-20.55	147.85	(1939/1990-2016)	BSh

*Köppen classification obtained from Peel et al. (2007).

In the case of Australian stations, the periods of observations vary between different climatic parameters. e.g. for the case (1939/1990-2016), the two dates separated with "/" show the starting date of the oldest and newest record of parameters used in calculations, respectively, while 2016 is the ending date of the records.

Table 2. Additional models of reduced parameters obtained from the international literature, which provide equivalent results to ET_o for short reference crop,

Reference	Abbreviation	Formula	Climate data requirements*
Droogers and Allen (2002)	DRAL1 (Eq.8)	$ET_o = 0.00102 R_a \left(T_{mean} + 16.8\right) \cdot \left(TD\right)^{0.5}$	T_{max}, T_{min}
Droogers and Allen (2002)	DRAL2 (Eq.9)	$ET_o = 0.0005304 R_a \left(T_{mean} + 17.0\right) \cdot \left(TD - 0.0123P\right)^{0.76}$	T_{max}, T_{min}, P
Alexandris et al. (2006)	Copais (Eq.10)	$ET_o = 0.057 + 0.227C_2 + 0.643C_1 + 0.0124C_1C_2$ $C_1 = 0.6416 - 0.00784RH + 0.372R_s - 0.00264R_sRH$ $C_2 = -0.0033 + 0.00812T_{mean} + 0.101R_s + 0.00584R_sT_{mean}$	T_{mean}, R_s, RH
Valiantzas (2013a, 2014)	VAL1 (Eq.11)	$ET_o = 0.0393R_s\sqrt{T_{mean} + 9.5} - 0.19R_s^{0.6}\varphi^{0.15} + 0.0061\left(T_{mean} + 20\right)\left(1.12T_{mean} - T_{min} - 2\right)^{0.7}$	T_{mean}, T_{min}, R_s
Valiantzas (2013a; 2014)	VAL2 (Eq.12)	$ET_o = 0.0393R_s\sqrt{T_{mean} + 9.5} - 0.19R_s^{0.6}\varphi^{0.15} + 0.078\left(T_{mean} + 20\right)\left(1 - \frac{RH}{100}\right)$	T_{mean}, R_s, RH
Valiantzas (2013b)	VAL3 (Eq.13)	$ET_o = 0.0393R_s\sqrt{T_{mean} + 9.5} - 2.4\left(\frac{R_s}{R_a}\right)^2 + Cu\left(T_{mean} + 20\right)\left(1 - \frac{RH}{100}\right)$	T_{mean}, R_s, RH (Cu=0.054 for RH>65% and Cu=0.083 for $RH \leq 65$%)
Ahooghalandari et al. (2016)	AKJ1 (Eq.14)	$ET_o = 0.252 \cdot 0.408R_a + 0.221T_{mean}\left(1 - \frac{RH}{100}\right)$	T_{mean}, RH
Ahooghalandari et al. (2016)	AKJ2 (Eq.15)	$ET_o = 0.29 \cdot 0.408R_a + 0.15T_{\max}\left(1 - \frac{RH}{100}\right)$	T_{max}, RH

* $T_{mean,\ max,\ min}$: Mean, maximum and minimum temperature (°C), TD: difference between maximum and minimum temperature (°C), R_s: incident solar radiation (MJ m^{-2} d^{-1}), R_a: extraterrestrial solar radiation (MJ m^{-2} d^{-1}), RH: relative humidity (%), φ: absolute value of latitude (rads), P: precipitation (mm $month^{-1}$)

Table 3. The % coverage* of *MAD%* classes based on mean annual values (according to Figs. 4), R^2 and *RMSD* based on comparisons of the mean monthly values of ET_o and R_s methods (comparisons based on 0.5 degree resolution maps).

MAD% range	†ET_o (ASCE-tall) for C_n=1600, C_d=0.38 (Eq.1)	†ET_o (P-T) for a_{pt}=1.26 (Eq.2)	†ET_o (H-S) for c_{hs2} = 0.0023 (Eq.4b)	‡R_s (H-S) for K_{RS}=0.17 (Eq.3)
≤ -50%	0.0%*	0.8%	0.0%	1.0%
-50 up to -25%	0.0%	14.8%	5.2%	2.2%
-25 up to -10%	0.0%	10.8%	15.4%	7.1%
-10 up to 10%	25.2%	21.3%	24.8%	55.3%
10 up to 25%	40.9%	22.5%	19.6%	32.8%
25 up to 50%	33.6%	21.9%	29.2%	1.6%
> 50%	0.3%	7.9%	5.8%	0.0%
R^2	0.98	0.77	0.89	0.92
RMSD	39.6§	36.0§	24.5§	2.4#

*The % coverage was estimated after conversion from WGS84 ellipsoid to projected Cylindrical Equal Area coordinate system without considering Antarctica.
† *MAD*% of the three ET_o methods is estimated versus ASCE-short.
‡ *MAD*% of the standard solar radiation method of H-S is estimated versus the R_s data of Sheffield et al. (2006).
§ The unit of *RMSD* for ET_o is mm month^{-1}.
# The unit of *RMSD* for R_s is MJ m^{-2} d^{-1}.

Table 4. Spatial extent of the major climatic groups CGs from Köppen-Geiger climate map (Peel et al., 2007), % prevalence of P-T versus H-S within each CG based on the *DMAD* values.

Climatic group (CG) of Köppen-Geiger	% extent of CGs* based on Peel et al. (2007) map	P-T versus H-S prevalence % inside a CG#		
		H-S (DMAD≤-1)	Trans. Zone -1<DMAD<1†	P-T (DMAD≥1)
A - tropical/megathermal	20.66%	32.0%	3.6%	64.4%
B - arid/semi-arid	32.90%	86.4%	1.3%	12.3%
C - temperate/mesothermal	14.58%	32.8%	3.2%	64.1%
D - continental/microthermal	27.00%	26.9%	2.1%	71.0%
E - polar/alpine (without Antarctica)	4.86%	71.1%	16.3%‡	12.5%

*The % coverage was estimated after conversion from WGS84 ellipsoid to projected Cylindrical Equal Area coordinate system without considering Antarctica.
% coverage of *DMAD* values were estimated after pixel resampling using the resolution of Köppen map.
†*DMAD* range were both methods present similar proximity to ASCE-short method (transitional zone).
‡Big part of this percentage corresponds to regions with annual ET_o equal to 0 (e.g. inner Greenland). Such cases are included in the trans. zone of Fig.5a.

Table 5. Statistical criteria from the comparisons **(a)** between ET_o values from ASCE-short and the methods used for estimating short reference crop evapotranspiration (i.e. P-T with standard and re-adjusted coefficients, H-S with standard and re-adjusted coefficients and all equations given in Table 2), **(b)** between ET_o values from ASCE-tall and P-T, H-S methods with re-adjusted coefficients for tall reference crop, **(c)** R_s values from stations and R_s obtained from the H-S radiation formula with standard and re-adjusted coefficients.

Case	Criterion	MAE	RMSE	NRMSE%	PBIAS%	R^2	bR^2	NSE	d	KGE
	Optimum value	0	0	0	0	1	1	1	1	1
a	P-T (Eq.2) with a_{pt}=1.26	36.92	48.87	90.9	33.3	0.763	0.591	0.173	0.849	0.539
	P-T (Eq.2) with a_{pt}=p.w.a.s.	22.71	29.43	40.3	7.5	0.856	0.832	0.837	0.956	0.883
	H-S (Eq.4b) with c_{hs2}=0.0023	21.19	30.36	53.2	10.8	0.858	0.772	0.717	0.941	0.746
	H-S (Eq.4b) with c_{hs2}=p.w.a.s.	17.13	22.72	34.4	2.5	0.895	0.878	0.881	0.971	0.921
	DRAL1 (Eq.8)	19.53	27.05	44.5	4.8	0.859	0.818	0.802	0.955	0.833
	DRAL2 (Eq.9)	22.92	30.28	45.0	3.2	0.818	0.808	0.798	0.949	0.894
	Copais (Eq.10)	14.49	20.70	34.3	7.3	0.940	0.870	0.882	0.974	0.829
	VAL1 (Eq.11)	21.36	31.87	59.8	15.1	0.888	0.763	0.642	0.932	0.657
	VAL2 (Eq.12)	12.13	17.96	29.3	4.2	0.948	0.900	0.914	0.981	0.859
	VAL3 (Eq.13)	11.45	15.94	24.1	1.4	0.949	0.934	0.942	0.986	0.940
	AKJ1 (Eq.14)	21.17	24.24	42.0	-10.6	0.955	0.887	0.824	0.964	0.771
	AKJ2 (Eq.15)	30.36	33.69	59.5	-16.3	0.938	0.820	0.645	0.931	0.718
b	P-T (Eq.2) with a_{pt}=p.w.a.t.	40.43	52.38	50.6	8.4	0.770	0.754	0.743	0.930	0.845
	H-S (Eq.4b) with c_{hs2}=p.w.a.t.	31.87	42.34	45.2	3.7	0.823	0.806	0.795	0.950	0.885
c	H-S R_s (Eq.3) with K_{RS}=0.17	1.64	1.99	29.6	-4.5	0.930	0.885	0.912	0.977	0.932
	H-S R_s (Eq.3) with K_{RS}=p.w.a.	1.05	1.43	22.3	-0.8	0.952	0.944	0.950	0.988	0.972

FIGURES

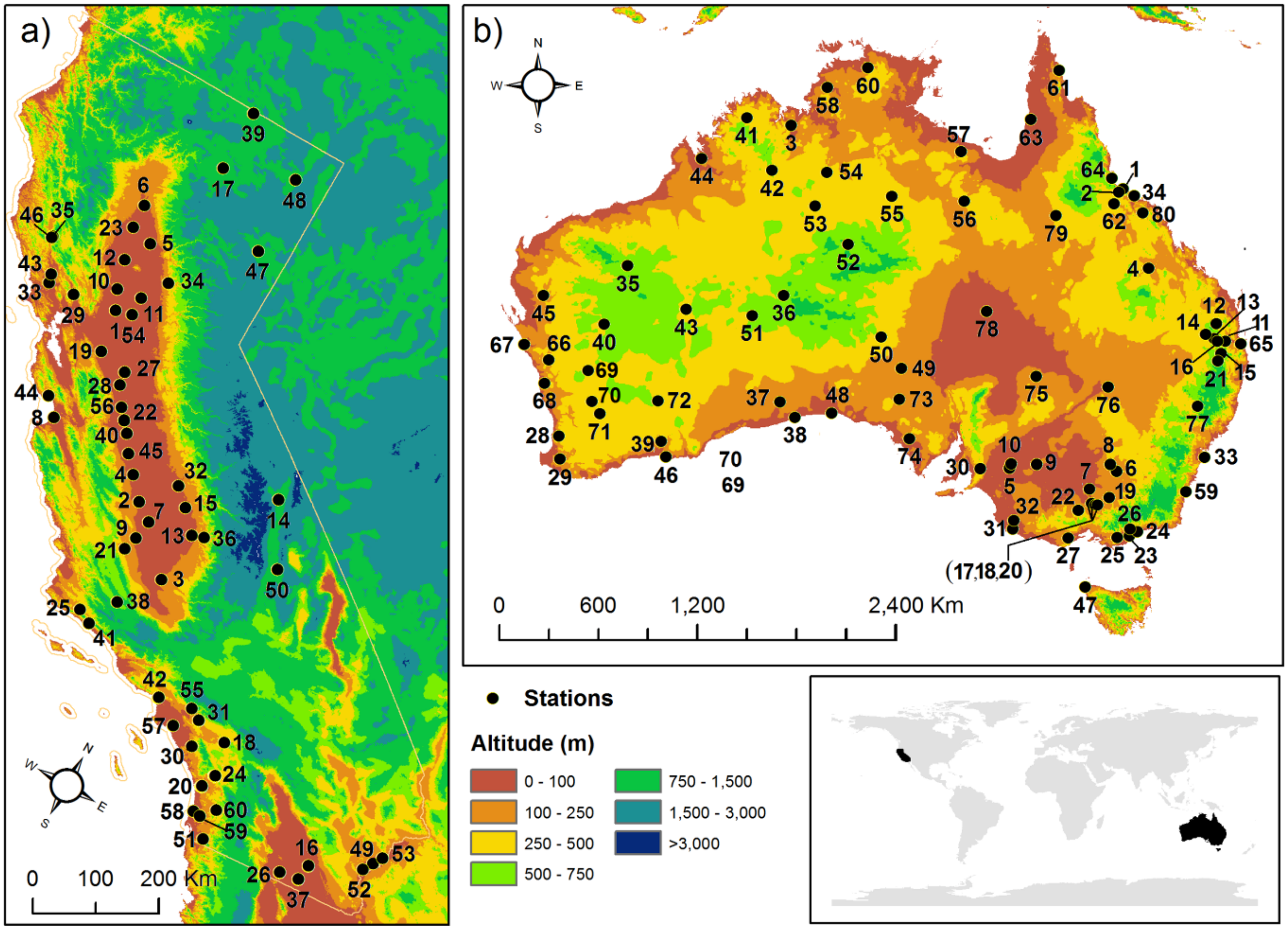

Figure 1. Position of stations **(a)** from California-USA obtained by CIMIS database and **(b)** from Australia obtained by AGBM database (the numbers indicate the No. of stations from Table 1 without the abbreviations CA- and A-).

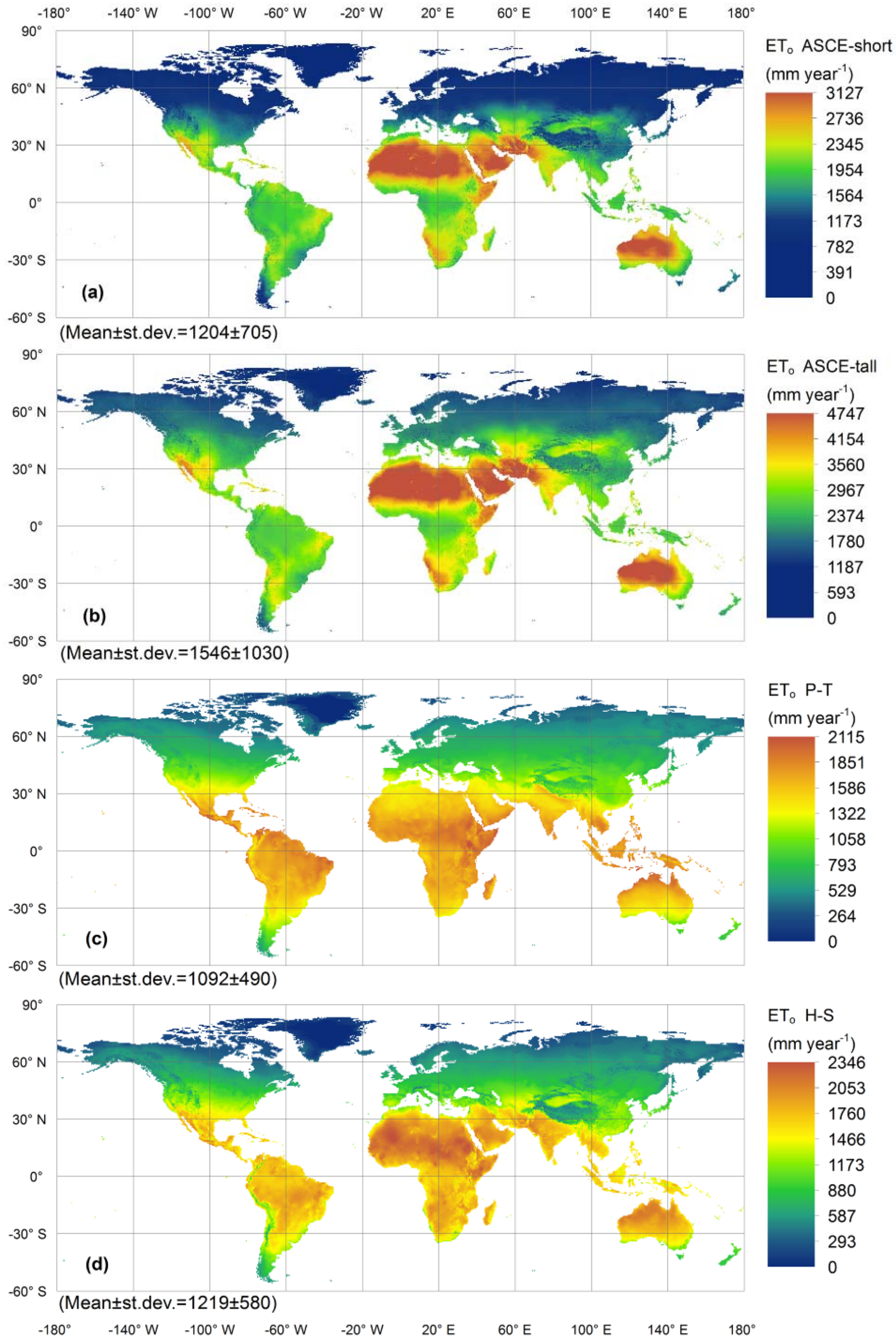

Figure 2. Mean annual values (mm year^{-1}) of ET_o for the period 1950-2000 using **(a)** the ASCE-short method, **(b)** the ASCE-tall method, **(c)** the standard P-T method for a_{pt}=1.26 and **(d)** the standard H-S method for c_{hs2}=0.0023 (0.5 degree resolution maps, mean±st.dev. are estimated after conversion from WGS84 to Cylindrical Equal Area coordinate system).

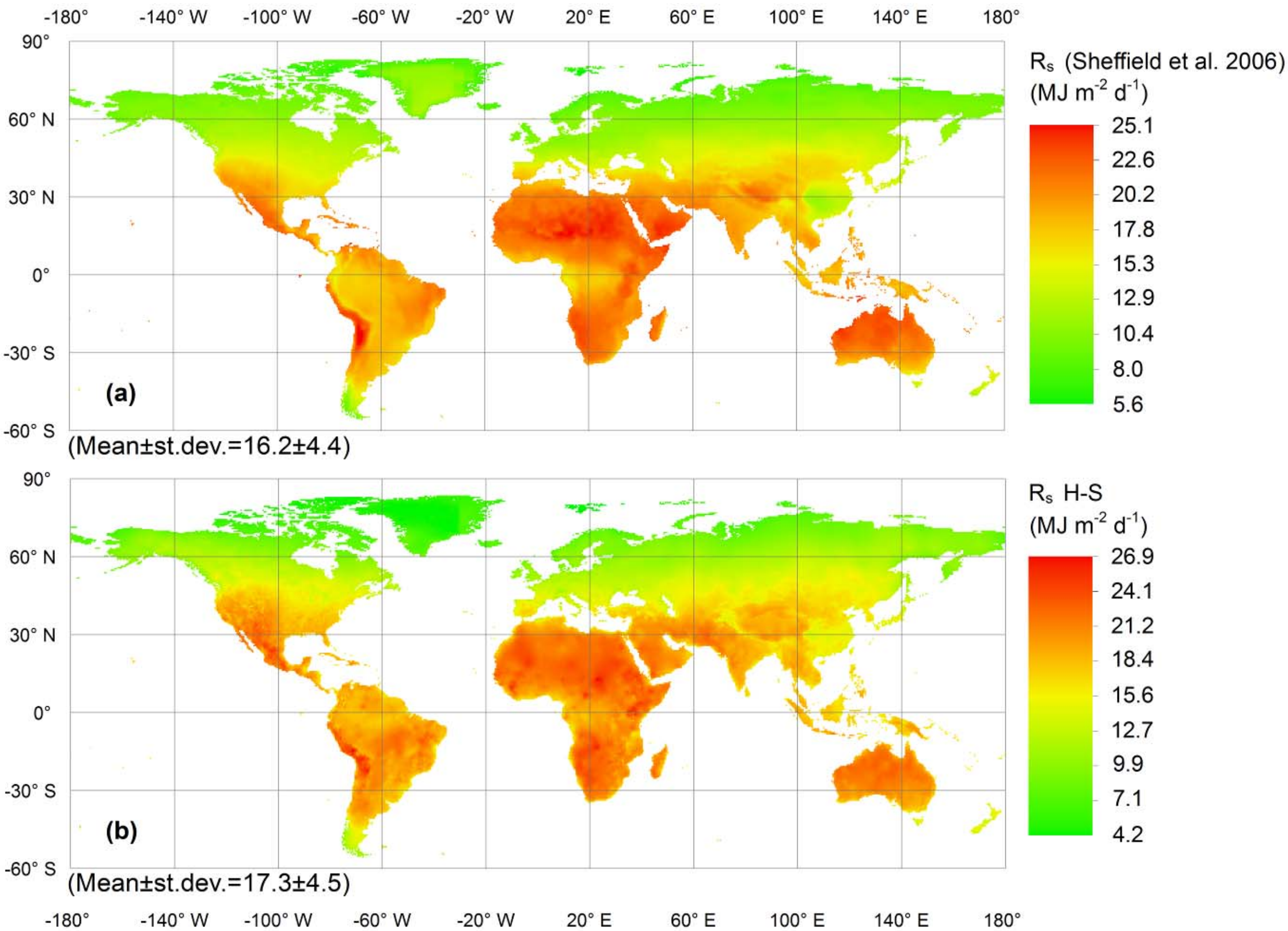

Figure 3. Mean annual values of R_s (MJ m^{-2} d^{-1}) for the period 1950-2000 **(a)** from the database of Sheffield et al. (2006) and **(b)** estimated using the standard H-S radiation formula for K_{RS}=0.17 (Eq.3) (0.5 degree resolution maps, mean±st.dev. are estimated after conversion from WGS84 to Cylindrical Equal Area coordinate system).

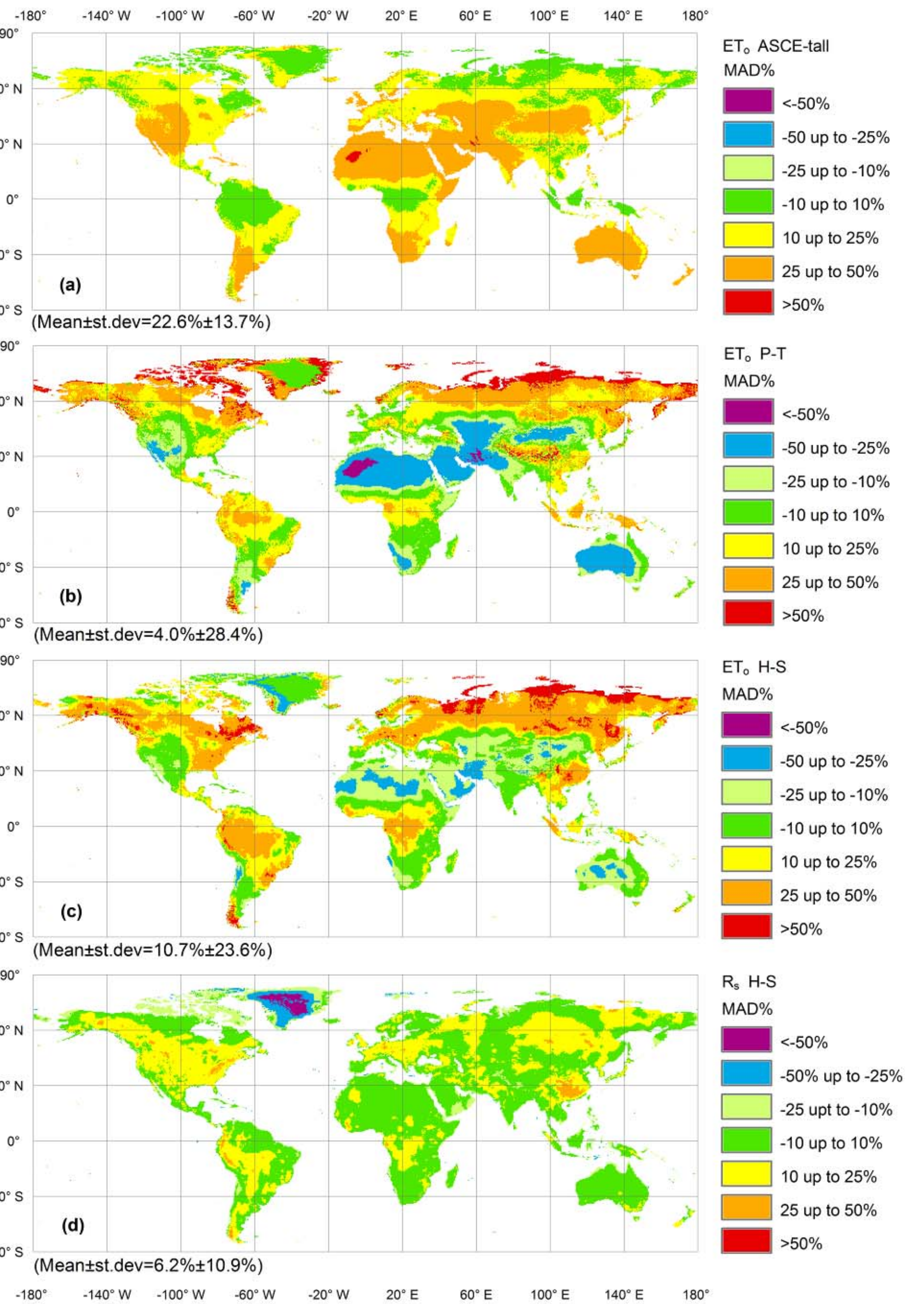

Figure 4. Mean annual difference % (*MAD*%) of ET_o between the ASCE-short and **(a)** the ASCE-tall method, **(b)** the standard P-T method for a_{pt}=1.26, **(c)** the standard H-S method for c_{hs2} = 0.0023, and **(d)** *MAD*% between R_s values of Sheffield et al. (2006) and the standard solar radiation formula of H-S for K_{RS}=0.17 (0.5 degree resolution maps, mean±st.dev. are estimated after conversion from WGS84 to Cylindrical Equal Area coordinate system).

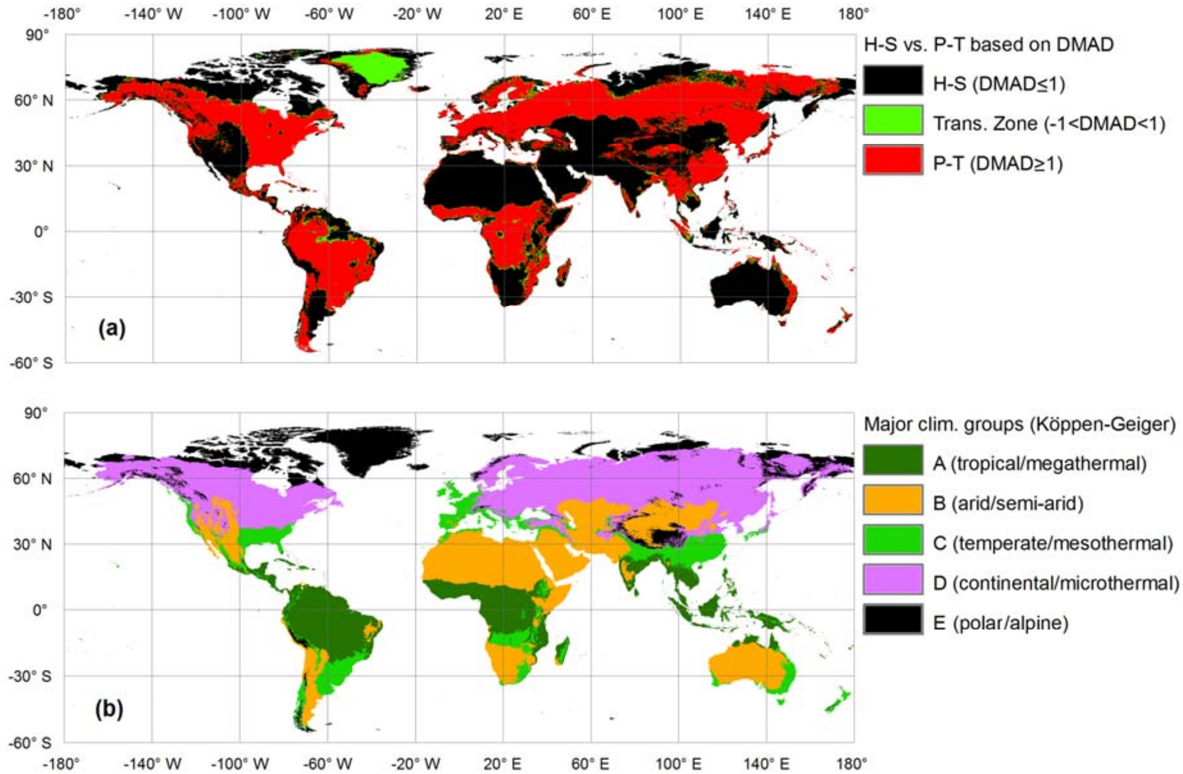

Figure 5. **(a)** P-T versus H-S prevalence according to their proximity to ASCE-short method expressed by the *DMAD* values (0.5 degree resolution map) and **(b)** Spatial extent of the major climatic groups of the Köppen-Geiger climate classification according to Peel et al. (2007).

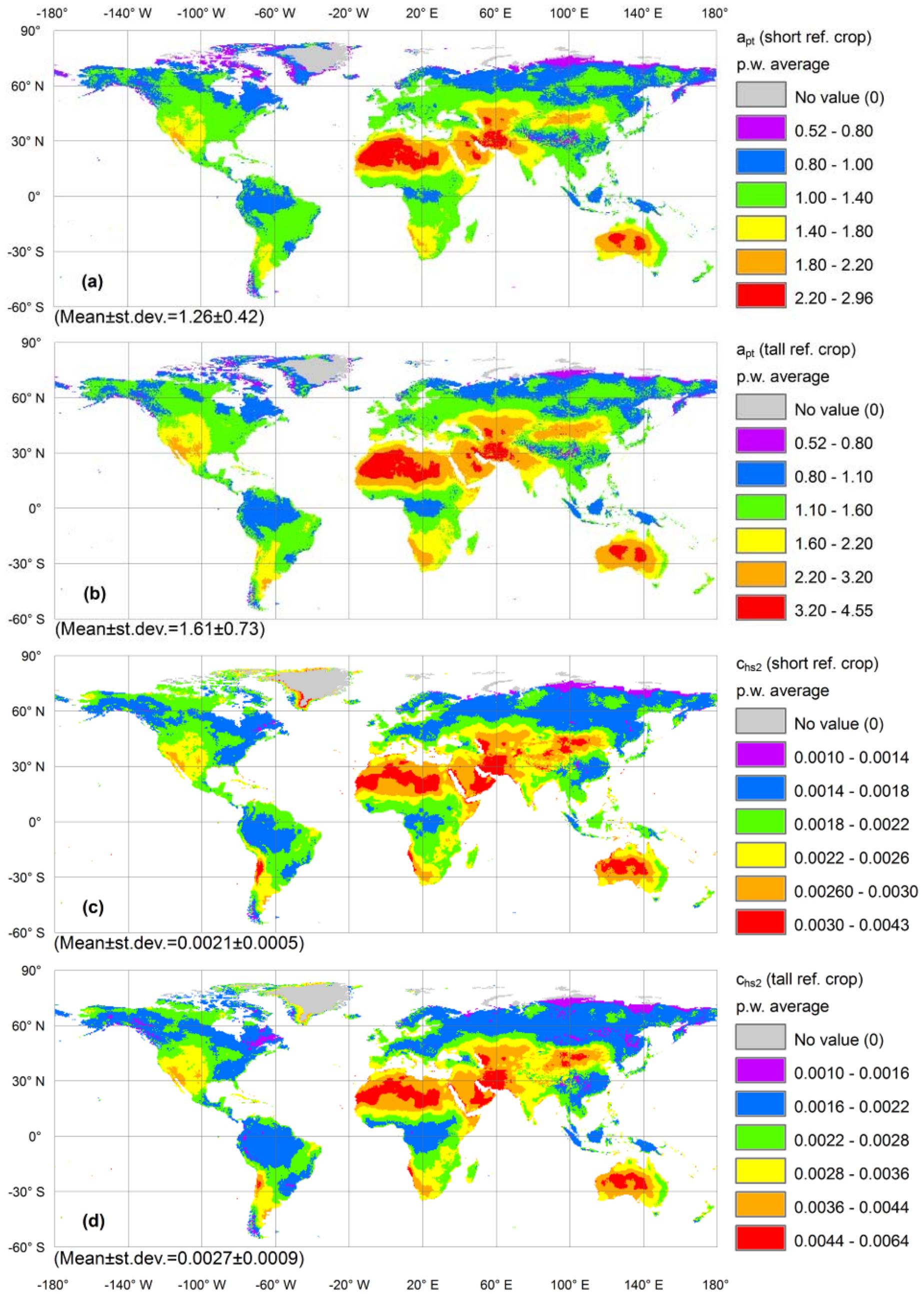

Figure 6. Partial weighted averages of mean monthly **(a)** a_{pt} for short reference crop, **(b)** a_{pt} for tall reference crop, **(c)** c_{hs2} for short reference crop and **(d)** c_{hs2} for tall reference crop (0.5 degree resolution maps, mean±st.dev. are estimated after conversion from WGS84 to Cylindrical Equal Area coordinate system excluding pixels of 0 value).

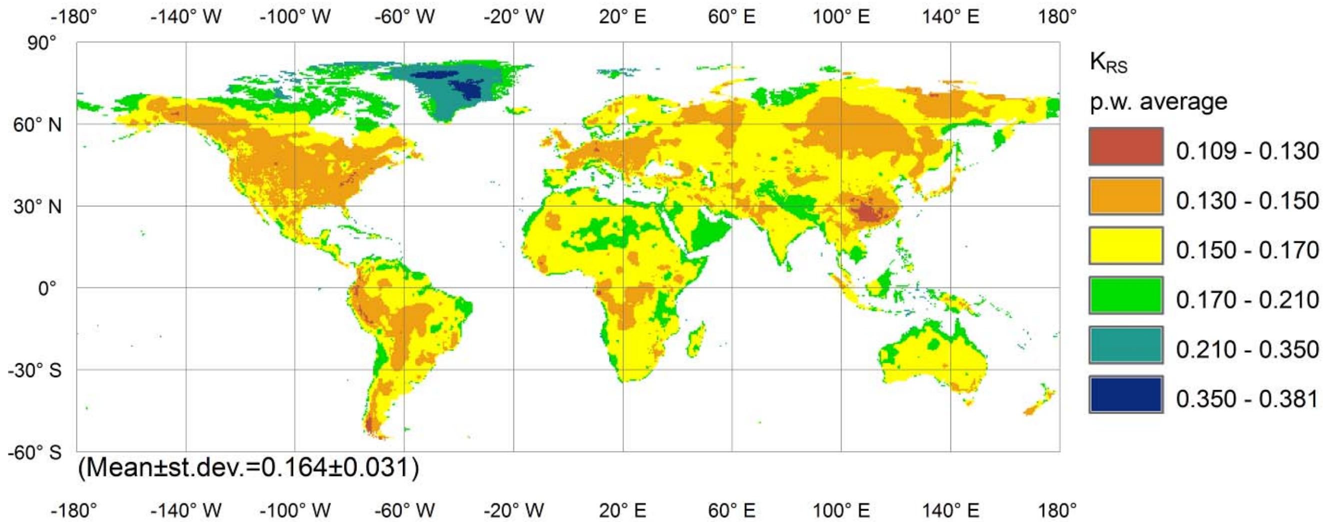

Figure 7. Partial weighted averages of mean monthly K_{RS} (0.5 degree resolution maps, mean±st.dev. are estimated after conversion from WGS84 to Cylindrical Equal Area coordinate system).

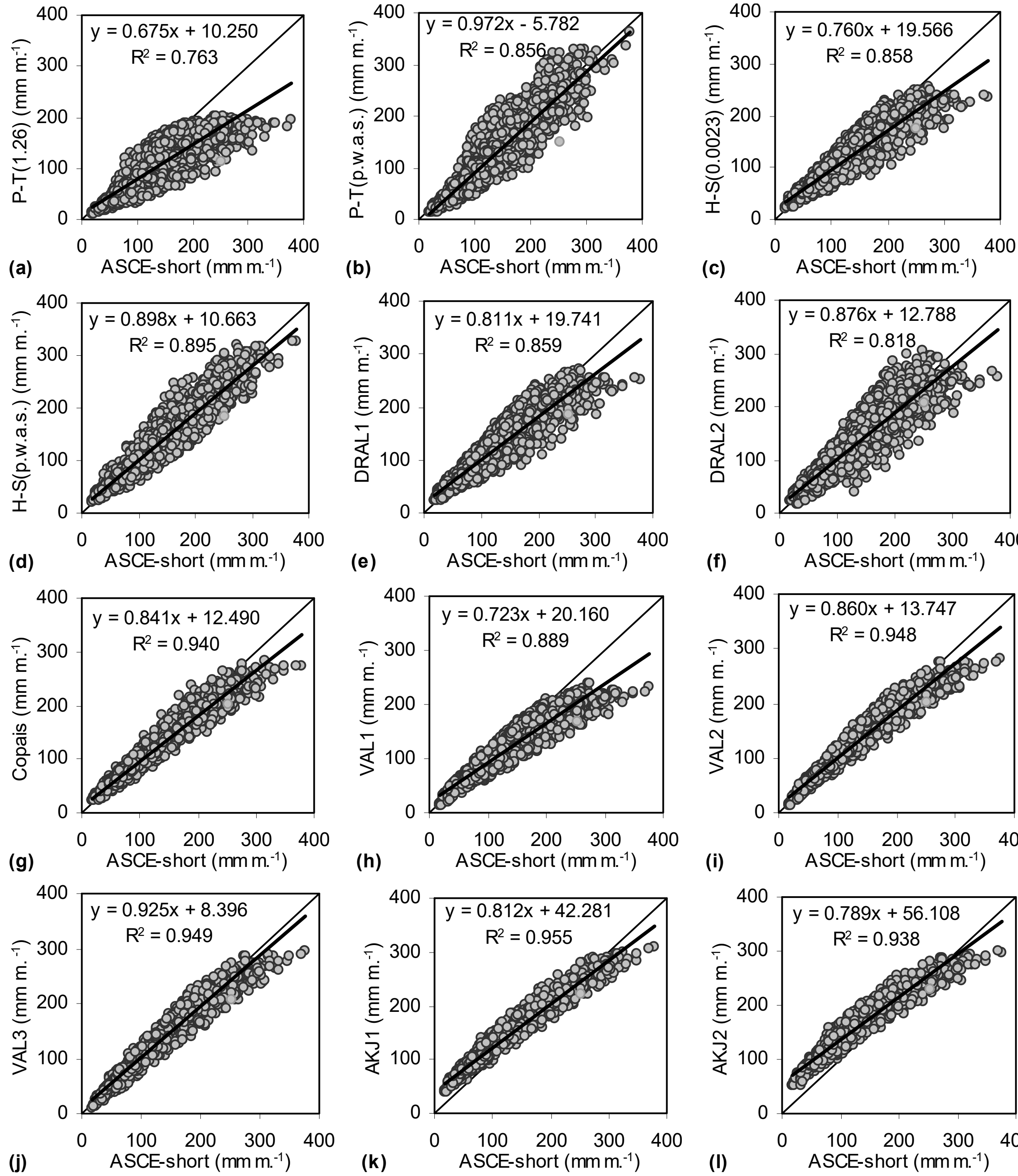

Figure 8. Comparative 1:1 plots between the results of ET_o ASCE-short (mm month^{-1}) versus **(a)** the standard P-T method with a_{pt}=1.26, **(b)** the P-T method with a_{pt}=p.w.a.s. (0.5 degree resolution), **(c)** the standard H-S method with c_{hs2}=0.0023. **(d)** the H-S method with c_{hs2}=p.w.a.s. (0.5 degree resolution), **(e)** DRAL1 (Eq.8)**, (f)** DRAL2 (Eq.9), **(g)** Copais (Eq.10), **(h)** VAL1 (Eq.11), **(i)** VAL2 (Eq.12), **(j)** VAL3 (Eq.13), **(k)** AKJ1 (Eq.14), **(l)** AKJ2 (Eq.15).

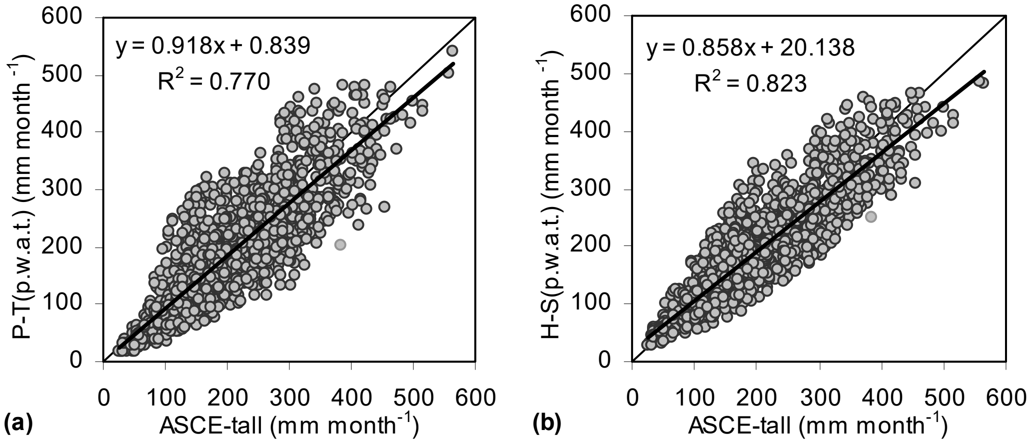

Figure 9. Comparative 1:1 plots between the results of ET_o ASCE-tall (mm month^{-1}) versus **(a)** the P-T method with a_{pt}=p.w.a.t. (0.5 degree resolution), **(b)** the H-S method with c_{hs2}=p.w.a.t. (0.5 degree resolution).

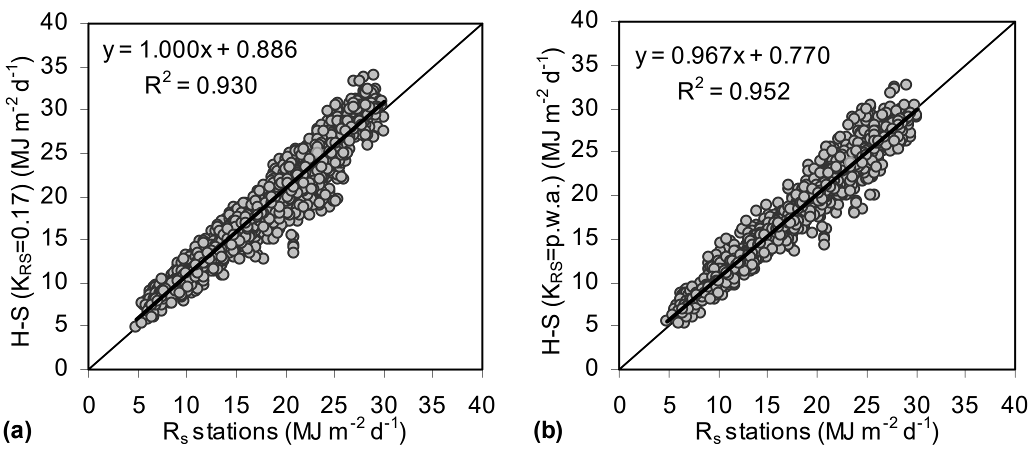

Figure 10. Comparative 1:1 plots between the R_s (MJ m^{-2} d^{-1}) values of CA-USA and Australia stations versus the results of H-S radiation formula (Eq.3) **(a)** with K_{RS}= 0.17, **(b)** with K_{RS}=p.w.a. (0.5 degree resolution).

Supplementary Material

Indirect verification of the data cleaning that was performed in the derived data from CIMIS database.

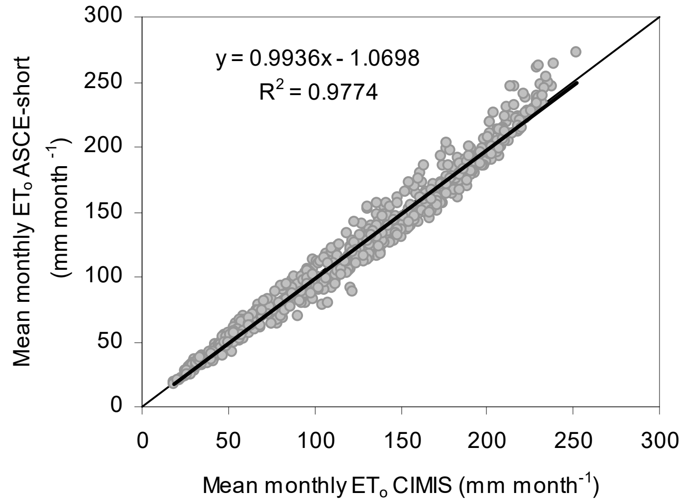

Fig.S1 Comparison between the mean monthly ET_o values of ASCE-short method using the final clean climatic data from CIMIS database versus the provided mean monthly values of ET_o by the database using the CIMIS evapotranspiration method.

General statistics of meteorological stations data (validation data) and comparison with the raster data (calibration data) used for developing the global maps of ET_o with ASCE method.

Table S1. General statistics* of the mean monthly observed values of climatic parameters from the 140 stations of California-USA and Australia that participate in the estimation of reference evapotranspiration with the ASCE method.

Parameter	T_{max}	T_{min}	R_s	RH	u_2	P	ET_o ASCE-short	ET_o ASCE-tall
Unit	°C	°C	MJ m^{-2} d^{-1}	%	m s^{-1}	mm $month^{-1}$	mm $month^{-1}$	mm $month^{-1}$
Average	25.3	11.4	18.8	56.4	2.6	41.5	138.4	190.5
Minimum	5.3	-7.2	4.9	19.0	0.9	0.0	17.9	26.2
Lower quartile	19.7	6.5	13.5	45.5	1.8	11.7	82.2	112.7
Upper quartile	31.1	15.8	24.4	68.2	3.2	50.6	186.9	254.2
Maximum	41.2	26.3	30.1	90.3	6.8	470.4	377.5	563.8
Range	35.9	33.5	25.2	71.3	5.9	470.4	359.6	537.6
Standard deviation	7.1	6.4	6.5	15.4	1.0	51.5	69.5	98.9
Coeff. of variation %	28.11%	56.13%	34.32%	27.36%	37.05%	123.90%	50.17%	51.93%

*The statistics are based on 1680 values (140 stations × 12 months)

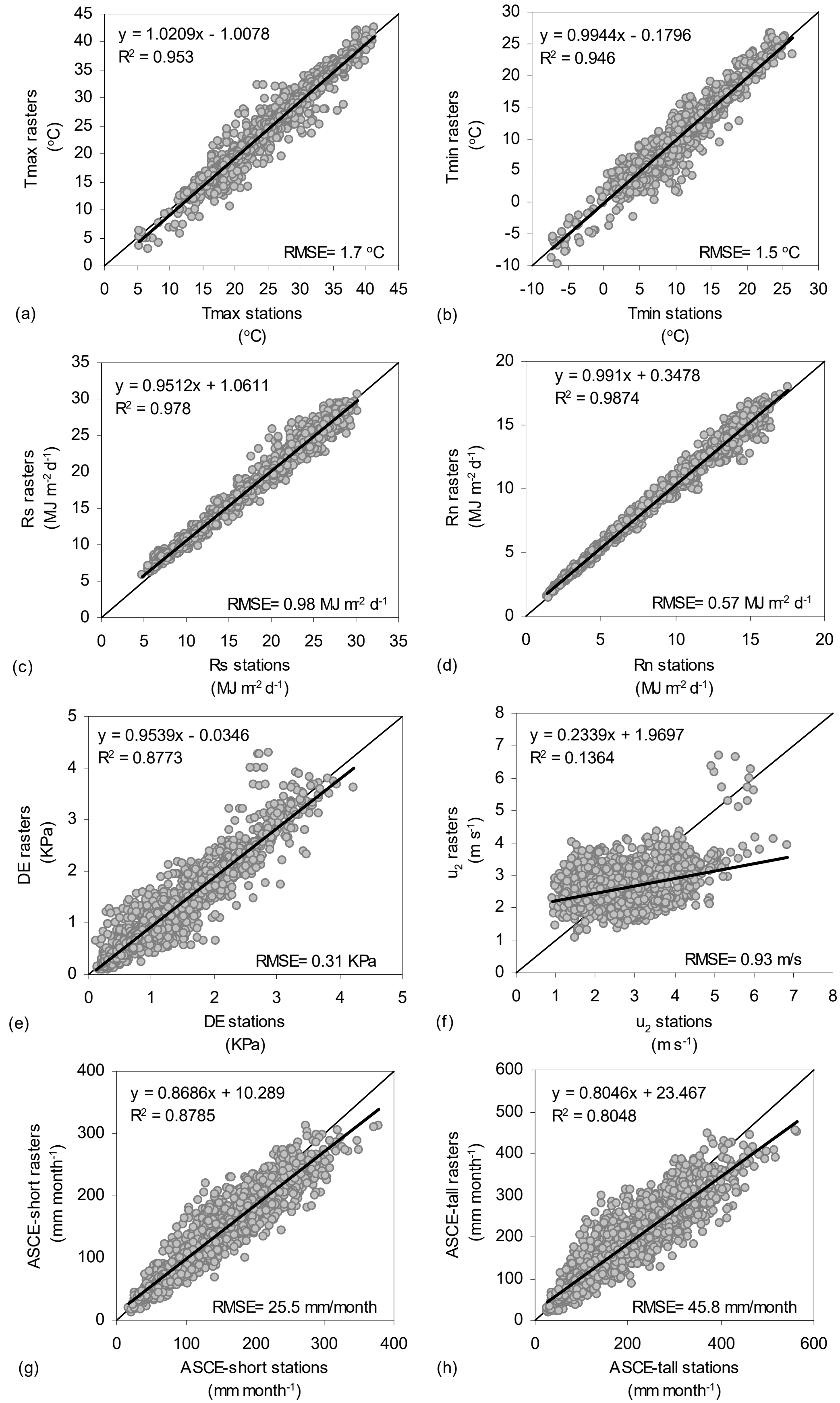

Fig.S2 Comparison of T_{max}, T_{min}, R_s, R_n, *DE* (vapour pressure deficit), u_2, ET_o ASCE-short, and ET_o ASCE-tall between the rasters (0.5 degree resolution) and the stations data.

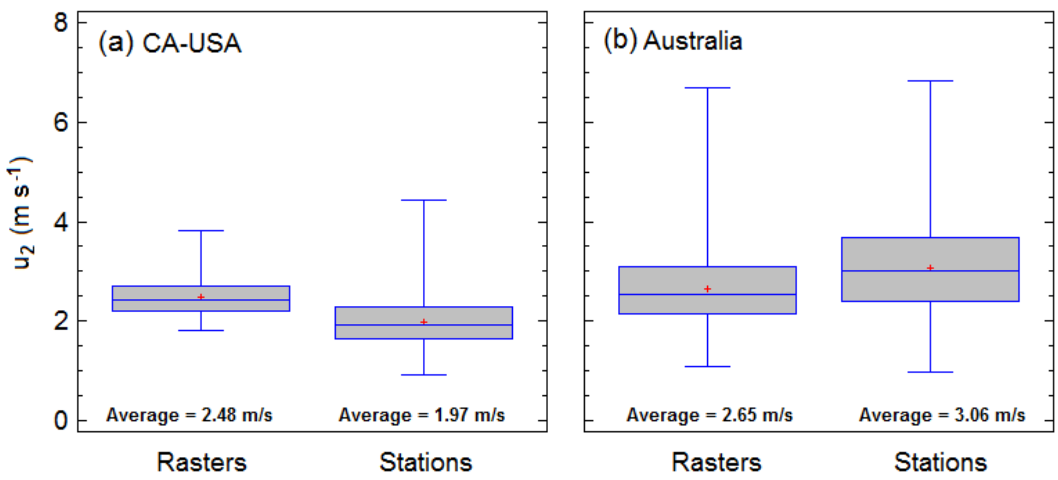

Fig.S3 Comparison of total averages of mean monthly u_2 values through Box-Whisker plots: a) between rasters (Sheffield et al., 2006) and California-USA stations, b) between rasters (Sheffield et al., 2006) and Australia stations.

Extracted values of the p.w.a. coefficients for each station in the validation dataset.

Table S2. Partial weighted averages of mean monthly coefficients (a_{pt}, c_{hs2}, K_{RS}) for each station extracted by the 0.5 degree resolution maps.

No.	Code	Station	Country	a_{pt} p.w.a.s. (0.5 deg)	a_{pt} p.w.a.t. (0.5 deg)	c_{hs2} p.w.a.s. (0.5 deg)	c_{hs2} p.w.a.t. (0.5 deg)	K_{RS} p.w.a. (0.5 deg)
CA-1	006	Davis	USA-CA	1.45	1.93	0.0022	0.0029	0.16
CA-2	002	FivePoints	USA-CA	1.53	2.06	0.0023	0.0030	0.16
CA-3	005	Shafter	USA-CA	1.48	1.97	0.0023	0.0031	0.16
CA-4	007	Firebaugh/Telles	USA-CA	1.48	1.99	0.0022	0.0029	0.15
CA-5	012	Durham	USA-CA	1.49	2.01	0.0024	0.0031	0.16
CA-6	008	Gerber	USA-CA	1.46	1.96	0.0023	0.0031	0.16
CA-7	015	Stratford	USA-CA	1.47	1.95	0.0023	0.0030	0.16
CA-8	019	Castroville	USA-CA	1.20	1.53	0.0023	0.0029	0.18
CA-9	021	Kettleman	USA-CA	1.49	1.99	0.0022	0.0030	0.15
CA-10	027	Zamora	USA-CA	1.45	1.93	0.0022	0.0029	0.16
CA-11	030	Nicolaus	USA-CA	1.45	1.93	0.0022	0.0029	0.16
CA-12	032	Colusa	USA-CA	1.49	2.01	0.0023	0.0030	0.15
CA-13	033	Visalia	USA-CA	1.48	1.96	0.0023	0.0031	0.16
CA-14	035	Bishop	USA-CA	1.71	2.38	0.0026	0.0036	0.15
CA-15	039	Parlier	USA-CA	1.45	1.92	0.0023	0.0030	0.16
CA-16	041	Calipatria/Mulberry	USA-CA	1.79	2.50	0.0025	0.0036	0.15
CA-17	043	McArthur	USA-CA	1.31	1.70	0.0022	0.0029	0.15
CA-18	044	U.C.Riverside	USA-CA	1.68	2.35	0.0025	0.0035	0.16
CA-19	047	Brentwood	USA-CA	1.45	1.94	0.0023	0.0030	0.16
CA-20	049	Oceanside	USA-CA	1.62	2.26	0.0029	0.0040	0.18
CA-21	054	Blackwells Corner	USA-CA	1.49	1.99	0.0022	0.0030	0.15
CA-22	056	Los Banos	USA-CA	1.47	1.95	0.0023	0.0030	0.16
CA-23	061	Orland	USA-CA	1.45	1.94	0.0023	0.0030	0.16
CA-24	062	Temecula	USA-CA	1.62	2.26	0.0029	0.0040	0.18
CA-25	064	Santa Ynez	USA-CA	1.36	1.81	0.0024	0.0032	0.17
CA-26	068	Seeley	USA-CA	1.93	2.76	0.0026	0.0037	0.15
CA-27	070	Manteca	USA-CA	1.43	1.89	0.0023	0.0030	0.16
CA-28	071	Modesto	USA-CA	1.43	1.89	0.0023	0.0030	0.16

CA-29	077	Oakville	USA-CA	1.37	1.82	0.0023	0.0030	0.16
CA-30	075	Irvine	USA-CA	1.65	2.29	0.0027	0.0038	0.17
CA-31	078	Pomona	USA-CA	1.72	2.39	0.0027	0.0038	0.16
CA-32	080	Fresno State	USA-CA	1.45	1.92	0.0023	0.0030	0.16
CA-33	083	Santa Rosa	USA-CA	1.24	1.63	0.0021	0.0027	0.16
CA-34	084	Browns Valley	USA-CA	1.45	1.93	0.0024	0.0031	0.17
CA-35	085	Hopland F.S.	USA-CA	1.38	1.87	0.0021	0.0028	0.15
CA-36	086	Lindcove	USA-CA	1.48	1.96	0.0023	0.0031	0.16
CA-37	087	Meloland	USA-CA	1.91	2.71	0.0025	0.0036	0.14
CA-38	088	Cuyama	USA-CA	1.37	1.81	0.0025	0.0033	0.17
CA-39	091	Tulelake F.S.	USA-CA	1.39	1.81	0.0022	0.0029	0.15
CA-40	092	Kesterson	USA-CA	1.47	1.95	0.0023	0.0030	0.16
CA-41	094	Goletta foothills	USA-CA	1.37	1.81	0.0025	0.0033	0.17
CA-42	099	Santa Monica	USA-CA	1.63	2.24	0.0027	0.0037	0.17
CA-43	103	Windsor	USA-CA	1.28	1.68	0.0021	0.0028	0.16
CA-44	104	De Laveaga	USA-CA	1.20	1.53	0.0023	0.0029	0.18
CA-45	105	Westlands	USA-CA	1.48	1.97	0.0023	0.0030	0.16
CA-46	106	Sanel Valley	USA-CA	1.10	1.39	0.0019	0.0024	0.16
CA-47	57	Buntingville	USA-CA	1.55	2.11	0.0023	0.0031	0.15
CA-48	90	Alturas	USA-CA	1.33	1.74	0.0023	0.0030	0.15
CA-49	151	Ripley	USA-CA	2.01	2.88	0.0028	0.0040	0.16
CA-50	183	Owens Lake North	USA-CA	1.43	1.89	0.0026	0.0034	0.17
CA-51	147	Otay Lake	USA-CA	1.71	2.39	0.0026	0.0037	0.15
CA-52	175	Palo Verde II	USA-CA	1.98	2.84	0.0027	0.0038	0.15
CA-53	135	Blynthe NE	USA-CA	2.01	2.88	0.0028	0.0040	0.16
CA-54	155	Bryte	USA-CA	1.45	1.93	0.0022	0.0029	0.16
CA-55	159	Monrovia	USA-CA	1.72	2.39	0.0027	0.0038	0.16
CA-56	161	Patterson	USA-CA	1.48	1.98	0.0023	0.0030	0.16
CA-57	174	Long Beach	USA-CA	1.52	2.08	0.0029	0.0040	0.20
CA-58	173	Torrey Pines	USA-CA	1.62	2.26	0.0029	0.0040	0.18
CA-59	150	Miramar	USA-CA	1.62	2.26	0.0029	0.0040	0.18
CA-60	153	Escondido SPV	USA-CA	1.62	2.24	0.0025	0.0035	0.16
A-1	32040	Townsville Aero	Australia	1.28	1.66	0.0026	0.0033	0.19
A-2	33307	Woolshed	Australia	1.28	1.66	0.0026	0.0033	0.19
A-3	2056	Kununurra Aero	Australia	1.56	2.11	0.0025	0.0034	0.18
A-4	35264	Emerald	Australia	1.29	1.63	0.0021	0.0027	0.16
A-5	24024	Loxton R.C.	Australia	1.63	2.21	0.0024	0.0032	0.15
A-6	74037	Yanco AG.I.	Australia	1.48	1.95	0.0023	0.0031	0.16
A-7	74258	Deniliquin Airp.AWS	Australia	1.49	1.99	0.0023	0.0030	0.16
A-8	75041	Griffith Airp.AWS	Australia	1.51	2.02	0.0024	0.0032	0.16
A-9	76031	Mildura Airp.	Australia	1.67	2.30	0.0025	0.0034	0.16
A-10	24048	Renmark Apt.1	Australia	1.63	2.21	0.0024	0.0032	0.15
A-11	40082	University of QLD G.	Australia	1.27	1.63	0.0021	0.0027	0.16
A-12	40922	Kingaroy Airp.	Australia	1.23	1.56	0.0021	0.0026	0.16
A-13	41359	Oakey Aero	Australia	1.23	1.55	0.0021	0.0026	0.16
A-14	41522	Dalby Airp.	Australia	1.26	1.60	0.0021	0.0026	0.16
A-15	41525	Warwick	Australia	1.22	1.55	0.0021	0.0027	0.16
A-16	41529	Toowoomba Airp.	Australia	1.25	1.58	0.0021	0.0026	0.16
A-17	80091	Kyabram	Australia	1.43	1.88	0.0022	0.0030	0.16
A-18	81049	Tatura I.S.A.	Australia	1.43	1.88	0.0022	0.0030	0.16
A-19	81124	Yarrawonga	Australia	1.39	1.80	0.0022	0.0028	0.15
A-20	81125	Shepparton Airp.	Australia	1.43	1.88	0.0022	0.0030	0.16
A-21	41175	Applethorpe	Australia	1.20	1.49	0.0021	0.0026	0.16
A-22	81123	Bendigo Airp.	Australia	1.43	1.89	0.0023	0.0030	0.15
A-23	85072	East sale Airp.	Australia	1.34	1.80	0.0023	0.0031	0.16
A-24	85279	Bairnsdale Airp.	Australia	1.40	1.88	0.0024	0.0032	0.16
A-25	85280	Morwell L.V.Airp.	Australia	1.38	1.86	0.0023	0.0031	0.15

A-26	85296	Mount Moornapa	Australia	1.43	1.94	0.0023	0.0031	0.15
A-27	90035	Colac	Australia	1.46	2.00	0.0024	0.0033	0.16
A-28	9538	Dwellingup	Australia	1.36	1.80	0.0023	0.0031	0.17
A-29	9617	Bridgetown	Australia	1.32	1.73	0.0022	0.0029	0.16
A-30	23373	Nuriootpa Pirsa	Australia	1.54	2.07	0.0024	0.0032	0.16
A-31	26021	Mount Gambier Aero	Australia	1.38	1.85	0.0024	0.0032	0.16
A-32	26091	Coonawarra	Australia	1.49	2.03	0.0023	0.0032	0.15
A-33	66062	Sydney (Obs.Hill)	Australia	1.18	1.52	0.0022	0.0029	0.17
A-34	33002	Ayr DPI Res.St.	Australia	1.22	1.54	0.0023	0.0029	0.18
A-35	7176	Newman Aero	Australia	2.04	2.94	0.0031	0.0044	0.18
A-36	13017	Giles	Australia	2.18	3.20	0.0032	0.0046	0.17
A-37	11052	Forrest	Australia	1.78	2.52	0.0027	0.0038	0.15
A-38	11003	Eucla	Australia	1.68	2.39	0.0029	0.0041	0.17
A-39	12071	Salmon Gums	Australia	1.65	2.28	0.0027	0.0038	0.16
A-40	7045	Meekatharra Airp.	Australia	1.98	2.84	0.0031	0.0044	0.18
A-41	1025	Doongan	Australia	1.38	1.82	0.0027	0.0035	0.19
A-42	2012	Halls Creek Airp.	Australia	1.72	2.39	0.0025	0.0034	0.17
A-43	13015	Carnegie	Australia	2.12	3.09	0.0030	0.0044	0.17
A-44	3080	Curtin Aero	Australia	1.59	2.17	0.0026	0.0036	0.18
A-45	6022	Gascoyne Junction	Australia	1.97	2.83	0.0029	0.0041	0.17
A-46	9789	Esperance	Australia	1.53	2.12	0.0027	0.0038	0.17
A-47	91223	Marrawah	Australia	1.10	1.47	0.0023	0.0030	0.19
A-48	18106	Nullarbor	Australia	1.77	2.52	0.0027	0.0039	0.16
A-49	16090	Coober Pedy Airp.	Australia	2.05	2.98	0.0030	0.0044	0.17
A-50	16085	Marla Police St.	Australia	2.05	2.98	0.0030	0.0044	0.17
A-51	13011	Warburton Airfield	Australia	2.19	3.22	0.0031	0.0046	0.17
A-52	15528	Yuendumu	Australia	2.14	3.13	0.0032	0.0046	0.17
A-53	15666	Rabbit Flat	Australia	2.15	3.14	0.0029	0.0042	0.16
A-54	14829	Lajamanu Airp.	Australia	1.85	2.63	0.0026	0.0036	0.17
A-55	15135	Tennant Creek Airp.	Australia	2.05	2.98	0.0031	0.0045	0.18
A-56	37010	Camooweal Township	Australia	1.93	2.78	0.0027	0.0038	0.16
A-57	14707	Wollogorang	Australia	1.56	2.12	0.0028	0.0037	0.19
A-58	14938	Mango Farm	Australia	1.37	1.79	0.0023	0.0030	0.17
A-59	69134	Batemans Bay	Australia	1.19	1.51	0.0021	0.0027	0.16
A-60	14198	Jabiru Airp.	Australia	1.28	1.60	0.0023	0.0028	0.18
A-61	28008	Lockhart River Airp.	Australia	1.27	1.63	0.0026	0.0033	0.19
A-62	34084	Charters Towers Airp.	Australia	1.27	1.60	0.0022	0.0028	0.17
A-63	29038	Kowanyama Airp.	Australia	1.29	1.65	0.0024	0.0030	0.19
A-64	32078	Ingham Composite	Australia	1.34	1.76	0.0025	0.0032	0.18
A-65	40854	Logan City W.T.P.	Australia	1.33	1.79	0.0023	0.0031	0.17
A-66	8095	Mullewa	Australia	1.78	2.51	0.0027	0.0038	0.16
A-67	8251	Kalbarri	Australia	1.58	2.18	0.0028	0.0038	0.18
A-68	8225	Eneabba	Australia	1.82	2.60	0.0029	0.0041	0.17
A-69	7139	Paynes Find	Australia	1.81	2.54	0.0027	0.0038	0.17
A-70	10007	Bencubbin	Australia	1.61	2.20	0.0025	0.0034	0.16
A-71	10092	Merredin	Australia	1.62	2.21	0.0025	0.0035	0.16
A-72	12038	Kalgoorlie-Boulder Airp.	Australia	1.79	2.52	0.0028	0.0040	0.17
A-73	16098	Tarcoola Aero	Australia	1.95	2.80	0.0028	0.0041	0.16
A-74	18195	Minnipa Pirsa	Australia	1.73	2.44	0.0027	0.0038	0.16
A-75	46126	Tibooburra Airp.	Australia	2.02	2.92	0.0029	0.0042	0.17
A-76	48245	Boorke Airp. AWS	Australia	1.68	2.30	0.0025	0.0034	0.16
A-77	55325	Tamworth Airp. AWS	Australia	1.21	1.48	0.0020	0.0024	0.15
A-78	38026	Birdsville Airp.	Australia	2.36	3.52	0.0032	0.0047	0.16
A-79	30161	Richmond Airp.	Australia	1.64	2.25	0.0024	0.0033	0.16
A-80	33013	Collinsville Airp.	Australia	1.38	1.81	0.0024	0.0031	0.17

Table S3. Ranking of models for each criterion (1 is the best, 12 is the worst).

Model	MAE	RMSE	NRMSE%	PBIAS%	R^2	bR^2	NSE	d	KGE
P-T (Eq.2) with a_{pt}=1.26	12	12	12	12	12	12	12	12	12
P-T (Eq.2) with a_{pt}=p.w.a.s.	9	7	5	7	10	6	5	6	4
H-S (Eq.4b) with c_{hs2}=0.0023	7	9	9	9	9	10	9	9	9
H-S (Eq.4b) with c_{hs2}=p.w.a.s.	4	4	4	2	6	4	4	4	2
DRAL1 (Eq.8)	5	6	7	5	8	8	7	7	6
DRAL2 (Eq.9)	10	8	8	3	11	9	8	8	3
Copais (Eq.10)	3	3	3	6	4	5	3	3	7
VAL1 (Eq.11)	8	10	11	10	7	11	11	10	11
VAL2 (Eq.12)	2	2	2	4	3	2	2	2	5
VAL3 (Eq.13)	1	1	1	1	2	1	1	1	1
AKJ1 (Eq.14)	6	5	6	8	1	3	6	5	8
AKJ2 (Eq.15)	11	11	10	11	5	7	10	11	10

Analysis of Dc (distance from the coastline) and DT (difference between max and min monthly temperature) effects on K_{RS} coefficient.

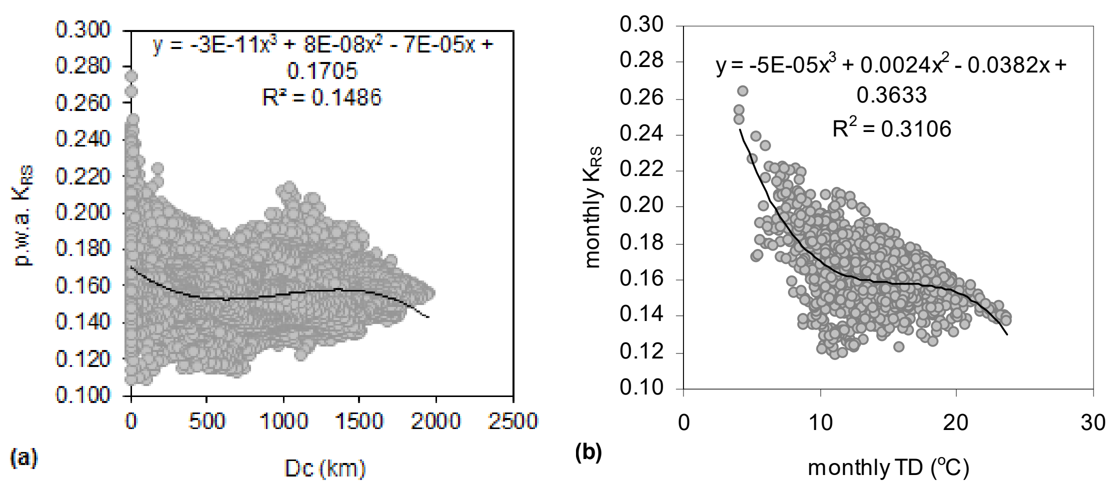

Fig.S4 Correlation between **(a)** p.w.a. K_{RS} and *Dc* (59031 observations derived by 0.5 degree resolution maps, all regions included except Greenland that showed extremely high K_{RS} values in inland areas, see Fig.7 in the manuscript) and (b) monthly K_{RS} and monthly *TD* values (1680 mean monthly observations derived by the 140 stations of Table 1 in the manuscript).

Example case using the Hargreaves-Samani method of evapotranspiration for the stations of California with revised coefficients.

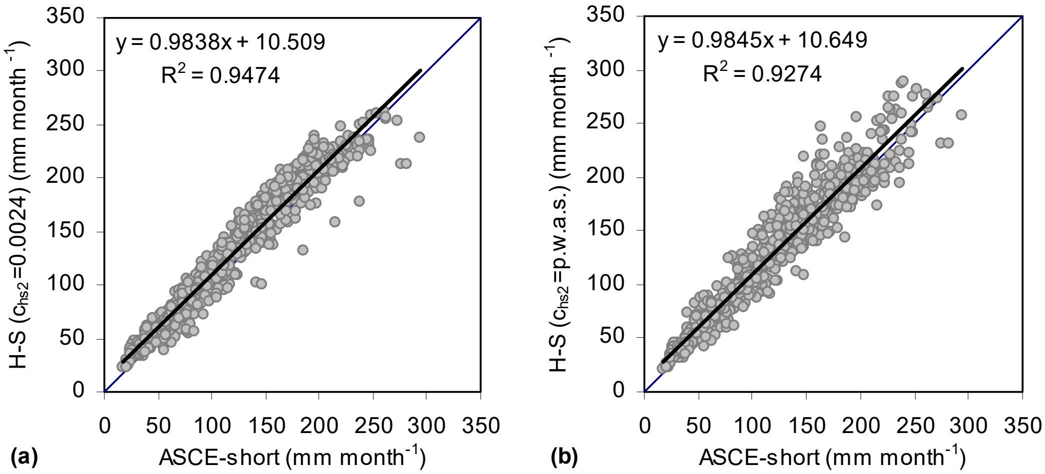

Fig.S5 Comparative 1:1 plots between the results of ASCE-short versus **(a)** the H-S method with c_{hs2}=0.0024 (mean value of p.w.a.s. c_{hs2} coefficients of all California stations obtained from Table S.2), **(b)** the H-S method using the individual values of c_{hs2}=p.w.a.s. for each station of California stations (Table S.2).

Table S4. Statistical criteria from the respective comparisons given in Fig.S5.

		H-S vs. ASCE-short	
Criterion	Optimum value	H-S (Eq.4b) with c_{hs2}=0.0024	H-S (Eq.4b) with c_{hs2}=p.w.a.s.
MAE	0	13.237*	14.297
RMSE	0	16.693*	19.119
NRMSE%	0	26.900*	30.500
PBIAS%	0	-7.100*	-7.200
R^2	1	0.947*	0.927
bR^2	1	0.887*	0.863
NSE	1	0.928*	0.907
d	1	0.982*	0.976
KGE	1	0.924*	0.916

*The asterisk is used to indicate the best value of each criterion.

Attributes of the datasets provided in the context of this study

Table S5. Contents of the database produced in this study (all five resolutions are included: 30 arc-sec, 2.5 arc-min, 5 arc-min, 10 arc-min, 0.5 deg.). The order of contents follows the alphabetical order of file names as they are stored in PANGAEA (https://doi.pangaea.de/10.1594/PANGAEA.868808)

No.	Content/resolution	File name	Method	Comment
1	Re-adjusted Priestley-Taylor coefficient for short ref.crop ETo (rescaled ×100) (unitless)/(30 arc-sec)	apts1_30s.zip	Re-calibration of Priestley-Taylor coefficient apt=1.26 for ETo method (Priestley and Taylor, 1972) using ASCE-EWRI method (Allen et al., 2005) for short ref.crop	the zip contains 1 raster (ESRI-grid) (partial weighted average of mean monthly values). For zero values use the closest non-zero value.
2	Re-adjusted Priestley-Taylor coefficient for tall ref.crop ETo (rescaled ×100) (unitless)/(30 arc-sec)	aptt1_30s.zip	Re-calibration of Priestley-Taylor coefficient apt=1.26 for ETo method (Priestley and Taylor, 1972) using ASCE-EWRI method (Allen et al., 2005) for tall ref.crop	the zip contains 1 raster (ESRI-grid) (partial weighted average of mean monthly values). For zero values use the closest non-zero value.
3	Re-adjusted Hargreaves-Samani coefficient for short ref.crop ETo (rescaled ×100,000) (unitless)/(30 arc-sec)	chs2s1_30s.zip	Re-calibration of Hargreaves-Samani coefficient chs2=0.0023 for ETo method (Hargreaves and Samani, 1982, 1985) using ASCE-EWRI method (Allen et al., 2005) for short ref.crop	the zip contains 1 raster (ESRI-grid) (partial weighted average of mean monthly values). For zero values use the closest non-zero value.
4	Re-adjusted Hargreaves-Samani coefficient for tall ref.crop ETo (rescaled ×100,000) (unitless)/(30 arc-sec)	chs2t1_30s.zip	Re-calibration of Hargreaves-Samani coefficient chs2=0.0023 for ETo method (Hargreaves and Samani, 1982, 1985) using ASCE-EWRI method (Allen et al., 2005) for tall ref.crop	the zip contains 1 raster (ESRI-grid) (partial weighted average of mean monthly values). For zero values use the closest non-zero value.
5	Hargeaves-Samani versus Priestley-Taylor (comparison between original methods versus ASCE-short) (DMADhp) (%)/(30 arc-sec)	dmadhp1_30s.zip	abs(madhs)-abs(madpt), higher negative values suggest better performance of original Hargreaves-Samani ETo method while higher positive values suggest better performance of original Priestley-Taylor ETo method using as reference the ASCE-short	the zip contains 1 raster (ESRI-grid)
6	Mean monthly ASCE-ETo for short reference crop (clipped grass) (mm/month)/(30 arc-sec)	etos1_30s.zip	ASCE-EWRI method (Allen et al., 2005) using climatic data from Hijmans et al. (2005) and Sheffield et al. (2006)	the zip contains 12 rasters (ESRI-grids) for each month (January is the first month)
7	Mean monthly ASCE-ETo for tall reference crop (alfalfa) (mm/month)/(30 arc-sec)	etot1_30s.zip	ASCE-EWRI method (Allen et al., 2005) using climatic data from Hijmans et al. (2005) and Sheffield et al. (2006)	the zip contains 12 rasters (ESRI-grids) for each month (January is the first month)
8	Re-adjusted coefficient for solar radiation formula of Hargreaves-Samani (rescaled ×1000) (unitless)/(30 arc-sec)	krs1_30s.zip	Re-calibration of Hargreaves-Samani coefficient krs=0.16-0.19 for solar radiation formula (Hargreaves and Samani, 1982, 1985) using solar radiation data (from Sheffield et al., 2006)	the zip contains 1 raster (ESRI-grid) (partial weighted average of mean monthly values)

9	Expected Mean Annual Difference/Error (MAD%) between original Hargreaves-Samani ETo and ASCE-ETo for short ref.crop (%)/(30 arc-sec)	madhs1_30s.zip	100*[(Annual ETo H-S)-(Annual ETo ASCE-short)]/(Annual ETo ASCE-short), Annual ETo H-S is estimated with the typical value chs2=0.0023	the zip contains 1 raster (ESRI-grid)
10	Expected Mean Annual Difference/Error (MAD%) between original Priestley-Taylor ETo and ASCE-ETo for short ref.crop (%)/(30 arc-sec)	madpt1_30s.zip	100*[(Annual ETo P-T)-(Annual ETo ASCE-short)]/(Annual ETo ASCE-short), Annual ETo P-T is estimated with the typical value apt=1.26	the zip contains 1 raster (ESRI-grid)
11	Expected Mean Annual Difference/Error (MAD%) between original Hargreaves-Samani radiation formula versus solar radiation data (%)/(30 arc-sec)	madrs1_30s.zip	100*[(Annual RS of H-S)-(Annual RS data)]/(Annual RS data), Annual RS H-S is estimated with the typical value krs=0.17 and RS obtained from Sheffield et al. (2006)	the zip contains 1 raster (ESRI-grid)
12	Re-adjusted Priestley-Taylor coefficient for short ref.crop ETo (rescaled ×100) (unitless)/(2.5 arc-min)	apts2_2-5m.zip	Re-calibration of Priestley-Taylor coefficient apt=1.26 for ETo method (Priestley and Taylor, 1972) using ASCE-EWRI method (Allen et al., 2005) for short ref.crop	the zip contains 1 raster (ESRI-grid) (partial weighted average of mean monthly values)
13	Re-adjusted Priestley-Taylor coefficient for tall ref.crop ETo (rescaled ×100) (unitless)/(2.5 arc-min)	aptt2_2-5m.zip	Re-calibration of Priestley-Taylor coefficient apt=1.26 for ETo method (Priestley and Taylor, 1972) using ASCE-EWRI method (Allen et al., 2005) for tall ref.crop	the zip contains 1 raster (ESRI-grid) (partial weighted average of mean monthly values)
14	Re-adjusted Hargreaves-Samani coefficient for short ref.crop ETo (rescaled ×100,000) (unitless)/(2.5 arc-min)	chs2s2_2-5m.zip	Re-calibration of Hargreaves-Samani coefficient chs2=0.0023 for ETo method (Hargreaves and Samani, 1982, 1985) using ASCE-EWRI method (Allen et al., 2005) for short ref.crop	the zip contains 1 raster (ESRI-grid) (partial weighted average of mean monthly values)
15	Re-adjusted Hargreaves-Samani coefficient for tall ref.crop ETo (rescaled ×100,000) (unitless)/(2.5 arc-min)	chs2t2_2-5m.zip	Re-calibration of Hargreaves-Samani coefficient chs2=0.0023 for ETo method (Hargreaves and Samani, 1982, 1985) using ASCE-EWRI method (Allen et al., 2005) for tall ref.crop	the zip contains 1 raster (ESRI-grid) (partial weighted average of mean monthly values)
16	Hargeaves-Samani versus Priestley-Taylor (comparison between original methods versus ASCE-short) (DMADhp) (%)/(2.5 arc-min)	dmadhp2_2-5m.zip	abs(madhs)-abs(madpt), higher negative values suggest better performance of original Hargreaves-Samani ETo method while higher positive values suggest better performance of original Priestley-Taylor ETo method using as reference the ASCE-short	the zip contains 1 raster (ESRI-grid)
17	Mean monthly ASCE-ETo for short reference crop (clipped grass) (mm/month)/(2.5 arc-min)	etos2_2-5m.zip	ASCE-EWRI method (Allen et al., 2005) using climatic data from Hijmans et al. (2005) and Sheffield et al. (2006)	the zip contains 12 rasters (ESRI-grids) for each month (January is the first month)

18	Mean monthly ASCE-ETo for tall reference crop (alfalfa) (mm/month)/(2.5 arc-min)	etot2_2-5m.zip	ASCE-EWRI method (Allen et al., 2005) using climatic data from Hijmans et al. (2005) and Sheffield et al. (2006)	the zip contains 12 rasters (ESRI-grids) for each month (January is the first month)
19	Re-adjusted coefficient for solar radiation formula of Hargreaves-Samani (rescaled ×1000) (unitless)/(2.5 arc-min)	krs2_2-5m.zip	Re-calibration of Hargreaves-Samani coefficient krs=0.16-0.19 for solar radiation formula (Hargreaves and Samani, 1982, 1985) using solar radiation data (from Sheffield et al., 2006)	the zip contains 1 raster (ESRI-grid) (partial weighted average of mean monthly values)
20	Expected Mean Annual Difference/Error (MAD%) between original Hargreaves-Samani ETo and ASCE-ETo for short ref.crop (%)/(2.5 arc-min)	madhs2_2-5m.zip	100*[(Annual ETo H-S)-(Annual ETo ASCE-short)]/(Annual ETo ASCE-short), Annual ETo H-S is estimated with the typical value chs2=0.0023	the zip contains 1 raster (ESRI-grid)
21	Expected Mean Annual Difference/Error (MAD%) between original Priestley-Taylor ETo and ASCE-ETo for short ref.crop (%)/(2.5 arc-min)	madpt2_2-5m.zip	100*[(Annual ETo P-T)-(Annual ETo ASCE-short)]/(Annual ETo ASCE-short), Annual ETo P-T is estimated with the typical value apt=1.26	the zip contains 1 raster (ESRI-grid)
22	Expected Mean Annual Difference/Error (MAD%) between original Hargreaves-Samani radiation formula versus solar radiation data (%)/(2.5 arc-min)	madrs2_2-5m.zip	100*[(Annual RS of H-S)-(Annual RS data)]/(Annual RS data), Annual RS H-S is estimated with the typical value krs=0.17 and RS obtained from Sheffield et al. (2006)	the zip contains 1 raster (ESRI-grid)
23	Re-adjusted Priestley-Taylor coefficient for short ref.crop ETo (rescaled ×100) (unitless)/(5 arc-min)	apts3_5m.zip	Re-calibration of Priestley-Taylor coefficient apt=1.26 for ETo method (Priestley and Taylor, 1972) using ASCE-EWRI method (Allen et al., 2005) for short ref.crop	the zip contains 1 raster (ESRI-grid) (partial weighted average of mean monthly values)
24	Re-adjusted Priestley-Taylor coefficient for tall ref.crop ETo (rescaled ×100) (unitless)/(5 arc-min)	aptt3_5m.zip	Re-calibration of Priestley-Taylor coefficient apt=1.26 for ETo method (Priestley and Taylor, 1972) using ASCE-EWRI method (Allen et al., 2005) for tall ref.crop	the zip contains 1 raster (ESRI-grid) (partial weighted average of mean monthly values)
25	Re-adjusted Hargreaves-Samani coefficient for short ref.crop ETo (rescaled ×100,000) (unitless)/(5 arc-min)	chs2s3_5m.zip	Re-calibration of Hargreaves-Samani coefficient chs2=0.0023 for ETo method (Hargreaves and Samani, 1982, 1985) using ASCE-EWRI method (Allen et al., 2005) for short ref.crop	the zip contains 1 raster (ESRI-grid) (partial weighted average of mean monthly values)
26	Re-adjusted Hargreaves-Samani coefficient for tall ref.crop ETo (rescaled ×100,000) (unitless)/(5 arc-min)	chs2t3_5m.zip	Re-calibration of Hargreaves-Samani coefficient chs2=0.0023 for ETo method (Hargreaves and Samani, 1982, 1985) using ASCE-EWRI method (Allen et al., 2005) for tall ref.crop	the zip contains 1 raster (ESRI-grid) (partial weighted average of mean monthly values)

27	Hargeaves-Samani versus Priestley-Taylor (comparison between original methods versus ASCE-short) (DMADhp) (%)/(5 arc-min)	dmadhp3_5m.zip	abs(madhs)-abs(madpt), higher negative values suggest better performance of original Hargreaves-Samani ETo method while higher positive values suggest better performance of original Priestley-Taylor ETo method using as reference the ASCE-short	the zip contains 1 raster (ESRI-grid)
28	Mean monthly ASCE-ETo for short reference crop (clipped grass) (mm/month)/(5 arc-min)	etos3_5m.zip	ASCE-EWRI method (Allen et al., 2005) using climatic data from Hijmans et al. (2005) and Sheffield et al. (2006)	the zip contains 12 rasters (ESRI-grids) for each month (January is the first month)
29	Mean monthly ASCE-ETo for tall reference crop (alfalfa) (mm/month)/(5 arc-min)	etot3_5m.zip	ASCE-EWRI method (Allen et al., 2005) using climatic data from Hijmans et al. (2005) and Sheffield et al. (2006)	the zip contains 12 rasters (ESRI-grids) for each month (January is the first month)
30	Re-adjusted coefficient for solar radiation formula of Hargreaves-Samani (rescaled ×1000) (unitless)/(5 arc-min)	krs3_5m.zip	Re-calibration of Hargreaves-Samani coefficient krs=0.16-0.19 for solar radiation formula (Hargreaves and Samani, 1982, 1985) using solar radiation data (from Sheffield et al., 2006)	the zip contains 1 raster (ESRI-grid) (partial weighted average of mean monthly values)
31	Expected Mean Annual Difference/Error (MAD%) between original Hargreaves-Samani ETo and ASCE-ETo for short ref.crop (%)/(5 arc-min)	madhs3_5m.zip	100*[(Annual ETo H-S)-(Annual ETo ASCE-short)]/(Annual ETo ASCE-short), Annual ETo H-S is estimated with the typical value chs2=0.0023	the zip contains 1 raster (ESRI-grid)
32	Expected Mean Annual Difference/Error (MAD%) between original Priestley-Taylor ETo and ASCE-ETo for short ref.crop (%)/(5 arc-min)	madpt3_5m.zip	100*[(Annual ETo P-T)-(Annual ETo ASCE-short)]/(Annual ETo ASCE-short), Annual ETo P-T is estimated with the typical value apt=1.26	the zip contains 1 raster (ESRI-grid)
33	Expected Mean Annual Difference/Error (MAD%) between original Hargreaves-Samani radiation formula versus solar radiation data (%)/(5 arc-min)	madrs3_5m.zip	100*[(Annual RS of H-S)-(Annual RS data)]/(Annual RS data), Annual RS H-S is estimated with the typical value krs=0.17 and RS obtained from Sheffield et al. (2006)	the zip contains 1 raster (ESRI-grid)
34	Re-adjusted Priestley-Taylor coefficient for short ref.crop ETo (rescaled ×100) (unitless)/(10 arc-min)	apts4_10m.zip	Re-calibration of Priestley-Taylor coefficient apt=1.26 for ETo method (Priestley and Taylor, 1972) using ASCE-EWRI method (Allen et al., 2005) for short ref.crop	the zip contains 1 raster (ESRI-grid) (partial weighted average of mean monthly values)
35	Re-adjusted Priestley-Taylor coefficient for tall ref.crop ETo (rescaled ×100) (unitless)/(10 arc-min)	aptt4_10m.zip	Re-calibration of Priestley-Taylor coefficient apt=1.26 for ETo method (Priestley and Taylor, 1972) using ASCE-EWRI method (Allen et al., 2005) for tall ref.crop	the zip contains 1 raster (ESRI-grid) (partial weighted average of mean monthly values)

36	Re-adjusted Hargreaves-Samani coefficient for short ref.crop ETo (rescaled ×100,000) (unitless)/(10 arc-min)	chs2s4_10m.zip	Re-calibration of Hargreaves-Samani coefficient chs2=0.0023 for ETo method (Hargreaves and Samani, 1982, 1985) using ASCE-EWRI method (Allen et al., 2005) for short ref.crop	the zip contains 1 raster (ESRI-grid) (partial weighted average of mean monthly values)
37	Re-adjusted Hargreaves-Samani coefficient for tall ref.crop ETo (rescaled ×100,000) (unitless)/(10 arc-min)	chs2t4_10m.zip	Re-calibration of Hargreaves-Samani coefficient chs2=0.0023 for ETo method (Hargreaves and Samani, 1982, 1985) using ASCE-EWRI method (Allen et al., 2005) for tall ref.crop	the zip contains 1 raster (ESRI-grid) (partial weighted average of mean monthly values)
38	Hargeaves-Samani versus Priestley-Taylor (comparison between original methods versus ASCE-short) (DMADhp) (%)/(10 arc-min)	dmadhp4_10m.zip	abs(madhs)-abs(madpt), higher negative values suggest better performance of original Hargreaves-Samani ETo method while higher positive values suggest better performance of original Priestley-Taylor ETo method using as reference the ASCE-short	the zip contains 1 raster (ESRI-grid)
39	Mean monthly ASCE-ETo for short reference crop (clipped grass) (mm/month)/(10 arc-min)	etos4_10m.zip	ASCE-EWRI method (Allen et al., 2005) using climatic data from Hijmans et al. (2005) and Sheffield et al. (2006)	the zip contains 12 rasters (ESRI-grids) for each month (January is the first month)
40	Mean monthly ASCE-ETo for tall reference crop (alfalfa) (mm/month)/(10 arc-min)	etot4_10m.zip	ASCE-EWRI method (Allen et al., 2005) using climatic data from Hijmans et al. (2005) and Sheffield et al. (2006)	the zip contains 12 rasters (ESRI-grids) for each month (January is the first month)
41	Re-adjusted coefficient for solar radiation formula of Hargreaves-Samani (rescaled ×1000) (unitless)/(10 arc-min)	krs4_10m.zip	Re-calibration of Hargreaves-Samani coefficient krs=0.16-0.19 for solar radiation formula (Hargreaves and Samani, 1982, 1985) using solar radiation data (from Sheffield et al., 2006)	the zip contains 1 raster (ESRI-grid) (partial weighted average of mean monthly values)
42	Expected Mean Annual Difference/Error (MAD%) between original Hargreaves-Samani ETo and ASCE-ETo for short ref.crop (%)/(10 arc-min)	madhs4_10m.zip	100*[(Annual ETo H-S)-(Annual ETo ASCE-short)]/(Annual ETo ASCE-short), Annual ETo H-S is estimated with the typical value chs2=0.0023	the zip contains 1 raster (ESRI-grid)
43	Expected Mean Annual Difference/Error (MAD%) between original Priestley-Taylor ETo and ASCE-ETo for short ref.crop (%)/(10 arc-min)	madpt4_10m.zip	100*[(Annual ETo P-T)-(Annual ETo ASCE-short)]/(Annual ETo ASCE-short), Annual ETo P-T is estimated with the typical value apt=1.26	the zip contains 1 raster (ESRI-grid)
44	Expected Mean Annual Difference/Error (MAD%) between original Hargreaves-Samani radiation formula versus solar radiation data (%)/(10 arc-min)	madrs4_10m.zip	100*[(Annual RS of H-S)-(Annual RS data)]/(Annual RS data), Annual RS H-S is estimated with the typical value krs=0.17 and RS obtained from Sheffield et al. (2006)	the zip contains 1 raster (ESRI-grid)

45	Re-adjusted Priestley-Taylor coefficient for short ref.crop ETo (rescaled ×100) (unitless)/(0.5 deg)	apts5_0-5d.zip	Re-calibration of Priestley-Taylor coefficient apt=1.26 for ETo method (Priestley and Taylor, 1972) using ASCE-EWRI method (Allen et al., 2005) for short ref.crop	the zip contains 1 raster (ESRI-grid) (partial weighted average of mean monthly values)
46	Re-adjusted Priestley-Taylor coefficient for tall ref.crop ETo (rescaled ×100) (unitless)/(0.5 deg)	aptt5_0-5d.zip	Re-calibration of Priestley-Taylor coefficient apt=1.26 for ETo method (Priestley and Taylor, 1972) using ASCE-EWRI method (Allen et al., 2005) for tall ref.crop	the zip contains 1 raster (ESRI-grid) (partial weighted average of mean monthly values)
47	Re-adjusted Hargreaves-Samani coefficient for short ref.crop ETo (rescaled ×100,000) (unitless)/(0.5 deg)	chs2s5_0-5d.zip	Re-calibration of Hargreaves-Samani coefficient chs2=0.0023 for ETo method (Hargreaves and Samani, 1982, 1985) using ASCE-EWRI method (Allen et al., 2005) for short ref.crop	the zip contains 1 raster (ESRI-grid) (partial weighted average of mean monthly values)
48	Re-adjusted Hargreaves-Samani coefficient for tall ref.crop ETo (rescaled ×100,000) (unitless)/(0.5 deg)	chs2t5_0-5d.zip	Re-calibration of Hargreaves-Samani coefficient chs2=0.0023 for ETo method (Hargreaves and Samani, 1982, 1985) using ASCE-EWRI method (Allen et al., 2005) for tall ref.crop	the zip contains 1 raster (ESRI-grid) (partial weighted average of mean monthly values)
49	Hargeaves-Samani versus Priestley-Taylor (comparison between original methods versus ASCE-short) (DMADhp) (%)/(0.5 deg)	dmadhp5_0-5d.zip	abs(madhs)-abs(madpt), higher negative values suggest better performance of original Hargreaves-Samani ETo method while higher positive values suggest better performance of original Priestley-Taylor ETo method using as reference the ASCE-short	the zip contains 1 raster (ESRI-grid)
50	Mean monthly ASCE-ETo for short reference crop (clipped grass) (mm/month)/(0.5 deg)	etos5_0-5d.zip	ASCE-EWRI method (Allen et al., 2005) using climatic data from Hijmans et al. (2005) and Sheffield et al. (2006)	the zip contains 12 rasters (ESRI-grids) for each month (January is the first month)
51	Mean monthly ASCE-ETo for tall reference crop (alfalfa) (mm/month)/(0.5 deg)	etot5_0-5d.zip	ASCE-EWRI method (Allen et al., 2005) using climatic data from Hijmans et al. (2005) and Sheffield et al. (2006)	the zip contains 12 rasters (ESRI-grids) for each month (January is the first month)
52	Re-adjusted coefficient for solar radiation formula of Hargreaves-Samani (rescaled ×1000) (unitless)/(0.5 deg)	krs5_0-5d.zip	Re-calibration of Hargreaves-Samani coefficient krs=0.16-0.19 for solar radiation formula (Hargreaves and Samani, 1982, 1985) using solar radiation data (from Sheffield et al., 2006)	the zip contains 1 raster (ESRI-grid) (partial weighted average of mean monthly values)
53	Expected Mean Annual Difference/Error (MAD%) between original Hargreaves-Samani ETo and ASCE-ETo for short ref.crop (%)/(0.5 deg)	madhs5_0-5d.zip	100*[(Annual ETo H-S)-(Annual ETo ASCE-short)]/(Annual ETo ASCE-short), Annual ETo H-S is estimated with the typical value chs2=0.0023	the zip contains 1 raster (ESRI-grid)

54	Expected Mean Annual Difference/Error (MAD%) between original Priestley-Taylor ETo and ASCE-ETo for short ref.crop (%)/(0.5 deg)	madpt5_0-5d.zip	100*[(Annual ETo P-T)-(Annual ETo ASCE-short)]/(Annual ETo ASCE-short), Annual ETo P-T is estimated with the typical value apt=1.26	the zip contains 1 raster (ESRI-grid)
55	Expected Mean Annual Difference/Error (MAD%) between original Hargreaves-Samani radiation formula versus solar radiation data (%)/(0.5 deg)	madrs5_0-5d.zip	100*[(Annual RS of H-S)-(Annual RS data)]/(Annual RS data), Annual RS H-S is estimated with the typical value krs=0.17 and RS obtained from Sheffield et al. (2006)	the zip contains 1 raster (ESRI-grid)